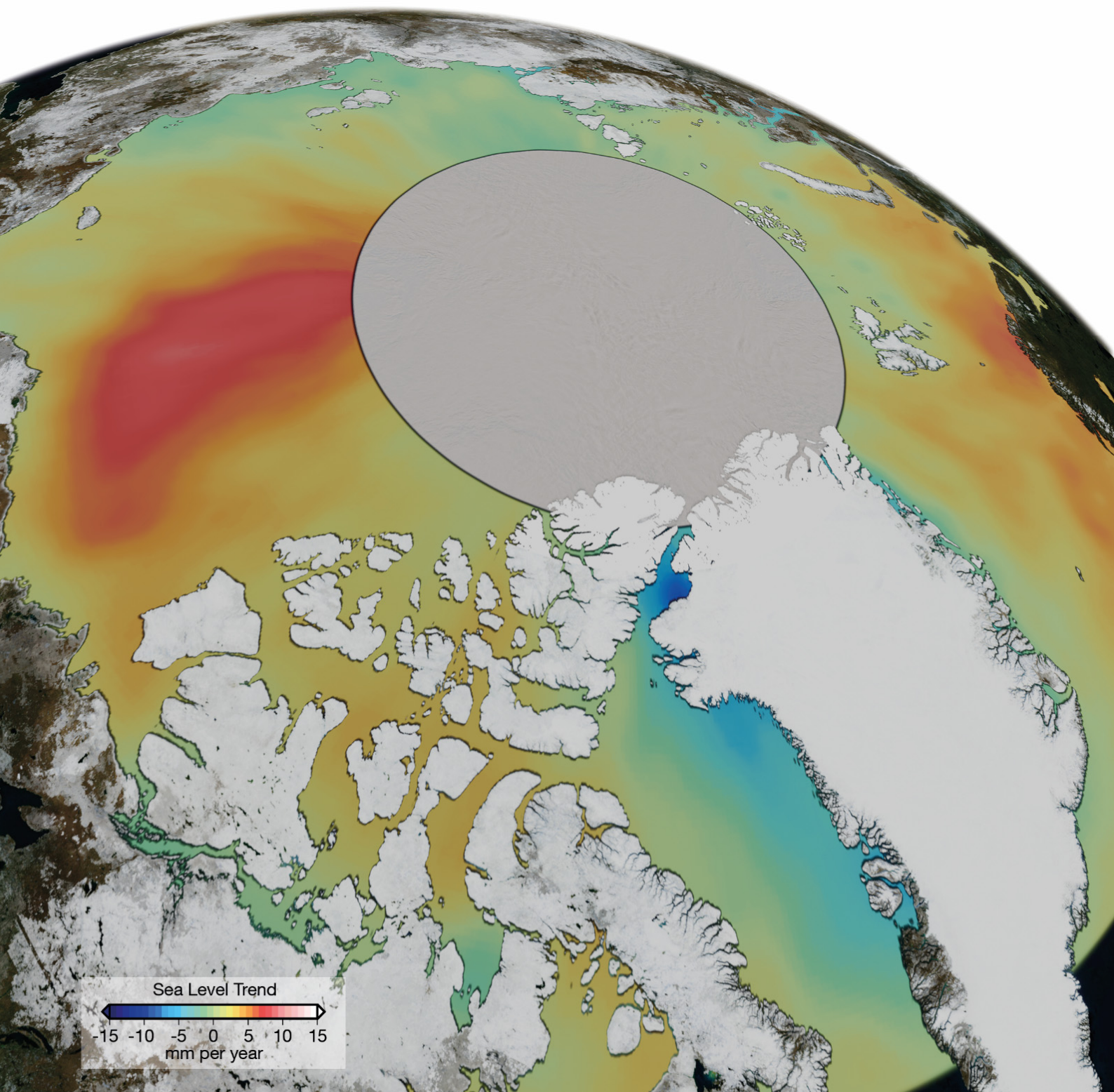


Annual Report 2019

Deutsches Geodätisches Forschungsinstitut
der Technischen Universität München
(DGFI-TUM)



Front cover: Long-term sea level change in the Arctic Ocean

The picture displays the change of the Arctic Ocean sea level over the past 22 years. Regions affected by sea level rise are colored in red and yellow. Blue colors, on the contrary, indicate a drop of the sea level. On average, the sea level of the Arctic Ocean has risen by 2.2 mm per year over the indicated period, but regional differences are strong. This is the result of a study conducted as part of ESA's Sea Level Climate Change Initiative (CCI) project in collaboration with the Technical University of Denmark (DTU Space).

The study resulted in the most complete and precise view of sea level changes in the Arctic Ocean to date. A comprehensive data set has been created based on more than 1.5 billion radar measurements of different altimetry satellites. Since vast areas of the Arctic Ocean are covered by sea ice, dedicated waveform classification and retracking algorithms had to be developed. These algorithms now make it possible to evaluate radar echoes reflected by water where it reaches the surface through cracks in the ice. This way, observations of sea level changes can be extended to regions for which the radar systems were blind in the past. The data means an important source of information for estimating future sea levels and for studying climate-related environmental changes in this particularly sensitive region. Details on the data processing and the results of the study are presented in Section 2.2 of this report.

Technische Universität München
Fakultät für Luftfahrt, Raumfahrt und Geodäsie
Deutsches Geodätisches Forschungsinstitut (DGFI-TUM)

Arcisstr. 21
D - 80333 München

www.dgfi.tum.de

Contents

Preface	1
1 Research Area Reference Systems	5
1.1 Analysis of Space-Based Microwave Observations	6
1.2 Analysis of Satellite Laser Ranging Observations	9
1.3 Computation of Satellite Orbits	12
1.4 Determination of Reference Frames	15
2 Research Area Satellite Altimetry	25
2.1 Multi-Mission Analysis	25
2.2 Sea Surface	27
2.3 Inland Altimetry	37
3 Cross-Cutting Research Topics	44
3.1 Atmosphere	44
3.2 Regional Gravity Field	57
3.3 Standards and Conventions	61
4 Scientific Transfer	66
4.1 Functions in Scientific Bodies	66
4.2 Publications	71
4.3 Presentations	74
4.4 Participation in Meetings, Symposia, Conferences	82
4.5 Guests	86
4.6 Internet Portals	86
5 Projects	90
6 Personnel	91
6.1 Lectures and Courses at Universities	91
6.2 Lectures at Seminars, Schools, and Public Relations	91
6.3 Thesis Supervision	92
6.4 Awards	92

Preface

The Institute

The Deutsches Geodätisches Forschungsinstitut (DGFI-TUM) is a research institute of the Technical University of Munich (TUM). It is part of the Chair of Geodetic Geodynamics within the newly established TUM Department of Aerospace and Geodesy (Fakultät für Luftfahrt, Raumfahrt und Geodäsie, LRG).

With a scientific focus on basic research in the field of Space Geodesy, the DGFI-TUM pursues the goal to provide a comprehensive and long-term valid metric of the Earth system for science and practice at the highest level of precision and consistency. In strong international and interdisciplinary collaboration, the institute processes, analyzes and combines observations from all relevant space-geodetic observing systems and complementary data sources.

For almost seven decades, the institute has continuously been involved in a broad variety of national and international research activities of which many were of high significance for the scientific advancement of geodesy. A central aspect of the institute's research has always been the precise determination of the Earth's geometrical shape and its temporal changes. For the solid Earth, this involves in particular the realization of horizontal and vertical terrestrial reference systems on global and regional scale and of the celestial reference system. With respect to water surfaces, the DGFI-TUM has a key focus on the precise determination of the changing sea level, the ocean's surface dynamics and water stages of inland water bodies using satellite altimetry.

The strategic direction of the DGFI-TUM is reflected by its organization into the two research areas *Reference Systems* and *Satellite Altimetry* (Fig. 1). The research areas are complemented by three overarching research topics, covering the investigation of the state and dynamics of the atmosphere (with a strong focus on ionospheric disturbances and space-weather impacts), the determination of high resolution regional gravity fields, and the enhancement of consistency in geodetic data analysis by establishing unique standards and conventions in an international context.

In the frame of the Research Group Satellite Geodesy (Forschungsgruppe Satellitengeodäsie, FGS), the institute contributes to the scientific data processing of the Geodetic Observatories Wettzell (Germany) and AGGO (Argentina). Furthermore, it operates several worldwide distributed GNSS stations.

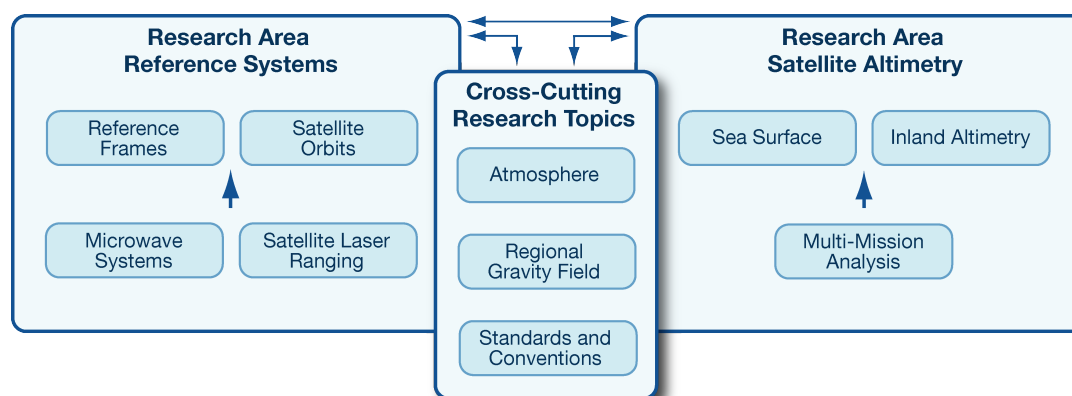


Figure 1: Research Areas of the DGFI-TUM

National and international involvement

The institute was established in 1952 as an independent research facility at the Bavarian Academy of Sciences and Humanities (BAdW) in Munich, and with effect from January 1, 2015 the DGFI became part of the TUM. The institute is intensively networked with renowned research institutions all over the world, and over its history it has been involved in a multitude of internationally coordinated scientific activities. During the first decades after its foundation, DGFI achieved outstanding results particularly in the fields of geodetic-astronomical observations and electro-optical distance measurements for the determination of the German and European triangulation as well as in gravimetric surveys for gravity networks. The DGFI was involved in the first worldwide network of satellite triangulation and played an important role in the development of dynamical methods of satellite geodesy for precise orbit determination, point positioning and gravity field modeling.

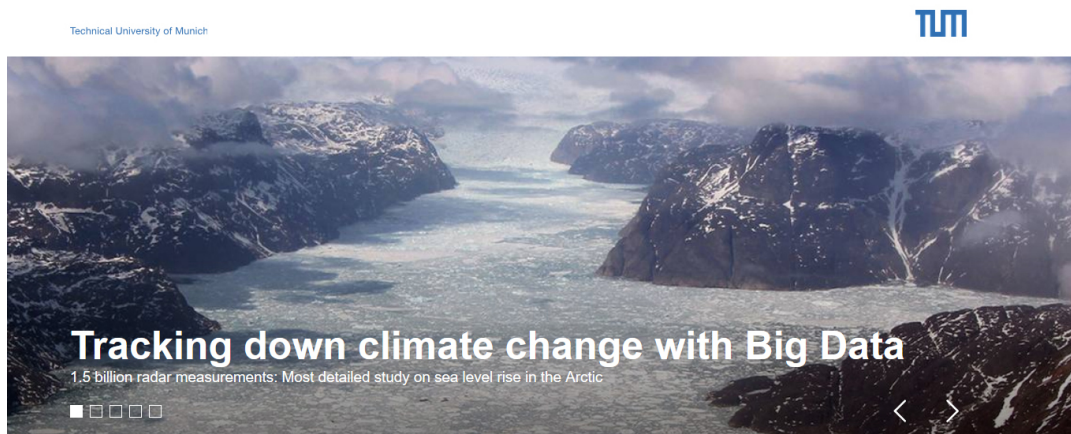
The DGFI-TUM collaborates at key positions in international scientific organizations, especially within the framework of the International Union of Geodesy and Geophysics (IUGG), the International Astronomical Union (IAU), and the International Association of Geodesy (IAG) (see Section 4.2). Since many years, it has been an important pillar of IAG's Global Geodetic Observing System (GGOS). GGOS advocates for the implementation of geodetic infrastructure and analysis capacity necessary for monitoring the Earth system and global change research, and it coordinates the generation of high-quality science data products under predefined standards and conventions. The DGFI-TUM provides the current GGOS Vice President, chairs one of the two GGOS Bureaus (Bureau of Products and Standards) and leads two of the three GGOS Focus Areas (FA Unified Height System; FA Geodetic Space Weather Research). Moreover, the institute recognizes the outstanding significance of IAG's Scientific Services which form the backbone of national and international spatial data infrastructure. In this framework, the DGFI-TUM operates data centers, analysis centers and research centers. It has been taking leading roles and supporting functions in IAG's Commissions, Projects, Working and Study Groups, and thus contributes to shaping the future direction of international geodetic research.

The institute participates in research programs of the European Union (EU) and the European Space Agency (ESA), and it cooperates in activities of the United Nations (UN). In this regard, the DGFI-TUM is involved in the implementation of a UN Resolution for a Global Geodetic Reference Frame (GGRF) and provides an IAG representative to the UN Committee of Experts on Global Geospatial Information Management (UN-GGIM) Working Group for the GGRF.

Research highlights of particular scientific and public interest

During the year 2019, several scientific results gained broad attention in the scientific community and in the public. The following activities and publications can be highlighted:

- **DGFI-TUM staff member elected GGOS Vice President:** Effective from November 2019, DGFI-TUM scientist Laura Sánchez was elected new Vice President of the Global Geodetic Observing System (GGOS) of the International Association of Geodesy (IAG). For the period 2019-2023, the new GGOS Coordinating Board will promote the advancement of the global geodetic infrastructure and organize the generation of high-quality geodetic products as backbone for studying the Earth system and for many other scientific and societal applications.
- **Long-term measurements document sea level rise in the Arctic (title page):** A collaborative study of scientists from the Technical University of Denmark (DTU) and the DGFI-TUM (*Arctic Ocean Sea Level Record from the Complete Radar Altimetry Era: 1991-2018*,



Remote Sensing, 2019, doi:[10.3390/rs11141672](https://doi.org/10.3390/rs11141672)) attained broad media coverage in 2019. The effort resulted in the most complete and precise view of the sea level changes in the Arctic Ocean to date, documenting the climate-related regional differences of sea level trends in this sensitive area. Further details on the study can be found in Section 2.2.

- Surface currents in Polar Oceans:** In a joint study of DGFI-TUM and the Alfred Wegener Institute (AWI), a novel dataset of geostrophic ocean surface currents in the northern Nordic Seas has been created from a combination of satellite altimetry and ocean model data (*Geostrophic currents in the northern Nordic Seas from a combination of multi-mission satellite altimetry and ocean modeling*, Earth System Science Data, 2019, doi:[10.5194/essd-11-1765-2019](https://doi.org/10.5194/essd-11-1765-2019)). The dataset (doi:[10.1594/PANGAEA.900691](https://doi.org/10.1594/PANGAEA.900691)) provides surface circulation information within the sea ice area between 1995 and 2012 to support a deeper comprehension of ocean dynamics in a region characterized by rapidly changing environmental conditions. See Section 2.2 for details.
- River levels tracked from space:** Flood forecasting and protection along rivers relies on monitoring data of water stages. At the example of the Mekong, TUM scientists from geodesy and mathematics developed an approach enabling the extensive assessment of water level changes within complex river systems under the influence of extreme weather events solely from satellite data. Flow patterns of the river network are modeled using the statistical method known as Universal Kriging. The model links data from different altimetry missions and makes it possible to extrapolate water levels observed at certain points to determine the levels at almost any location in the river system. It was demonstrated that including the precise and densely distributed SAR measurements of Cryosat-2 in the



model greatly improves the quality of the results. A TUM press release of January 2019 addressed the potential of satellite data for comprehensive monitoring of large river systems. Further details can be found in the article *Observing water level extremes in the Mekong River Basin: The benefit of long-repeat orbit missions in a multi-mission satellite altimetry approach* (Journal of Hydrology, 2019, doi:[10.1016/j.jhydrol.2018.12.041](https://doi.org/10.1016/j.jhydrol.2018.12.041)) and in previous DGFI-TUM annual reports.

- DGFI-TUM is a new Associate Analysis Centre (AAC) of the International DORIS Service (IDS):** In 2019, the Governing Board of the IDS accepted DGFI-TUM as an AAC, recognizing DGFI-TUM's specialized DORIS products. Among them are precise orbits of DORIS-tracked altimetry and other Earth observation satellites, as well as 3D-positions of DORIS ground stations.
- High-resolution Global Ionosphere Maps (GIM):** A new approach enables to determine almost concurrently global maps of the Vertical Total Electron Content (VTEC). It is based on algorithms, specifically tailored to the globally inhomogeneous distribution of GNSS observations. In comparison with the VTEC products of the International GNSS Service (IGS), the maps are of comparable quality, but they are available with a latency of only 2-3 hours instead of 2 weeks. The IGS Ionosphere Working Group recommended to add DGFI-TUM's VTEC GIMs as a new product contributing to the IGS combined VTEC solution; for details see Section 3.1.
- Regional geoid contribution to IAG's "1 cm Geoid Experiment":** The IAG Joint Study Group 2.2.2 initiated an experiment to compare different methodologies for the computation of geoid heights, height anomalies, and geopotential values from the combination of gravity data from different sources. DGFI-TUM's solution showed the smallest misfit of height anomaly and geoid height results at the benchmarks with respect to the mean values of all fourteen participants; see Sections 1.4 (Vertical Reference Systems) and 3.2 for details.
- P.M. Wissen magazine reports on geodetic model of the Alps:** The creation of a comprehensive model of the present-day surface-kinematics in the Alpine-Adriatic region based on high-level data analysis of more than 300 continuously operating GNSS stations was subject of a study led by DGFI-TUM in 2018 (see last year's annual report). The related TUM press release informing about the Alpine motions obtained considerable attention. In October 2019, the study was also subject of a TV report of the *P.M. Wissen* magazine on Servus TV (see www.dgfi.tum.de/en/dgfi-tum-in-the-media/).



1 Research Area Reference Systems

Theoretical and practical aspects of the realization of global and regional reference systems on Earth and in space at highest precision has been a key topic of the institute since decades. The computation of reference frames relies on the space geodetic observation techniques Very Long Baseline Interferometry (VLBI), Satellite and Lunar Laser Ranging (SLR/LLR), Global Navigation Satellite Systems (GNSS), and Doppler Orbitography and Radiopositioning Integrated by Satellite (DORIS). The work in this research area involves a refined modeling and analysis of these observation techniques and the development of advanced combination methods. As a backbone for its investigations, DGFI-TUM employs the proprietary software package DOGS (DGFI Orbit and Geodetic parameter estimation Software) with the components DOGS-OC for SLR and DORIS data processing and precise orbit determination, DOGS-RI for the analysis of VLBI observations, and DOGS-CS for the combination of the different observations on the normal equation level (Table 1.1). GNSS data are analyzed with the Bernese software.

Table 1.1: Components of the DGFI Orbit and Geodetic parameter estimation Software (DOGS).

Component	Purpose
DOGS-OC	SLR and DORIS data processing and precise orbit determination
DOGS-RI	VLBI data processing
DOGS-CS	Combination of space-geodetic observations on the normal equation level

All DOGS software packages are continuously updated to incorporate the latest developments and the state-of-the-art models for the data processing. In 2019, the institute further enhanced the DOGS-OC software for the analysis of DORIS observations.

The research benefits from DGFI-TUM's engagement in international scientific organizations, in particular in the frame of the International Association of Geodesy (IAG) and the International Astronomical Union (IAU). Mostly by virtue of long-term commitments, DGFI-TUM operates data centers, analysis centers, and research centers (Table 1.2).

Table 1.2: Long-term commitments of DGFI-TUM in international organizations related to the Research Area Reference Systems.

IAG Service	DGFI-TUM Commitments
International Earth Rotation and Reference Systems Service (IERS)	International Terrestrial Reference System (ITRS) ITRS Combination Center
International GNSS Service (IGS)	Regional Network Associate Analysis Center for SIRGAS (RNAAC-SIR),
International Laser Ranging Service (ILRS)	Global Data and Operation Center (EDC), Analysis Center
International VLBI Service for Geodesy and Astrometry (IVS)	Analysis Center, Combination Center (together with BKG)
International DORIS Service (IDS)	Associate Analysis Center

1.1 Analysis of Space-Based Microwave Observations

VLBI data analysis

Very Long Baseline Interferometry (VLBI) data analysis has been part of DGFI-TUM's research since many years. The institute has been an operational Analysis Center (AC) of the IVS since 2008. The IVS organizes the world-wide collaboration in performing VLBI observations and analysis. According to our corresponding duties, we continued to provide solutions (in the form of datum-free normal equations) for the twice-weekly rapid turnaround VLBI sessions in 2019. For the processing, we used our proprietary VLBI analysis software DOGS-RI, the Radio Interferometry component of the DOGS software package.

In 2019, we worked on two major topics with respect to VLBI. First, we investigated the impact of non-tidal loading, a geophysical effect that is only partly considered in VLBI analysis yet. Next to the non-tidal atmospheric loading, which is already included for the IVS solutions, we also applied non-tidal oceanic and hydrological loading, both individually and as a whole. Furthermore, we examined two application levels: the observation and the normal equation level. We found that the correction for non-tidal loading can mitigate various systematic effects in the VLBI analysis, mostly independent of the application level. For example, the weighted root mean square (WRMS) values of the estimated station heights are improved (i.e. decreased; Fig. 1.1).

Second, we prepared DOGS-RI for the upcoming 2020 realization of the International Terrestrial Reference System. The most important modifications were the implementation of

- the secular pole function as agreed upon at the Unified Analysis Workshop (UAW) 2017,
- the Desai and Sibois [2016] model for sub-daily EOP variation due to ocean tides,
- the latest realization of the International Celestial Reference System (ICRF3, including Galactic Aberration), and
- the empirical model for the gravitational deformation of selected VLBI antennas.

All these new models also have to be considered for the official IVS solutions starting from January 2020.

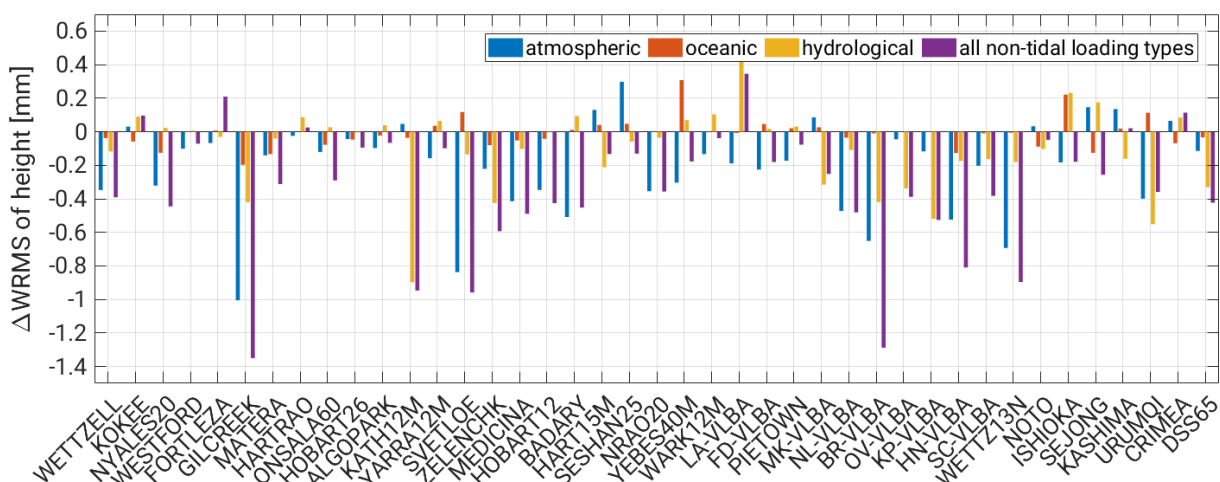


Figure 1.1: Change in the WRMS values of VLBI station heights when different non-tidal loading corrections are applied at observation level. Loading data was obtained from the GeoForschungsZentrum (GFZ) Potsdam.

DORIS data analysis

Precise orbits of altimetry satellites are fundamental for altimetry investigations since they provide positions of altimetry satellites in a well-defined reference frame. In the recent years, macro-models and satellite specific information of non-spherical satellites Jason-1, Jason-2 and Jason-3 have been implemented in DOGS-OC used for precise orbit determination (POD; Zeithöfler 2019, Bloßfeld et al., 2020). In 2018, the processing of DORIS observations in the IDS 2.2 format was implemented in this software. To reach a better orbit quality, processing of observation-based attitude data in the quaternion form for satellite main body and solar panel angles has been implemented and tested.

Using DOGS-OC, orbits of Jason satellites were computed based on DORIS 2 GHz measurements in the IDS 2.2 format available from IDS at the time intervals 13 January 2002 to 30 June 2013 for Jason-1 and 20 July 2008 to 7 January 2018 for Jason-2. The information about the satellite mass and its center of mass, the DORIS phase center coordinates, and the satellite macro-model were used according to Cerri et al. (2019)¹. The force models and the background models used for the computation of station coordinates are described in Bloßfeld et al. (2020). For each pass, a station-dependent frequency bias was estimated. The average RMS fits of DORIS observations are 0.495 mm/s for Jason-1 and 0.467 mm/s for Jason-2 (Fig. 1.2).

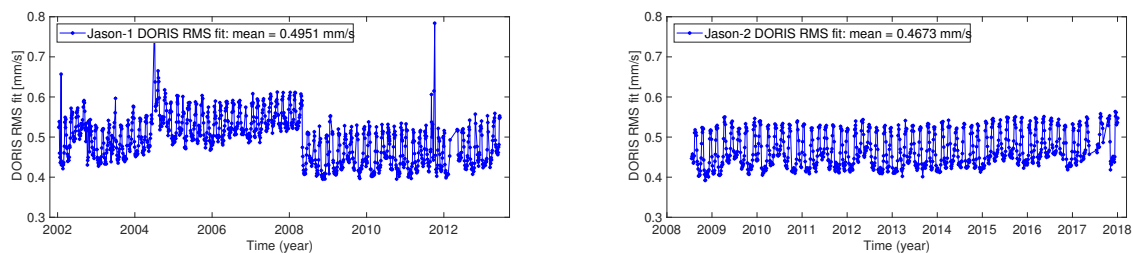


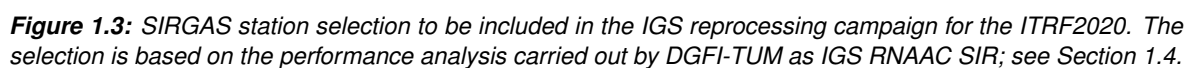
Figure 1.2: RMS values of the DORIS observation fits obtained for Jason-1 (left) and Jason-2 (right).

GNSS data analysis

In the frame of different international cooperation projects, DGFI-TUM has installed 21 continuously observing GNSS stations since 1998 in Europe and South America. The operation of these stations is supported by local partner institutions, which take care of the functioning of the equipment and the opportune data delivery to the processing centers. The DGFI-TUM permanent stations are integrated in different international initiatives such as the IGS Multi-GNSS Experiment (MGEX), the IGS Tide Gauge Benchmark Monitoring (TIGA), assessment of surface deformations in mountainous areas (especially in the Alps and the Andes), and the ITRF densification in Latin America by SIRGAS. In the particular case of SIRGAS, DGFI-TUM acts as the IGS Regional Network Associate Analysis Center for SIRGAS (IGS RNAAC SIR) since June 1996, and its main objective is the development of analysis strategies to ensure the long-term reliability and stability of the regional reference frame (see SIRGAS and DIGERATI, Section 1.4). In this context, DGFI-TUM's research is focused on:

- Computation of multi-year solutions to estimate the kinematics of the reference frame and to model the station velocity field as a basis for the determination of regional surface deformations;

¹Cerri L., et al.: DORIS satellites models implemented in POE processing. 1st ed.; 14th review; Ref.: SALP-NT-BORD-OP-16137-CN. Available online: <ftp://ftp.ids-doris.org/pub/ids/satellites/DORISatelliteModels.pdf>, 2019.



- Estimation of co-seismic deformation models derived from discrete station positions to incorporate seismic discontinuities in the computation of the reference frame and to support the precise transformation of coordinates referring to pre-seismic and post-seismic reference frame realizations;
- Modeling of seasonal movements at the combination level of the weekly solutions.

Additionally, DGFI-TUM supports IERS and IGS on the selection of regional stations of high performance to be included in new releases of the ITRF. As an example, Fig. 1.3 shows the SIRGAS stations added to the IGS reprocessing campaign for the ITRS realization 2020. DGFI-TUM makes the SIRGAS science data products available via www.sirgas.org and [ftp.sirgas.org](ftp://ftp.sirgas.org).

1.2 Analysis of Satellite Laser Ranging Observations

SLR data analysis

Since many years, DGFI-TUM has been an active Analysis Center (AC) of the International Laser Ranging Service Analysis Standing Committee (ILRS-ASC). Beside the daily routine analysis of SLR observations to multiple satellites, DGFI-TUM focuses on the consistent reprocessing of all available SLR observations since the beginning of this geodetic tracking technique in the 1980s.

DGFI-TUMs routinely computed products for the ILRS are summarized in Table 1.3. The “v170” and “v70” solutions are routinely processed on a daily and weekly basis and contain station coordinate (TRF) and Earth Orientation Parameter (EOP) solutions based on observations to the spherical near-Earth satellites LAGEOS-1 and -2 (LA-1/-2) and Etalon-1 and -2 (ET-1/-2). The weekly processing chain is also used to submit orbit solutions of these four satellites to the ILRS Combination Center in the so called “SP3c” data format.

For the new ITRS realization 2020, preprocessed SLR observations to the four above mentioned satellites and LARES will be applied. Therefore, DGFI-TUM currently analyzes all available LARES observations. Fig. 1.4 shows the arc-wise SLR orbit fits (RMS over observation residuals) for the spherical satellites LAGEOS-1/-2, Etalon-1/-2 and LARES.

It is clearly visible from Fig. 1.4 that before 1993.0, only LAGEOS-1 observations are analyzed. After 1993, LAGEOS-2 and both Etalon satellites contribute to the solution. Finally, in early 2012, LARES was launched and continuously tracked since then.

In the framework of the reprocessing for the ITRS realization 2020, DGFI-TUM also contributes to the ILRS-ASC pilot project (PP) on the systematic error monitoring of all stations (“v230” solution, see Tab. 1.3). For this PP, several model updates have been implemented in DGFI-TUM’s orbit computation software DOGS-OC, such as a new SLRF2014 TRF model, a new Center of Mass model, an updated ILRS site eccentricity file, the new ILRS secular pole model and the new ILRS high-frequency EOP model. As a result, individual range biases for LA-1/-2 and combined range biases for ET-1/-2 were estimated for all SLR stations on a weekly basis.

Table 1.3: DGFI-TUM routine solutions and pilot project contributions.

ILRS solution	Description
v170	Daily LA-1/-2 and ET-1/-2 TRF and EOP solutions
v70	Weekly LA-1/-2 and ET-1/-2 TRF and EOP solutions
v70-sp3c	Weekly LA-1/-2 and ET-1/-2 orbit solutions
v230	Contribution to the ILRS ASC pilot project on systematic error monitoring

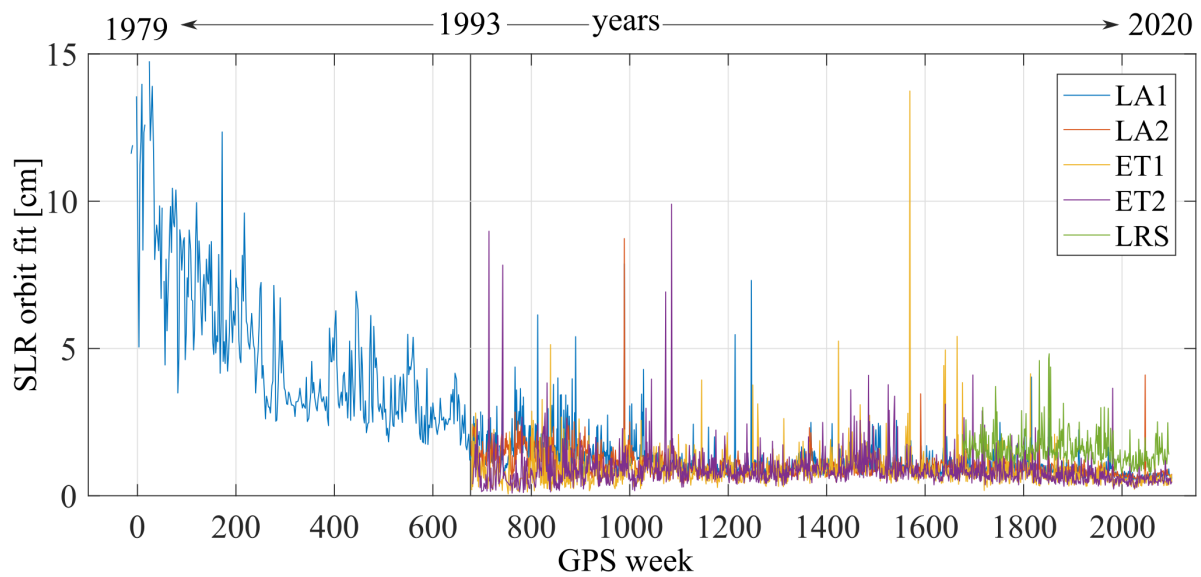


Figure 1.4: Arc-wise SLR orbit fits for the spherical satellites LAGEOS-1/-2, Etalon-1/-2 and LARES.

This time series of range biases is currently being combined with estimates from the other ILRS ACs at the ILRS Combination Center in order to obtain station- and satellite-specific long-term mean range biases to be applied in the final reprocessing run.

DGFI-TUM also investigates the quality of the current SLR tracking network which suffers from an insufficient network geometry due to a lack of stations especially in the southern hemisphere. Previous simulation studies have shown that the extension of the global SLR tracking network is indispensable for reaching the target accuracy of future TRFs in accordance with user requirements and the ambitious goals of the Global Geodetic Observing System (GGOS). A study performed in 2019 addressed the question where additional SLR stations would be most beneficial for an improved estimation of geodetic key parameters. Kehm et al. (2019) performed a simulation of a set of stations distributed homogeneously over the globe and compared different solutions, always adding one of the simulated stations to the existing SLR station network (see also Fig. 1.5). This approach has been chosen in order to be able to investigate the deficiencies of the existing SLR network and to judge in which regions an additional SLR station would be most valuable for the improvement of certain geodetic datum parameters of SLR-derived reference frames. For the determination of Earth Rotation Parameters (ERP), significant improvement could be reached through additional stations in polar regions (improvement of polar motion in y -direction up to 7%) and through stations along the equator (improvement for the Length of Day up to 1.5%). TRF parameters (see Fig. 1.6) would benefit from an additional station around the pierce points of the axes of the terrestrial reference frame (improvement for t_y up to 4%), in Arctic and the Pacific Ocean regions (t_z improved by up to 4.5%), and in the Antarctic and the Indian Ocean region (improved of the scale by up to 2.2%). Overall it was concluded that an additional SLR site in Antarctica should be of first priority, enabling improvements in the pole coordinates and the scale of the TRF; potential further sites are recommended close to the equator, especially beneficial for the origin of the realized TRF as well as for LOD.

DGFI-TUM will finish its reprocessing of SLR observations to other spherical satellites such as Starlette, Stella, Ajisai, Larets, BLITS and Westpac shortly. Moreover, in 2020, DGFI-TUM's ILRS AC staff will strongly be engaged in the final processing of the input data for the ITRS realization 2020 to be delivered to the ILRS Combination Center in early 2021.

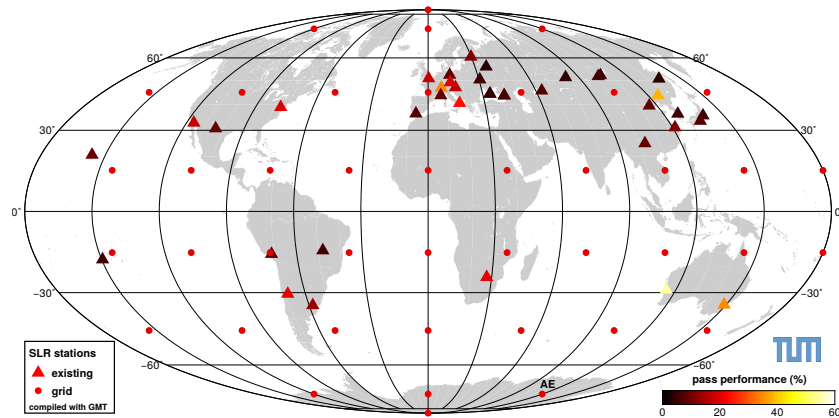


Figure 1.5: Global SLR network and locations of simulated SLR stations. Colors indicate the simulated performance; for existing stations, these were taken from Kehm et al. (2017), for each additional station, a performance of 20% has been assumed. The station marked with AE (Antarctica East) is the station for which an additional scenario with lower performance has been simulated.

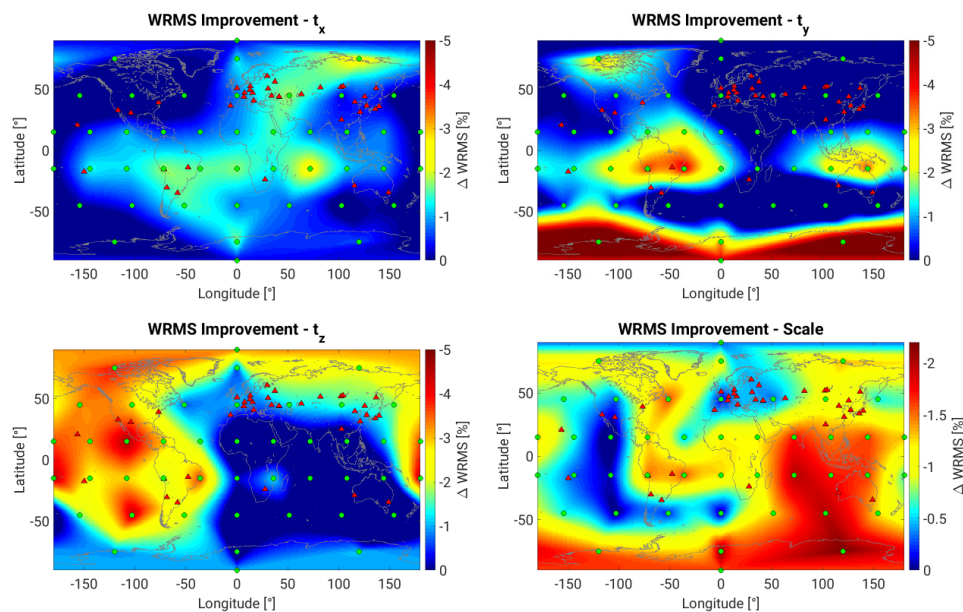


Figure 1.6: Improvement of the WRMS of estimated datum parameters by one additional station (for visualization a triangulation-based natural neighbor interpolation between grid points was applied).

SLR data management

DGFI(-TUM) has been operating the EUROLAS Data Center (EDC) since the foundation of the ILRS in 1998. It is one of worldwide two ILRS Data Centers (the second one is the Crustal Dynamics Data Information System, CDDIS, operated by NASA). The EDC, as an ILRS Operation Center (OC) and ILRS Data Center (DC), has to ensure the quality of submitted data sets by checking their format. Furthermore, a daily and hourly data exchange with the NASA OC and CDDIS is performed. All data sets and products are publicly available for the ILRS community via ftp (<ftp://edc.dgfi.tum.de>) and the dedicated website <http://edc.dgfi.tum.de>; see Section 4.6.

The EDC is running different mailing lists for the exchange of information, data and results. In 2019, 58243 Consolidated Prediction Format (CPF) files of 113 satellites were sent automatically to SLR stations. Besides, EDC distributed SLR-Mails (71 messages in 2019), SLR-Reports (1492 in 2019), SLR-Urgent (42 in 2019) and Rapid-Service-Mails (6 in 2019).

In 2019, 43 SLR stations observed 121 different satellites. There were 5 new satellite missions tracked by SLR stations, namely Astrocast-0.1, Astrocast-0.2, Glonass-139, Glonass-140 and Lightsail-2. ILRS stations, prediction providers and Analysis Centers were working on the implementation of the new format 2.0 for Consolidated Laser Ranging Data (CRD) and the Consolidated Prediction Format (CPF). This task shall be finished in December 2021.

1.3 Computation of Satellite Orbits

Observation-based attitude realization for Jason altimetry satellites

The altimetry satellite family Jason-1/-2/-3 has been providing continuous, precise measurements of the global and regional sea level since December 2001. The satellites have a non-spherical and complex shape, comprising two solar panel arrays and the main satellite body on which numerous measurement and positioning instruments are mounted. Precise investigation of the sea level and its changes requires the determination of satellite orbits at an accuracy level of sub-centimeters. Consequently, gravitational and non-gravitational perturbations need to be computed with high precision. Since the non-gravitational forces such as atmospheric drag, solar radiation pressure and Earth albedo depend on the satellite's effective cross-sectional area and the incidence angle of the perturbing force, the knowledge of the satellite's orientation in space is essential. Furthermore, the vector between the reference point of the tracking station and the spacecraft's center of mass is required. This vector depends on the position of the reference point of the tracking system mounted on the spacecraft which continuously changes its orientation with respect to the tracking station. These conditions require an accurate modeling of the satellite-body attitude and the solar panel orientation during the precise orbit determination (POD).

Attitude information for the satellites can be obtained in two ways: It can be modeled by a nominal yaw steering algorithm, or it can be determined from star tracking camera observations, for example in the form of quaternions, and rotation angles of the solar panels. The nominal yaw steering model consists of four regimes: sinusoidal and fixed yaw as well as the events ramp-up/ramp-down and yaw flip (Fig. 1.7).

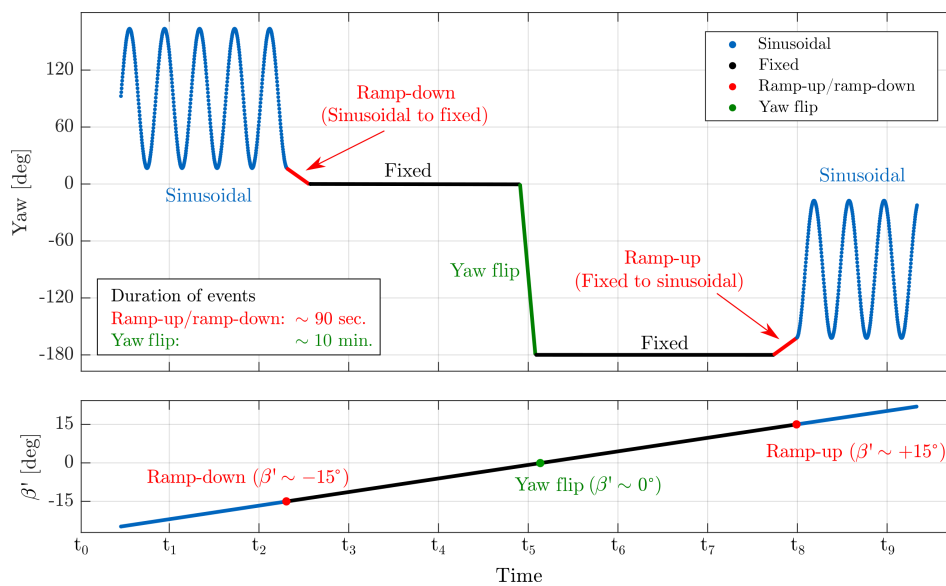


Figure 1.7: Principle of nominal yaw steering model for Jason satellites (top) depending on the angle (bottom); from Zeithöfler (2019).

DGFI-TUM has developed a preprocessing algorithm for satellite attitude information (attitude quaternions and solar panel rotation angles). It comprises a detailed analysis of the original data, detection and elimination of outliers, temporal resampling and the optimal interpolation of missing data. To accurately model the satellites' attitudes, a set of six parameters (four quaternion elements, two rotation angles) must be available at each epoch. As this requirement is not fulfilled in the original data, missing rotation angles are obtained by linear interpolation, missing quaternions are calculated using optimal spherical linear interpolation (Zeithöfler 2019).

Based on the analysis of SLR-only orbits of the Jason satellites over 25 years of operation, the benefit of using preprocessed observation-based attitude in contrast to a nominal yaw steering model for the POD was investigated by Bloßfeld et al. (2020). It was shown that using preprocessed observation-based attitude reduces (improves) the RMS of SLR observation residuals by 5.9% (Jason-1), 8.3% (Jason-2) and 4.5% (Jason-3). Parameters estimated within the orbit computation, e.g. the solar radiation scaling coefficient and empirical accelerations, are closer to the intended values for orbits with observed attitude. Furthermore, the station coordinate repeatability clearly improves at the draconitic period. Altimetry data analysis (see Section 2) indicates a clear improvement of the single-satellite crossover differences (6%, 15% and 16% reduction of the mean of absolute differences and 1.2%, 2.7% and 1.3% of their standard deviations for Jason-1/-2/-3 (Fig. 1.8) when using observation-based satellite attitude).

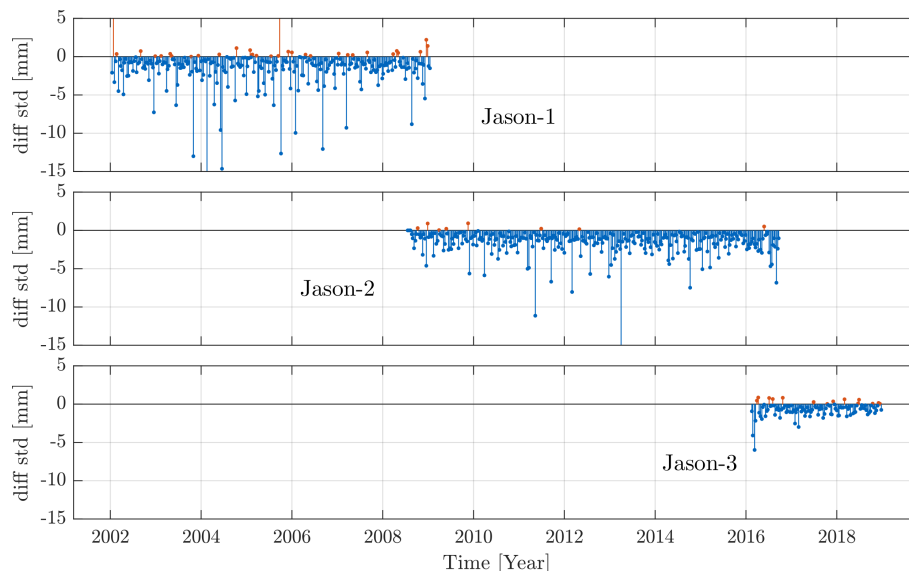


Figure 1.8: Single-satellite crossover differences (standard deviations per 10-day cycle) for the nominal orbit phases of the three Jason missions. Differences between the solutions using quaternion-based orbits and nominal orbits are shown. Negative differences mean improvements by observation-based attitude modeling (Bloßfeld et al. 2020).

Impact of TRF realizations on precise orbit determination (POD)

The precise orbit determination of Earth-orbiting satellites requires as an indispensable fundament an accurate terrestrial reference frame (TRF). The TRF provides the positions and motions of tracking stations from which the satellites are observed. In cooperation with the Deutsches Geoforschungszentrum Potsdam (GFZ), the DGFI-TUM investigated the impact of different TRF solutions on the quality of orbits of three altimetry satellites (TOPEX/Poseidon, Jason-1, and Jason-2) in the time interval from August 1992 to April 2015 and on altimetry products computed using these orbits (Rudenko et al., 2019). In particular, the International Terrestrial Reference Frame solutions ITRF2014 and its predecessor ITRF2008 have been compared. It was found that using ITRF2014 generally improves the orbit quality as compared

to using ITRF2008. The mean values of the RMS fits of SLR observations decreased (improved) by 2.4% and 8.8% for Jason-1 and Jason-2, respectively, but are almost not impacted for TOPEX/Poseidon when using ITRF2014 instead of ITRF2008. The internal orbit consistency in the radial direction (as derived from arc overlaps) is reduced (improved) by 6.6%, 2.3%, and 5.9% for TOPEX/Poseidon, Jason-1, and Jason-2, respectively. Single-satellite altimetry crossover analyses indicate reduction (improvement) in the absolute mean crossover differences by 0.2 mm (8.1%) for TOPEX, 0.4 mm (17.7%) for Jason-1, and 0.6 mm (30.9%) for Jason-2 with ITRF2014 instead of ITRF2008. The major improvement of the mean values of the RMS of crossover differences (0.13 mm; 0.3%) has been found for Jason-2. Multi-mission crossover analysis shows slight improvements in the standard deviations of radial errors: 0.1%, 0.2%, and 1.6% for TOPEX, Jason-1, and Jason-2, respectively. The standard deviations of geographically correlated mean Sea Surface Height (SSH) errors improved by 1.1% for Jason-1 and 5.4% for Jason-2 and degraded by 1.3% for TOPEX. The use of ITRF2014 instead of ITRF2008 causes changes in regional sea level trends of up to 0.4 mm/year between April 1993 and July 2008, and up to 1.0 mm/year between July 2008 and April 2015 (Figure 1.9).

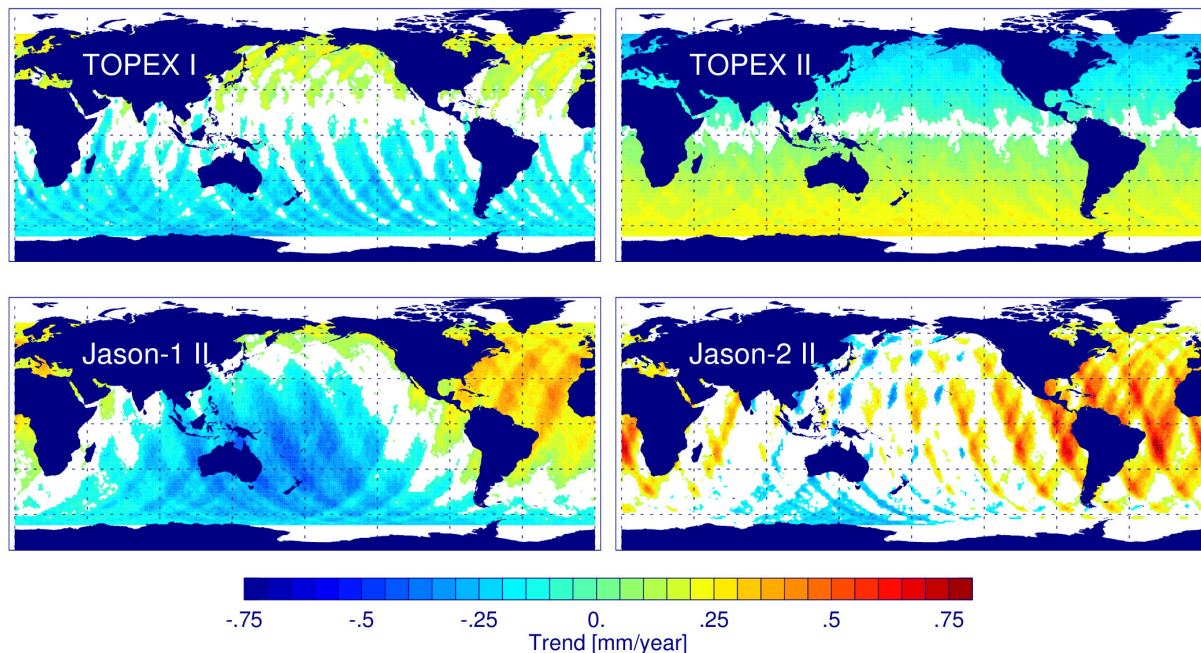


Figure 1.9: Impact of the use of ITRF2014 instead of ITRF2008 on the regional sea level trend for four periods. TOPEX I: April 1993–May 1997; TOPEX II: June 1997–September 2005; Jason-1 II: October 2007–February 2012; Jason-2 II: March 2012–April 2015. Regions with formal errors larger than the fitted value are masked out (white). From Rudenko et al., 2019.

Refined modeling of thermospheric density

DGFI-TUM performs studies to improve models of thermospheric density. The thermospheric density is, among others, an important information required to determine precise orbits of low Earth orbiting satellites, for mission planning, to predict satellite re-entries, and to avoid collisions of space objects. The investigations are predominantly based on the analysis of SLR observations to the spherical satellites ANDE-Pollux, ANDE-Castor and SpinSat. Resulting density information has been compared with results from different empirical and physical models at different altitudes. These investigations were part of the DFG **Project TIPOD** on which further details and results can be found in Section 3.1 (Research Topic Atmosphere).

1.4 Determination of Reference Frames

Analysis of DTRF2014 and preparation for DTRF2020

As one of worldwide three International Terrestrial Reference System (ITRS) Combination Centers of the International Earth Rotation and Reference Systems Service (IERS), DGFI-TUM is in charge of realizing the ITRS in regular intervals. DGFI-TUM's latest ITRS realization, the DTRF2014, was finalized and published in 2016. In the meantime, validations of DTRF2014, ITRF2014 (realization of IGN, France) and JTRF2014 (realization of NASA JPL, USA) have been performed by various groups. The results demonstrated the good performance of DTRF2014. In order to give a detailed description of the DTRF2014 solution together with a summary of the validation results, we prepared a comprehensive publication about the DTRF2014 (Seitz et al., in review).

The LOD (Length of Day) parameter series of the IVS contribution to the ITRS realizations 2014 are affected by a periodic signal of 13.65 days with a very significant amplitude of 0.029 ms w.r.t the reference series IERS 08 C04. The period seems to be related to the zonal lunar tide (M_f) with a period of 13.66 days. We performed detailed analyzes by inter-comparing the individual contributions of the IVS ACs to the combined IVS series and found that the LOD series of one of the ACs contained a signal of the same period and with an amplitude of 0.061 ms. Even though the combined DTRF2014 LOD series (with contributions from VLBI, GNSS and SLR) is not affected by the signal, in preparation of the ITRS realization 2020 systematic signals in the input series should be thoroughly investigated and removed in advance. This way, limitations of the accuracy of the ITRS realizations can be avoided.

The ITRS realizations 2020 will be based on solutions/normal equations of the four geodetic space techniques VLBI, SLR, GNSS and DORIS, which are reprocessed by applying new models and parametrizations (see also Sections 1.1, VLBI, and 1.2, SLR). Many of the changes will affect the scale, which is of particular importance in the case of SLR and VLBI as these techniques contribute substantially to the scale of the ITRS realizations 2020. The issue becomes even more important against the background of the critically discussed scale offset between SLR and VLBI as estimated in the ITRF2014 solution, which was not confirmed by DTRF2014 and JTRF2014.

DGFI-TUM contributes to both input series (SLR and VLBI) for the ITRS realizations 2020 through its operational (reprocessed) SLR and VLBI series, generated in the framework of the ILRS and IVS ACs operated by DGFI-TUM. In preparation for the DTRF2020, we started a detailed analysis of the different changes for the SLR and VLBI scales, extended by the analysis of GNSS data series provided by one of the IGS AC, and based on different GNSS systems (GPS, GLONASS, Galileo, Beidou). A major change in parametrization is planned by the ILRS: mean range biases will be determined for all satellites/stations and introduced in the SLR analysis. Figure 1.10 shows the SLR scale parameter time series of the DGFI-TUM solutions submitted to the ILRS for the computation of mean range biases. Range biases are set up for all stations/satellites. The scale differs on average by more than 7 mm from the DTRF2014 scale.

DTRF2014 was the first secular ITRS realization considering non-tidal loading corrections. We considered atmospheric and hydrological loading, while oceanic loading corrections were not available over the full time-span of DTRF2014. Recently, a detailed study on the application of different non-tidal loading models was performed for VLBI (see Section 1.1). It confirmed the strong reduction of the annual signal in the scale parameter time series found in the DTRF2014 analysis, when all components (or at least the hydrological component) of non-tidal loading are considered (Glomsda et al., in review).

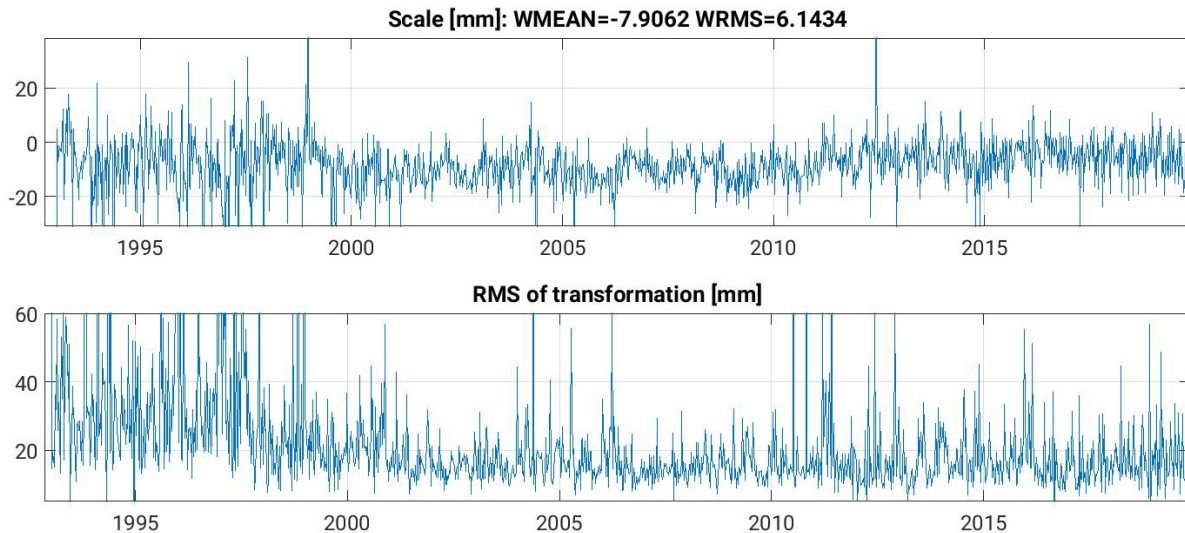


Figure 1.10: Scale differences of the DGFI-TUM SLR solution series w.r.t. DTRF2014 obtained from similarity transformations and the RMS of transformation. The SLR solutions include range biases for all stations/satellites and are submitted to the ILRS (solution “v230” in Tab. 1.3) for the computation of mean range biases, to be applied in the ILRS reprocessing for the ITRS realizations 2020.

Vertical reference systems

The International Association of Geodesy (IAG) released in July 2015 a resolution for the definition and realization of an International Height Reference System (IHRs). The IHRs is defined in terms of potential parameters: the vertical coordinates are geopotential numbers ($-W(P) = C(P) = W_0 - W(P)$) referring to an equipotential surface of the Earth's gravity field realized by the conventional value $W_0 = 62\,636\,853.4 \text{ m}^2/\text{s}^2$. The spatial reference of the position P for the potential $W(P) = W(X)$ is given by the ITRF coordinates X . At present, the main challenges are the establishment of the International Height Reference Frame (IHRF); i.e., a global reference network with precise geopotential numbers referring to the IHRs; and the preparation of required standards, conventions and procedures to ensure consistency between the definition (IHRs) and the realization (IHRF). DGFI-TUM supports this initiative by coordinating the GGOS Focus Area "Unified Height System", which defines and promotes the required international actions to establish the IHRF worldwide (Sánchez, 2019a). Regarding the IHRF reference network, DGFI-TUM proposed a preliminary station selection, which was distributed to regional and national experts to get advice about the availability of gravity data, and the addition of further geodetic sites to improve the density and distribution of the IHRF stations in their regions/countries. In April 2019, it was defined the first station selection and current actions are oriented to keep updated this network.

Regarding the computation of geopotential numbers as primary IHRs coordinates, we started an experiment focused on the estimation and comparison of (quasi-)geoid heights and potential values using the same input data and the own methodologies/software of colleagues involved in the gravity field modeling of high resolution. This experiment is based on (terrestrial and airborne) gravity data, terrain model and GNSS/levelling data made available by the US National Geodetic Survey (NGS) for an area of about 500 km x 800 km in Colorado, USA. Fourteen groups from thirteen countries participated in this experiment and delivered geoid and quasi-geoid models at a resolution of 11 for the complete area and geoid heights, height anomalies, and geopotential values at 223 benchmarks of the Geoid Slope Validation Survey 2017 (GSVS17). Figure 1.11 presents the comparison of the potential values delivered by the different groups. For the sake of facility, the potential values are converted to normal heights

after subtracting the reference potential W_0 from the point-wise potentials. The results show that twelve solutions agree within 1 cm to 2 cm in terms of standard deviation with respect to the mean value. These discrepancies only reflect the disagreement between the computation methods as the input data are assumed free of error and a proper error propagation analysis is not performed yet. However, it is evident that the discrepancies between the different solutions are highly correlated with the topography, suggesting further investigations on the handling of terrain gravity effects (model and strategy). Based on these outcomes, the next activities concentrate on generating a detailed document with standards for the determination of potential values; on investigating better strategies for the modeling of topographic effects, the determination of potential changes with time, and reliable approaches for the accuracy assessment.

The IHRS/IHRF activities are developed under a strong international cooperation promoted by the GGOS-JWG: Strategy for the IHRS realization (chaired by DGFI-TUM), IAG-SC2.2: Methodology for geoid and physical height systems, IAG-JWG2.2.2: The 1 cm geoid experiment, ICCT-JSG0.15: Regional geoid/quasi-geoid modeling - Theoretical framework for the sub-centimeter accuracy, and the International Gravity Field Service (IGFS).

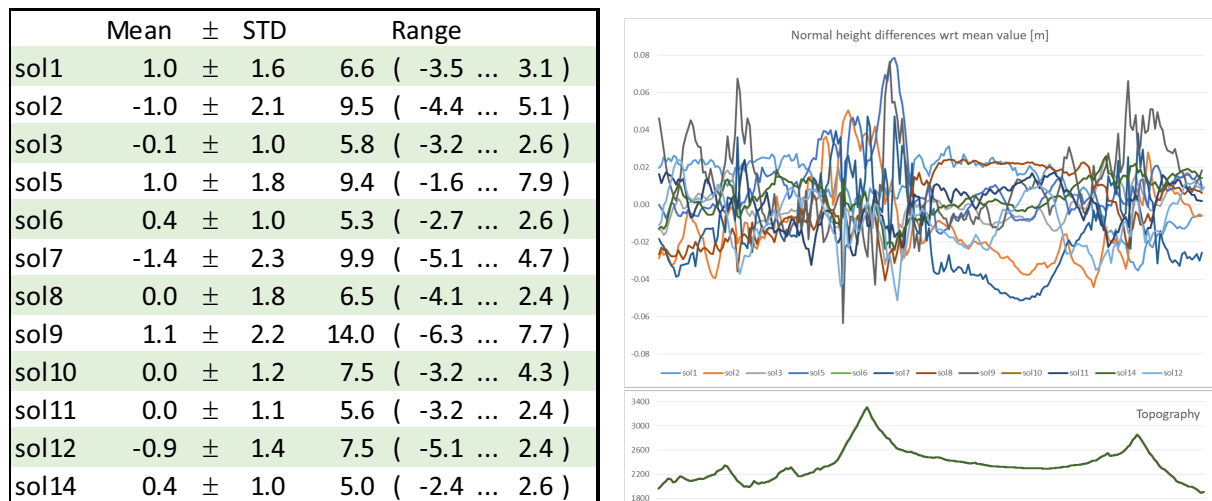


Figure 1.11: Comparison of potential values obtained by different methods for the regional gravity field modeling. The comparison is made in terms of normal heights.

Regional terrestrial reference frame in Latin America (SIRGAS)

SIRGAS (Sistema de Referencia Geocéntrico para las Américas) is the regional densification of the ITRF in Latin America. Currently, it is composed of about 400 continuously operating GNSS (GPS + GLONASS + GALILEO + BEIDOU) stations (Figure 1.12). 70 of these stations are included in the IGS global network, and some of them are used for the datum realization in the SIRGAS reference frame computation. The SIRGAS data processing strategy follows the IERS standards and the most-recent GNSS processing guidelines issued by the IGS. The only exception is that the GNSS satellite orbits and clock offsets as well as the Earth orientation parameters (EOPs) are not estimated within the SIRGAS processing, but fixed to the final weekly IGS values. The SIRGAS reference network is processed on a weekly basis to generate instantaneous weekly station positions aligned to the ITRF and multi-year (cumulative) reference frame solutions (Sánchez, 2019b). The instantaneous weekly positions are especially useful when strong earthquakes cause co-seismic displacements or strong relaxation motions at the SIRGAS stations disabling the use of previous coordinates. The multi-year solutions provide the most accurate and up-to-date SIRGAS station positions and velocities between two releases of the ITRF.

In Nov 2018, DGFI-TUM (as IGS RNAAC SIR) started the reprocessing of SIRGAS GNSS historical data from January 2000 to December 2019 using the IGS14 reference frame. This reprocessing includes not only SIRGAS regional stations, but also globally distributed IGS stations co-located with VLBI and SLR (Fig. 1.12). The main objective is to evaluate the reliability of the datum realization (origin, orientation, scale) in the regional network. The idea is to define the geodetic datum of the regional network by combining GNSS with SLR and VLBI normal equations and to compare the station coordinates with the GNSS-only frame computations (see project DIGERATI, below). In this frame, different scenarios were evaluated. The first one considered only those GNSS sites co-located with SLR and VLBI (blue circles and green dots in Fig. 1.12). As most of these stations are located in the northern hemisphere, this station distribution was not optimal for the GNSS data processing, especially when EOPs and GNSS satellite orbits have to be computed. Consequently, we had to introduce additional GNSS sites to ensure a homogeneous global distribution of the network as far as possible, also in view of the fact that the orientation of the combined reference frame should be realized via a NNR condition over a global subset of GNSS sites. After many empirical experiments, our main conclusion is to include the core stations of the IGS reference frame in the GNSS data processing.

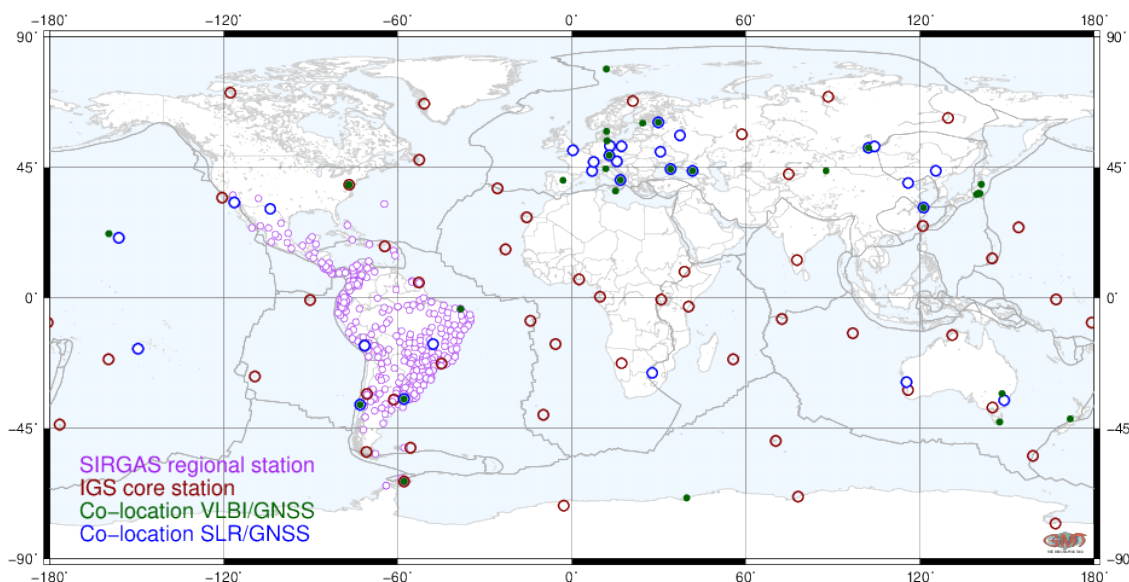


Figure 1.12: GNSS network configuration for the combination of GNSS, SLR and VLBI normal equations in the realization of a global geodetic datum in a regional reference frame. VLBI/GNSS (green dots) and SLR/GNSS (blue circles) co-located stations are necessary for the normal equation combination. IGS core stations (red circles) are necessary for a high-quality GNSS data processing.

A further research topic concentrated on the simultaneous determination of GNSS satellite orbits, satellite clock offsets, EOPs and station positions within the GNSS data processing. Although we use a global network in the computations, including all the SIRGAS regional stations reduces the reliability of the EOPs and GNSS orbits due to the dense station distribution in one particular region (see Fig. 1.12). Our recommendation is to follow a two-step procedure: (a) orbit and EOP determination based on a global network, and (b) processing of the GNSS data fixing the previous determined orbits and EOPs. As this procedure is currently applied in the computation of regional reference frames, we conclude that the SIRGAS computations, even though with a global station distribution, can continue be based on the IGS final products. Important is that the datum parameters given to GNSS normal equations by fixing the GNSS orbits and the EOPs are removed before the combination with the SLR and VLBI normal equations.

Determination of epoch regional geocentric reference frames

To explore the possibility of computing a regional geocentric reference frame (RGRF) epoch-wise and directly, i.e. without the usual transformation onto a global reference frame is the main objective of the DFG-funded **Project DIGERATI** (Direct Geocentric Realization of the American Reference Frame by Combination of Geodetic Observation Techniques). The epoch RGRF shall be computed by combining GNSS with the geodetic techniques SLR and VLBI using a minimum network configuration on a weekly basis. The origin of the epoch solutions should be realized by SLR only, whereas the scale is realized by a weighted mean of SLR and VLBI. Since an epoch-wise realization entails a variable SLR network configuration from epoch to epoch, one central aspect of the project is to investigate the effect of the variable station network on a stable datum realization.

In our analyses, the datum is realized directly by a combination of SLR (origin realized by SLR only), VLBI (contributing to the scale, together with SLR), and GNSS (orientation realized via NNR condition over a global selection of stations). The combination of the different techniques is performed at normal equation (NEQ) level, as this is the most flexible but - given harmonized geophysical background models - also a rigorous approach for the combination. The input data are IGS14-based NEQs from GNSS (see SIRGAS, above), SLR (re-processed datum-free weekly NEQs from ILRS standard processing with DOGS-OC) and VLBI (session-wise datum-free NEQs from IVS standard processing with DOGS-RI). As orbits are fixed in the GNSS processing, datum-free GNSS NEQs are reconstructed by introducing and reducing seven Helmert parameters as a first step. The combination is performed by introducing local ties (LTs) at co-location sites as weighted condition equations. Based on the LT table generated for the DTRF2014, the local ties are selected and weighted by comparing the weekly coordinate differences of the single-technique solutions to the measured LT.

Figure 1.13 shows the translation of the SLR-only solution (left) and of the technique-specific sub-networks of the combined solution with respect to ITRF2014 (weekly coordinates, post-seismic deformation applied). A seasonal variation at sub-cm level (amplitude 0.8 cm) reveals

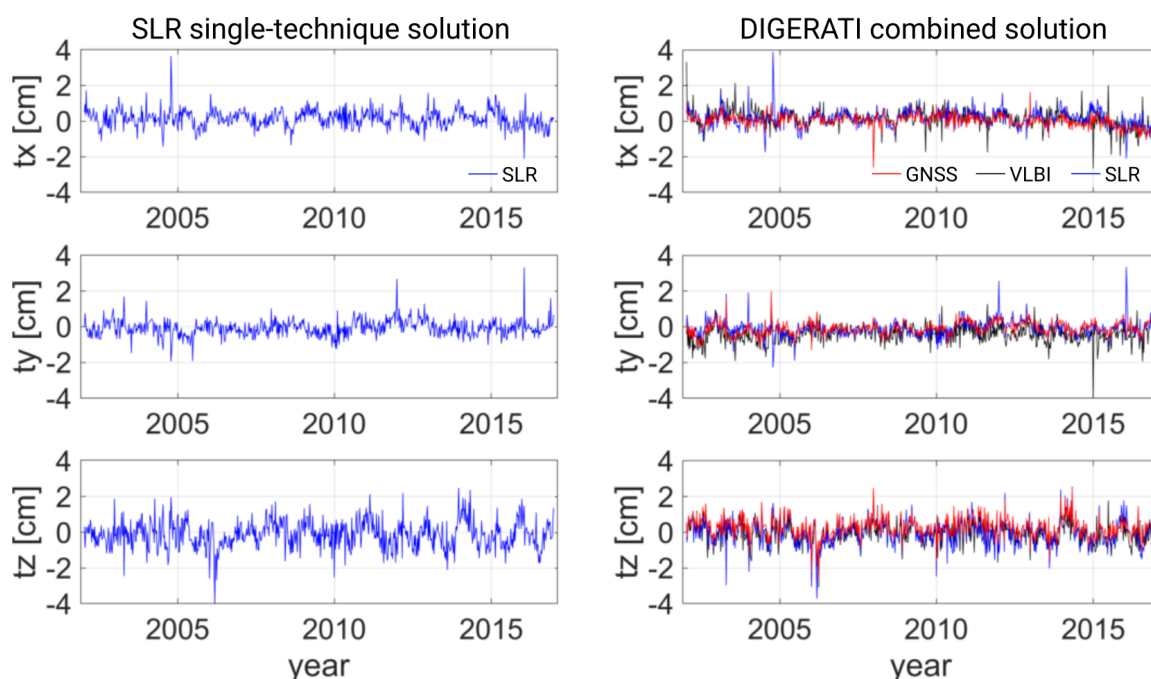


Figure 1.13: Translations of the SLR single-technique solution (left) and the technique-specific sub-networks of the combined solution (right) w.r.t. ITRF2014.

the variation of the origin of ITRF2014 with its, in general, linear station velocities with respect to the actual geocenter, which is better represented by the DIGNET epoch RGRF. The good agreement between the SLR-only and the combined solution confirms a good datum transfer. As the sub-networks of the combined solution have been transformed separately, it is obvious that the datum transfer between the techniques is successful.

Figures 1.14, 1.15 and 1.16 show the translations, the scale and the rotations between the SIRGAS regional operational solution (old solutions transformed to IGS14) and the DIGNET epoch RGRF. The translations agree well. The seasonal variations in the x- and y-translations are reduced due to the fact that the variations of the stations coincide with those in the DIGNET RGRF. However, an offset and a seasonal variation are visible in the z-translation. The offset confirms that the origin of the SIRGAS regional operational solution does not coincide with the geocenter since 90% of the stations of the network are located in the southern hemisphere. The seasonal variation in z can be related to seasonal variations in the Amazon basin, leading to the conclusion that the datum of the current SIRGAS operational solution is affected by the instability of its datum stations. Consequently, the complete reference frame performs a periodic North-South displacement. The large translations and rotations in 2002 occur as a sufficient number of reliable IGS stations is lacking. After 2010 the agreement improves due to an extension of the SIRGAS network to a larger area with more fiducial points, enabling an improved datum definition of the network. Jumps in the scale time series are caused by a change of the modeling of antenna phase center variations between ITRF realizations.

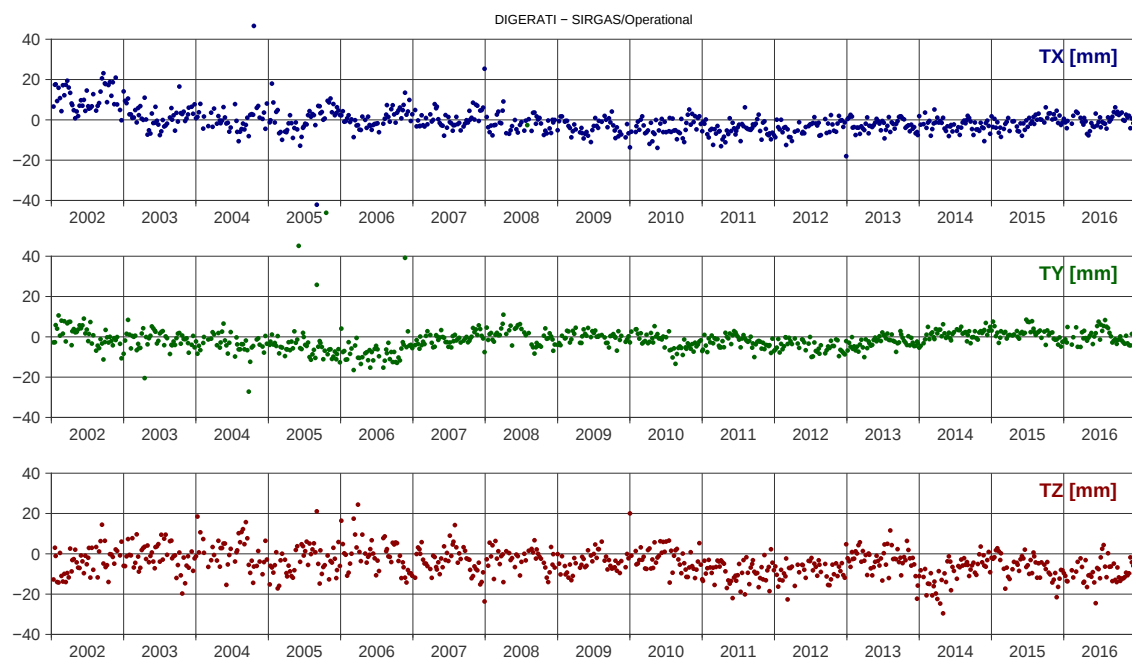


Figure 1.14: Translations between the DIGNET and the SIRGAS regional operational solution.

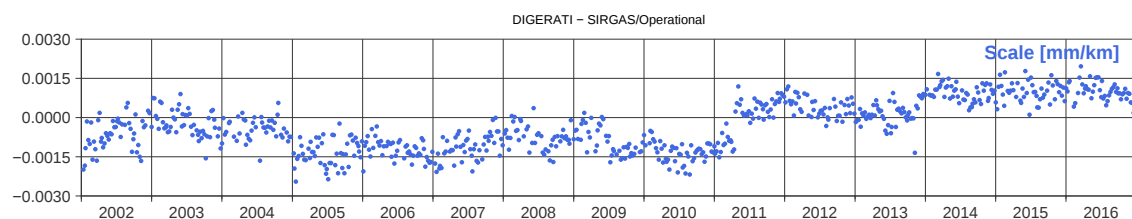


Figure 1.15: Scale difference between the DIGNET and the SIRGAS regional operational solutions.

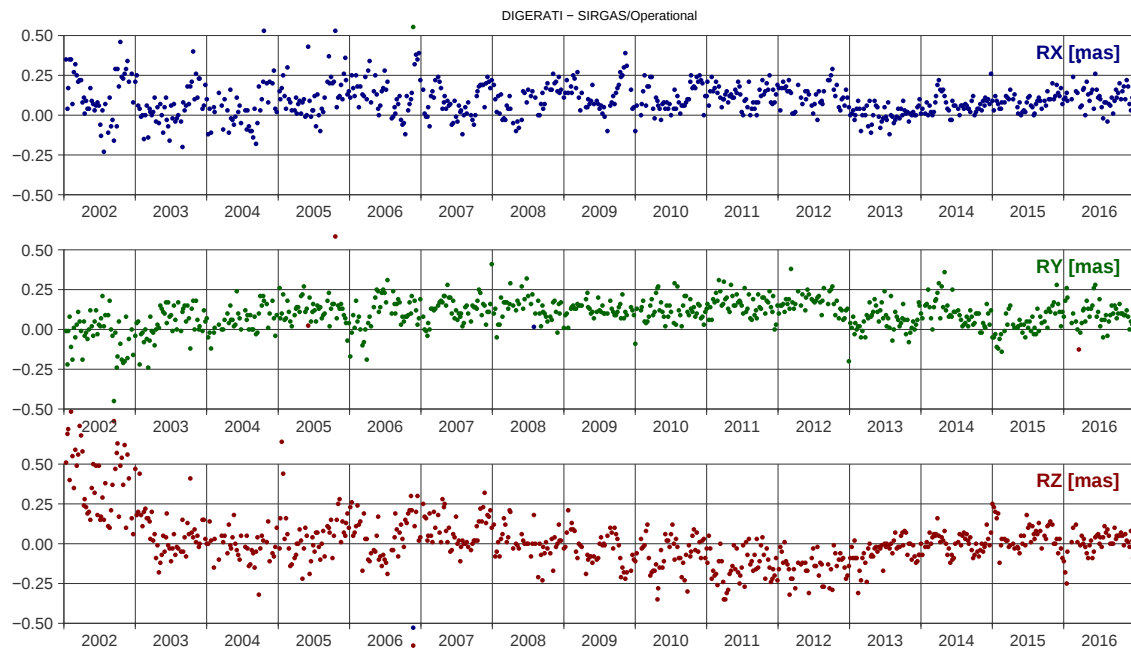


Figure 1.16: Rotations between the DIGERATI and the SIRGAS regional operational solutions.

Independent generation of Earth orientation parameters

The ESA project Independent Generation of Earth Orientation Parameters (**ESA-EOP**) aims at the development of a high-level EOP combination approach and its implementation in a respective software. EOPs are fundamental parameters for the description of the orientation between the terrestrial and the celestial reference frame as well as for the realization of precise time systems. DGFI-TUM is leading the project which includes partners from the TUM (Chair of Satellite Geodesy), the Bundesamt für Kartographie und Geodäsie (BKG), the Deutsches Geoforschungszentrum Potsdam (GFZ), and the TU Vienna.

The EOP combination of VLBI, SLR, GNSS and DORIS data is realized at the NEQ level. The approach has been chosen as it is the most flexible approach w.r.t. the source of the input data (as technique-specific contributions can be provided by different software packages), but still equivalent to a rigorous combination at observation level, given that common background models and parametrizations are used. In addition to the software development, the project includes the homogeneous setup of input normal equations of the four geodetic space techniques.

The combination shall result in consistent and highly accurate time series of Earth Rotation Parameters (ERPs; a subset of the EOPs), covering the time span from several years into the past until 90 days into the future. The combination shall run on an operational (e.g., daily) basis. Thereby, a special focus is put on the continuity of the final ERPs (about three weeks latency), the rapid ERPs (few hours latency) and the predicted ERPs (up to 90 days into the future). During the year 2019 the optimal processing and combination strategy was explored and defined. The scheme is displayed in Fig. 1.17.

Final ERP are combined using session-wise, daily or weekly NEQs of VLBI, GNSS, SLR, and DORIS. Rapid ERP are obtained from a combination of GNSS Rapid NEQs and VLBI-Intensive NEQs (daily 1-hour sessions); see Hellmers et al., 2019. In contrast to estimated ERPs based on geodetic observations, the predicted ERPs are based on effective angular momentum series obtained from geophysical model data by GFZ (right column in Fig. 1.17). Moreover, the ERP predictions follow deterministic signals obtained from the estimated final ERP series and start with the most recent ERP estimates obtained from the estimated rapid ERP series.

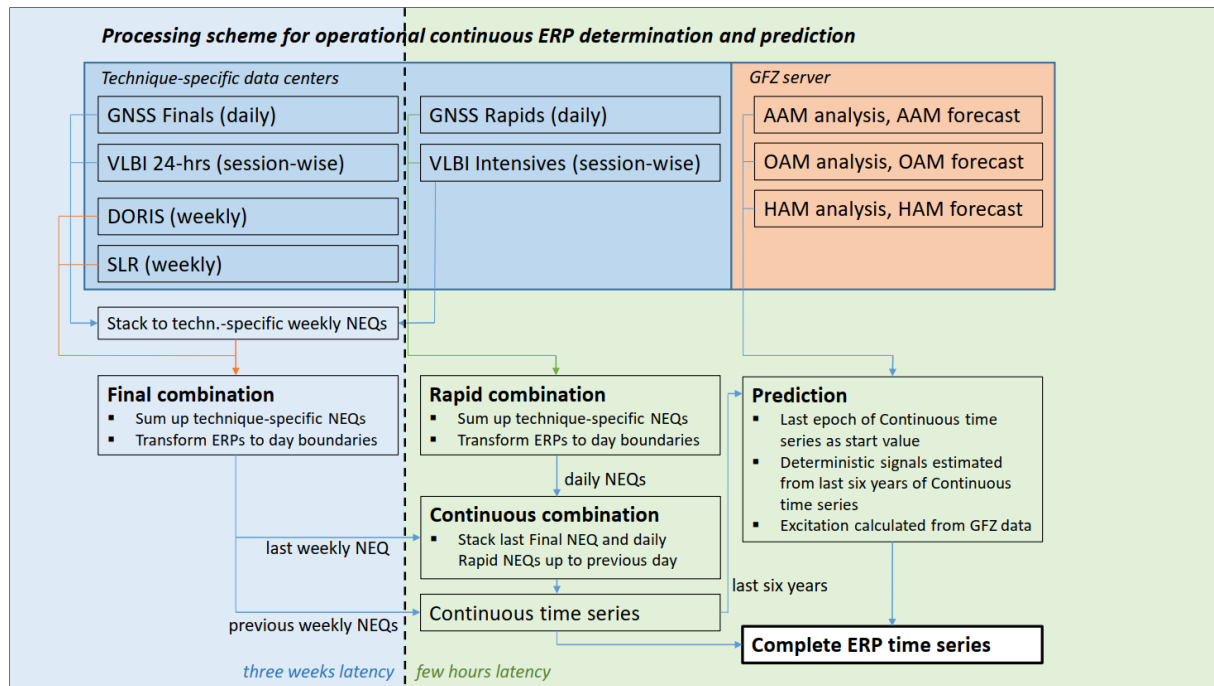


Figure 1.17: Realized processing scheme of the ERP estimation and prediction in the framework of the project ESA-EOP.

Fig. 1.18 shows the resulting continuous ERP time series covering past, present and future epochs (solutions from second half of 2019). The obtained time series is provided for further use in the same format as the standard IERS C04 EOP series.

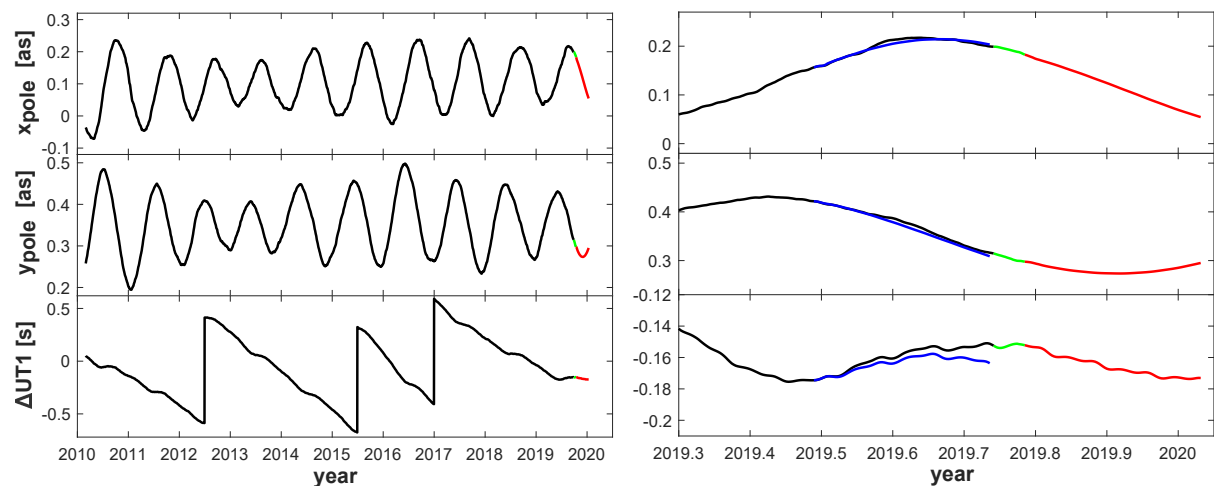


Figure 1.18: Left: full estimated ERP time series. Black: final combination; green: rapid combination part of continuous combination; red: prediction. Right: zoom at the end of the final-rapid-predicted time series shown above. Blue: Additional prediction based on final solution as can be used for internal validation of the prediction against the final combination, omitting the reduced quality of the rapid combination part of the continuous combination.

Mass transports in the cryosphere and their impact on Earth rotation

The determination of cryospheric mass changes (ice melting) and their impact on Earth rotation is the goal of the DFG **Project CIEROT**. Mass changes in the cryosphere are determined from GRACE (Gravity Recovery and Climate Experiment) satellite gravity field observations. These are transformed into changes of angular momentum which are related to polar motion excitation functions. The analysis of GRACE data requires the treatment of erroneous meridional stripes present in the observation data. Different filtering methods have been developed to reduce these disturbing signals, but they also attenuate the measurement signal and induces leakage effects.

A novel approach developed at DGF-TUM now allows for the reduction of these filter effects (attenuation and leakage) in polar motion excitation functions derived from GRACE mass variations (Göttl et al., 2019). It is independent from geophysical model information, works on global grid point scale and can thus be used for mass variation estimates of different subsystems of the Earth. Gain factors k for each grid point are determined from once and twice filtered GRACE equivalent water height values. Analysis of the results revealed, that the uncertainties of the GRACE-derived polar motion excitation functions can be reduced from 12-48% to 8-38%. Simulation studies have shown that the gain factors are a good approximation, but they are damped due to the filtering process. In order to counteract this phenomenon, scaling factors were introduced, derived from the ratio between original and filtered gain factors. Uncertainties could further be reduced to 5-29%. The largest improvement can be seen for the GRACE-derived polar motion excitation functions of the oceans (19 percentage points), followed by Greenland (7 percentage points), Antarctica (4 percentage points) and the continental hydrosphere (3 percentage points); see Fig. 1.19.

The approach was applied for the reduction of filter effects to the GRACE gravity field solutions GFZ RL06 and CSR RL06. Figure 1.20 shows that the agreement with the GRACE mascon solution CSR RL06M could be significantly improved, especially in Antarctica and Greenland (9 and 11 percentage points). Furthermore, comparisons with model-based oceanic excitations reveal that the accordance can be improved by up to 15 percentage points.

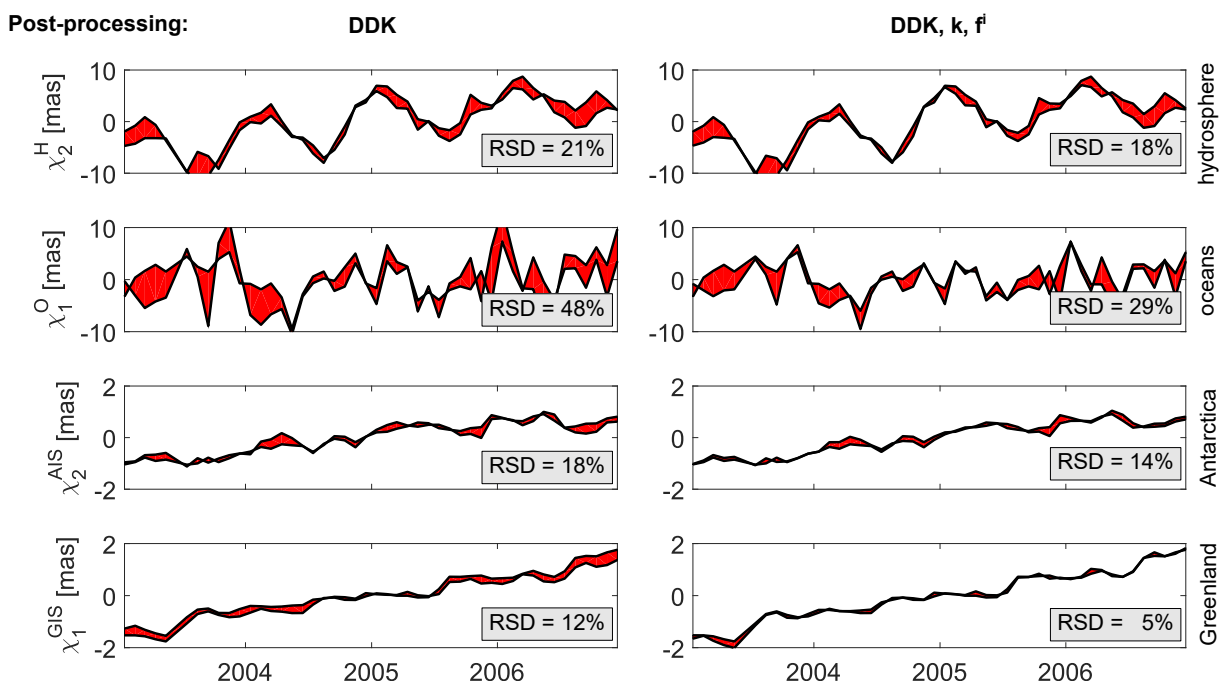


Figure 1.19: Comparison of GRACE-derived polar motion excitations: Original versus filtered time series

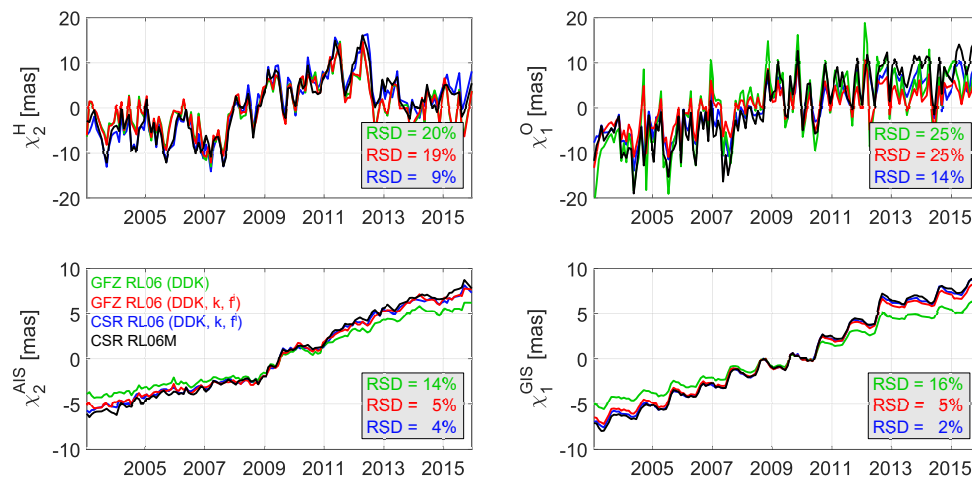


Figure 1.20: Validation of the developed approach with the GRACE mascon solution CSR RL06M

Related publications

- Bloßfeld M., Zeitlhöfler J., Rudenko S., Dettmering, D.: *Observation-based attitude realization for accurate Jason satellite orbits and its impact on geodetic and altimetry results*. Remote Sensing, 12(4), 682, doi:[10.3390/rs12040682](https://doi.org/10.3390/rs12040682), 2020
- Göttl F., Murböck M., Schmidt M., Seitz F.: *Reducing filter effects in GRACE-derived polar motion excitations*. Earth, Planets and Space, 71(117), doi:[10.1186/s40623-019-1101-z](https://doi.org/10.1186/s40623-019-1101-z), 2019
- Glomsda M., Bloßfeld M., Seitz M., Seitz F.: *Mitigating systematic effects in VLBI analysis by various applications of non-tidal loading*. Journal of Geodesy, 2020 (in review)
- Hellmers H., Thaller D., Bloßfeld M., Kehm A., Girdiuk A.: *Combination of VLBI Intensive Sessions with GNSS for generating Low latency Earth Rotation Parameters*. Advances in Geosciences, 50, 49–56, doi:[10.5194/adgeo-50-49-2019](https://doi.org/10.5194/adgeo-50-49-2019), 2019
- Kehm A., Bloßfeld M., König P., Seitz F.: *Future TRFs and GGOS – where to put the next SLR station?* Advances in Geosciences, 50, 17–25, doi:[10.5194/adgeo-50-17-2019](https://doi.org/10.5194/adgeo-50-17-2019), 2019
- Rudenko S., Esselborn S., Schöne T., Dettmering D.: *Impact of terrestrial reference frame realizations on altimetry satellite orbit quality and global and regional sea level trends: a switch from ITRF2008 to ITRF2014*. Solid Earth, 10(1), 293-305, doi:[10.5194/se-10-293-2019](https://doi.org/10.5194/se-10-293-2019), 2019
- Sánchez L.: *Report of the GGOS Focus Area Unified Height System and the Joint Working Group 0.1.2: Strategy for the Realization of the International Height Reference System (IHR)*. Reports 2015-2019 of the International Association of Geodesy, Travaux de l'AIG 41, Global Geodetic Observing System (GGOS), 42-51, 2019a
- Sánchez L.: *SIRGAS Regional Network Associate Analysis Centre Technical Report 2018*. In: Villiger A., Dach R. (Eds.), International GNSS Service Technical Report 2018 (IGS Annual Report), 109-125, doi:[10.7892/boris.130408](https://doi.org/10.7892/boris.130408), 2019b
- Seitz M., Bloßfeld M., Angermann D., Gerstl M., Seitz F.: *DTRF2014: The first secular ITRS realization considering non-tidal station loading*. Journal of Geodesy, 2020 (in review)
- Zeitlhöfler, J.: *Nominal and Observation-Based Attitude Realization for Precise Orbit Determination of the Jason Satellites*. Master Thesis, Technical University of Munich. Available online: https://mediatum.ub.tum.de/1535892?show_id=1535899, 2019

2 Research Area Satellite Altimetry

Satellite altimetry was originally designed in the late 1960s to provide information on the dynamic topography of the sea surface at an accuracy level of 10 cm for wavelengths of the order of 100 km or larger¹. Today, the technique can be applied for mapping much finer structures, not only in the open ocean but also in coastal regions and of inland waters. In addition, precision and accuracy are steadily increasing.

DGFI-TUM is working on advanced methods to further improve the quality and applicability of satellite altimetry observations for various phenomena in ocean and continental hydrosphere. The exact determination of the geometrical shape of the water surface in space and time, and the investigation of its temporal changes in terms of underlying dynamic processes in both components of the Earth's global water cycle is one of DGFI-TUM's primary research goals.

The prerequisite for these kinds of investigations is a large database of the complete observation record of all altimetry missions that have been launched until today. Whenever possible, we apply a multi-mission approach by combining all available missions after careful harmonization and cross-calibration (Section 2.1). Over the oceans (Section 2.2), we are working on sea level variability in different regions with special focus on coastal waters and sea-ice regions. In addition, we are focusing on surface currents, ocean tides, as well as sea state and its temporal evolution. In close cooperation with our Research Area Reference Systems, we are studying advanced methods to estimate coastal vertical land motion from a combination of altimetry data with tide gauge measurements. Over the continents (Section 2.3.), we are working on the automated estimation of improved water level time series for rivers, lakes, and reservoirs. Moreover, by combining the height information with additional remote sensing data (such as optical images), derived products relevant for hydrological applications are created, i.e. storage changes of lakes and river discharge.

2.1 Multi-Mission Analysis

To combine different altimetry missions with various sampling characteristics and measurement periods, and to enable long-term high-resolution applications, a cross-calibration is mandatory. This accounts for systematic differences between the missions, such as inter-mission biases, instrumental drifts, and different orbit realizations. In addition, cross-calibration is able to provide information on the quality of single missions and to reveal, e.g., instrument drifts or geographically correlated orbit errors.

DGFI-TUM performs a global multi-mission crossover analysis (MMXO)² on a regular basis. In our approach, the cross-calibration is realized globally by minimizing a large set of single- and dual-satellite sea surface height (SSH) crossover differences computed between all contemporaneous altimeter systems. In addition to the crossover differences, along-track consecutive differences of single missions are minimized to ensure smooth radial errors without the need to adjust a pre-defined analytical function. Iterative variance component estimation is applied to obtain an objective relative weighting between altimeter systems with different performances.

¹Kaula, W.M. (Ed.): The Terrestrial Environment: Solid-Earth and Ocean Physics (Williamstown 1968 Report). NASA CR-1579.

²Bosch W., Dettmering D., Schwatke C.: Multi-mission cross-calibration of satellite altimeters: constructing a long-term data record for global and regional sea level change studies. Remote Sensing 6(3): 2255-2281, doi: [10.3390/rs6032255](https://doi.org/10.3390/rs6032255), 2014

The analysis yields time series of radial errors of each mission and can be used to derive inter-mission biases, to identify potential altimeter drifts, as well as to extract information on the quality of precise orbit determination (POD; see Section 1.3) and geophysical corrections (e.g., wet tropospheric errors).

Systematic differences between Sentinel-3A and Jason-3

The MMXO reveals systematic differences between the missions Sentinel-3A and Jason-3. As reported last year, both missions show differences in global mean sea level trends of about 4 mm per year (Dettmering and Schwatke, 2019). This has been confirmed by analyzing a longer dataset of 3.5 years. However, with the start of a new processing baseline in 2018, the trend differences decrease to about 1 mm per year. Part of this behavior has been identified as resulting from a drift in the point target response width. Another likely cause is the sea state bias correction that is not yet tuned for SAR (Synthetic Aperture Radar). In addition to the temporal inconsistencies, significant differences in geographically correlated errors of up to 1 cm can be seen (Fig. 2.1). A similar pattern is visible for PLRM (Pseudo Low Resolution Mode) data. Since the end of January 2020 a reprocessed Sentinel-3 dataset is available (BC0004) with the expectation to improve the consistency between the two missions.

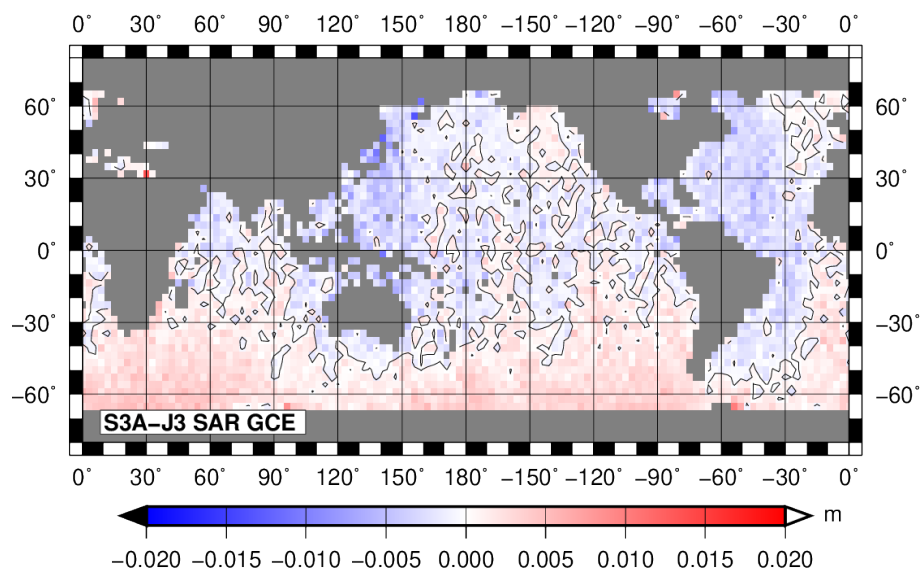


Figure 2.1: Differences in geographically correlated errors between Sentinel-3A SAR and Jason-3.

Impact of different satellite orbit solutions on sea level products

The cross-calibration has been used to investigate the impact of different orbit solutions on the sea level products. We studied the impact of switching from orbits related to ITRF2008 to orbits related to ITRF2014 for the three altimetry missions TOPEX, Jason-1 and Jason-2 (Rudenko et al., 2019). In general, the newer reference frame solution improved the orbit quality. Single-satellite absolute mean crossover differences are reduced by 8% for TOPEX, 18% for Jason-1 and 31% for Jason-2. When looking at the relative differences of the standard deviation of the radial errors (as estimated by the MMXO), one can clearly see the impact of extrapolating the ITRF2008 coordinates to later years (Fig. 2.2). The change from ITRF2008 to ITRF2014 has only minor effects on the estimation of the regional and global sea level trends on decadal time scales. However, on shorter timescales (3-8 years), large-scale coherent trend patterns can be observed.

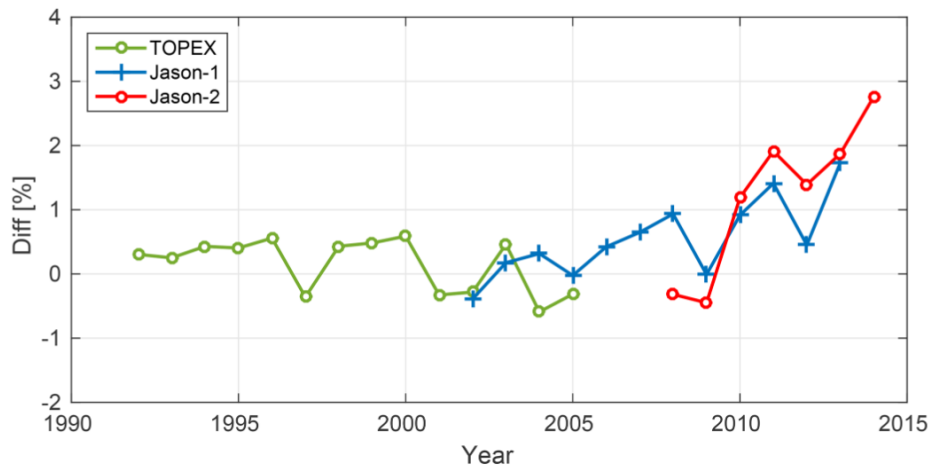


Figure 2.2: Relative differences of the standard deviations of radial errors per year (Rudenko et al., 2019). Positive values indicate improvements of orbits due to the change from ITRF2008 to ITRF2014.

2.2 Sea Surface

Arctic sea level

Global sea level is rising due to the combined impact of various effects related to climate change. In particular, the two most relevant factors are (1) the increasing average temperature of the ocean and the related expansion of water volume (so-called thermosteric effect) and (2) the additional water inflow due to glacier melting. While the average global sea level rise is a strong indicator of climate change, the sea level trend varies strongly depending on the regions of the global ocean. These regional discrepancies are mainly due to the fact that water masses constantly circulate and that ocean currents can be influenced, for example, by changes in the wind patterns (direction and strength of the wind) that force the ocean surface currents.

Sea level has been monitored along the coasts for more than one hundred years using in-situ stations (gauges). Since about 25 years, satellite altimetry allows for the monitoring of the global sea level. However, the monitoring of the ocean in high latitudes is highly challenging (Quartly et al., 2019a): First, not all of the satellites reach those regions due to their orbit characteristics; Furthermore, the presence of seasonal and permanent sea ice coverage hinders the retrieval of the water level as the radar pulses do not hit the ocean surface that is hidden below the ice. This lack of knowledge has to be tackled, since the Arctic Ocean is a hotspot of climate change impact, due to the enormous masses of rapidly melting land ice and the quickly disappearing sea ice, which can also cause changes to the global circulation that could influence the climate much beyond this region.

The European Space Agency (ESA), within its Climate Change Initiative (CCI), finances a study on the Sea Level (SL). The **Project SL-CCI** now resulted in the most comprehensive and accurate record of sea level change in the Arctic Ocean using all missions data available between 1996-2018 (Rose et al., 2019). The complete observation data has been re-processed using the latest methodologies, thus resulting in improved consistency. The most important innovations include a special treatment of sea level signals retrieved from openings and cracks in the sea ice (so-called leads), in order to extend the records to areas that are often not considered in the analysis. But as the respective satellite signals are highly distorted due to false reflections from surrounding sea ice, these signals have to be recognized, carefully analyzed and finally harmonized with the other signals coming from ice-free areas.

In collaboration with colleagues from the Technical University of Denmark (DTU), we have analyzed the dataset and found a mean sea level rise of 2.22 mm/yr for the Arctic Ocean between January 1996 and September 2018 with a 95% confidence interval from 1.67 to 2.54 mm/yr. Very strong differences were found for different sectors of the Arctic Ocean:

1. The sector with the largest trend across the whole period of study is the Beaufort Gyre region, located between Greenland and Alaska (5.8 mm/yr with confidence interval 4.1-6.4 mm/yr). The large trend is due to increasing fresh water accumulation caused by wind-driven water transport whose effect is increased by the thinning of the sea-ice layer.
2. Along the Greenland coast, the sea level trend is negative, i.e. the water stage is getting lower over time. This effect results from the melting of the Greenland ice sheet. As the ice is melting, its mass is decreasing - and along with the mass also its gravitational attraction to the sea water. As the powerful gravitational force that pulls the water towards Greenland is getting lower, the sea water is flowing away from Greenland.

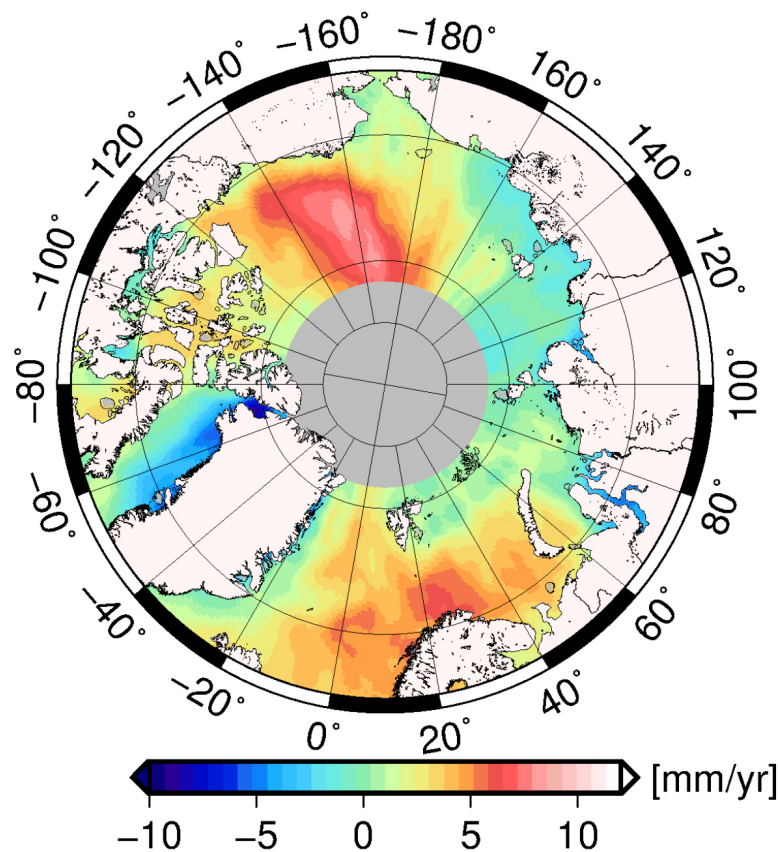


Figure 2.3: Trends of sea level in the Arctic Ocean from the DTU/TUM gridded sea level product at high latitudes. The map illustrates that the average change in the Arctic sea level varies regionally (Rose et al., 2019).

The results are supported by a good agreement with local sea level trends registered by the (very sparse) network of in-situ stations in the area. Other studies based on altimetry data obtained similar results for specific periods and regions over shorter time scales. New in our study is the very long time span over which the changes of the sea level have been computed which also allows for analyzing changes of the trend over time. Through the improved consistency, the re-processing of all available data, the incorporation of new satellites and the application of dedicated algorithms to analyze sea level changes including ice-covered regions, we obtained the most comprehensive and accurate data set that is currently available.

While uncertainties in the area remain higher than in the rest of the global ocean due to the data coverage and quality of data, especially where sea ice is still present, this study presents clear observational evidence of how climate-change related phenomena, such as disappearing sea-ice and glacier melting, have affected the sea level in the region.

Global coastal sea level

Within the ESA Sea Level Climate Change Initiative **SL-CCI** framework, research activities concerning coastal sea level are on-going. Efforts during 2019 have been focused on the creation of the first Sea Level CCI product to be tailored for coastal as well as open ocean sea level analysis, currently available in Eastern Africa, Mediterranean Sea and North East Atlantic Ocean (<http://www.esa-sealevel-cci.org/products>).

A dedicated analysis performed in the tracks along Eastern Africa has revealed interesting insights (Marti et al., 2019). Over the Jason-1 and Jason-2 period (2002-2016), estimated trends along the Jason tracks show gradients of trend from offshore to the coastline, which have been proved not to be caused either by errors in the fitting of the signal or by trends contained in the geophysical corrections. In most instances, the trends are roughly constant from 15 km to about 5 km to the coast, then change when approaching the coast. At some locations, a slight trend decrease is observed within the 0-4 km band followed by a sharp trend increase when approaching the coast. Such a behavior could be associated to coastal processes that were not visible with former altimetry products. This could be the result of wind-induced setup, river freshwater runoff, and wave forcing on shallow shelves. At embedded coasts and estuaries and shallow areas, cross-shore winds can drive important surge, such as observed off Senegal over the wide shelf during winter upwelling.

Only two tracks show a trend decrease within the 0-5 km to the coast. This is particularly clear on a track crossing the coast close to the Niger River estuary. Large river fresh water plumes can also change water density and affect coastal sea level. Influence of the river plume could be at the origin of the observed behavior. Indeed, the reflectance ratio derived by MODIS images, considered as a proxy of river discharge, showed similar trend with respect to the sea level anomaly observed by altimetry close to the mouth of the river itself.

Among the 24 Jason track portions covering the study region, 19 tracks allow estimating trends as close as 2-3 km to the coast. For three of them, distances of 1 km or less are reached. Such new data will allow investigating small-scale processes occurring in the coastal zone (Benveniste et al., 2019). This represents a real progress compared to what is available with standard sea level products and the first attempt to observe sea level trends by remote sensing at such a close distance to the coast.

Baltic Sea

The Baltic Sea, a semi-enclosed peripheral sea with depths up to 200 meters, features two conditions that severely limit the use of satellite altimetry in high latitude and coastal regions: the presence of seasonal sea ice coverage, and the proximity of the coast. New technological improvements (such as the advent of Delay-Doppler altimetry), improved signal processing (retracking), and advances in sea-ice classification methods and geophysical corrections (wet tropospheric correction, sea state bias), have pushed the exploitation of altimetry observations at the regional scale. These advances can be, therefore, exploited to improve product quality and applicability, particularly to high latitude and coastal regions.

In 2019, ESA started the wider Baltic region activity *Baltic+* looking at sea level, salinity dynamics, sea-land biogeochemical linkages, and height system unification. The initiative constitutes a coordinated approach to advance Earth-observation based science, novel applications and data exploitation infrastructures serving the specific needs of the Baltic community. The DGFI-TUM is involved in two of the *Baltic+* studies: It is leading the **Project Baltic+ SEAL** on the Baltic Sea Level (<http://balticseal.eu/>) (see below), and it is cooperation partner in the **Project Baltic+ SAR-HSU** (Geodetic SAR for Baltic Height System Unification, see <http://eo4society.esa.int/projects/sar-hsu/>) to provide expertise on reference frames and by defining consistent standards for the combination of geometric and gravimetric quantities.

Baltic+ SEAL is framed as a laboratory in which advanced solutions in preprocessing and post-processing of satellite altimetry can be assessed for integration into global initiatives such as the ESA SL-CCI. The project will create and validate novel multi-mission high spatio-temporal resolution grids of sea level anomalies to estimate sea level trends, produce an updated mean sea surface model for the Baltic Sea region, and map seasonal sea level variability.

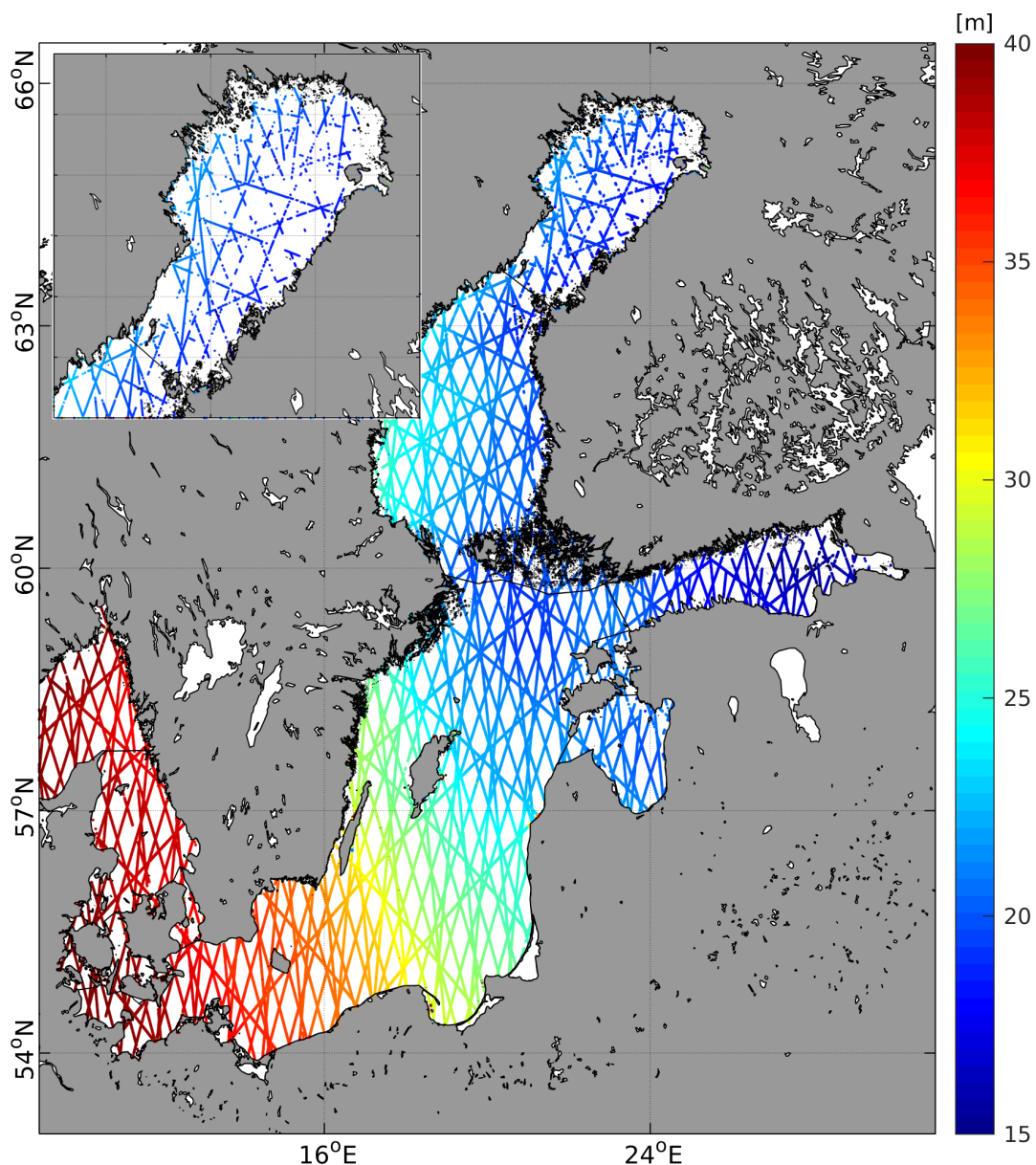


Figure 2.4: Along-track multi-mission cross-calibrated sea surface heights in February 2019 from Jason-3, Sentinel-3A, Sentinel-3B and Cryosat-2 missions. Zoom-in shows the Bay of Bothnia.

The activities of the first half of the project have focused on the processing chain needed to generate a dedicated along-track product. Among the processing steps, particular effort has been dedicated to:

1. The fitting algorithm of the radar signal, applied for open-ocean, coastal and sea-ice conditions (ALES+),
2. The unsupervised classification method developed to detect radar echoes reflected by open-water gaps within the sea-ice layer,
3. The application of a sea state bias correction aimed at reducing the correlated errors between sea level and wave height estimation (Quartly et al., 2019b), and
4. The calibration of the different missions in order to correct for geographically correlated errors (such as orbit errors)

The benefit of these processing steps can be observed in Fig. 2.4, which shows one month of Sea Surface Height observations in February 2019 using Jason-3, Sentinel-3A, Sentinel-3B and Cryosat-2 missions. The classification algorithm recognizes the openings among the sea ice area in the Bay of Bothnia (zoomed). The ALES+ retracking algorithm derives the corresponding heights and the multi-mission cross-calibration allows to consider the heights coming from different missions in an absolute sense.

Geostrophic surface currents in the Greenland Sea

Geostrophic currents are horizontal surface movements of sea water. They result from the balance between horizontal pressure gradients and the Coriolis force. The horizontal pressure gradients are proportional to the sea level slope, which means that elevation differences in the sea surface cause an acceleration of the water masses. The so-called geostrophic flow explains major ocean current patterns (e.g. the Gulf Stream) on the rotating Earth without the influences of wind- or wave induced current motions (i.e. ageostrophic currents). Geostrophic ocean surface currents can be computed by applying the geostrophic equations to height differences of the so-called Dynamic Ocean Topography (DOT) derived from satellite altimetry observations. The DOT is defined as the difference between the sea surface height, a direct measured quantity by the altimeter, and the geoid.

Over last years, a novel dataset of geostrophic currents in the northern Nordic Seas has been created, based on a combination of along-track satellite altimetry data with an ocean model. The work commenced within the framework of the DFG project NEG-OCEAN (until 2018) with the aim to describe and investigate ocean surface currents at the North Eastern coast of Greenland and the northern Nordic Seas. The scientific challenge and innovation consist in providing a comprehensive description of the temporal evolution of surface currents by combining satellite altimetry data, Earth gravity field models, and ocean modeling in a region, which is affected by sea-ice and rapidly changing environmental conditions.

The ocean model is used to fill-in gaps of altimetry observations (e.g. due to ice coverage) with the aim to obtain a homogeneous DOT representation that enables consistent investigations of ocean surface current changes. The ocean model applied is the global Finite Element Sea-ice Ocean Model (FESOM). Gaps in observation data are bridged with simulated differential water heights which are very similar to altimetry derived DOT elevations. Both quantities were combined by applying the method of Principal Component Analysis (PCA). After reducing both quantities by their constant offsets and seasonal signals, the most dominant spatial patterns of the modeled water heights as provided by the PCA are linked with the temporal variability of the

estimated DOT from altimetry. The constant offsets and annual signals are re-added in order to reference the combined data sets to the altimetry height level. Beforehand, a comparison of both data sets was performed. It revealed a good agreement in terms of the included annual variability and the spatial structures. Even though, the seasonal sea level variability differs by a few centimeters, residual heights show similar patterns and high temporal correlations. Small differences are mostly related to sea-ice coverage and artifacts in the geoid (Müller et al., 2019a).

The combination is based on DOT observations from the ESA satellites ERS-2 and Envisat, covering a period of nearly 17 years. Daily meshes of geostrophic currents are computed from slope gradients directly on the finite elements, thus exploiting the Finite-Element formulation of the model and minimizing unnecessary damping effects (Müller et al., 2019b). The combined DOT and geostrophic current data sets were made publicly available via PANGAEA (Müller et al., 2019c). Figure 2.5 shows a field for July 2008.

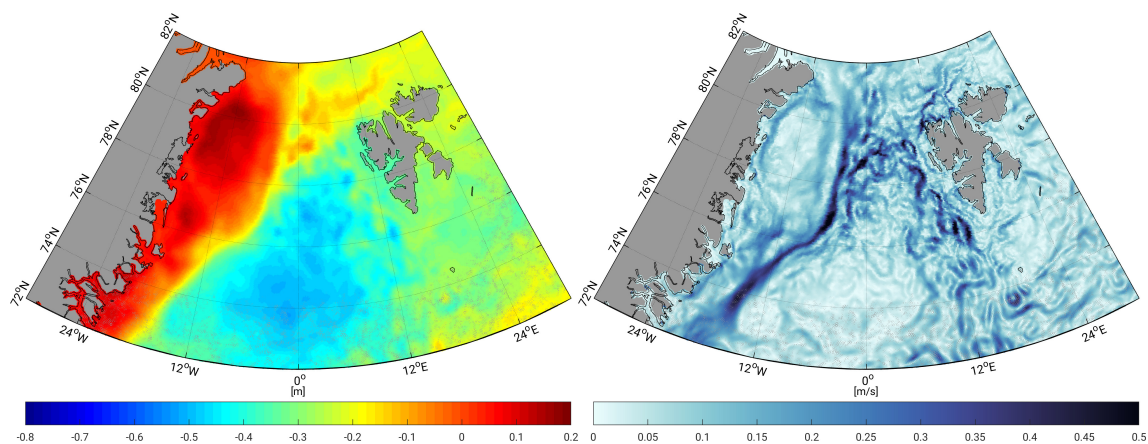


Figure 2.5: Examples for data sets derived from the combination of satellite altimetry with ocean modeling: Dynamic Ocean Topography (left) and absolute geostrophic surface velocities (right) for July 18th, 2008)

Significant wave height estimation

The sea state (i.e. the condition of the ocean due to the action of wind waves and swell) is one of the so-called Essential Climate Variables (ECV) and thus a key quantity to record and investigate the processes of climate change. One important sea state parameter is the significant wave height (SWH) that can be measured by satellite altimetry.

In June 2018, ESA launched the Sea State Climate Change Initiative (**SS-CCI**). DGFI-TUM takes a key role in that project by leading the Algorithm Development (AD) Team for the satellite altimetry part. The main goal of the study is the estimation and exploitation of consistent climate-quality time-series of SWH across different satellite missions. One of the focus areas of the project is the coastal zone, given the current decrease in performance of standard altimetry products when approaching land and the significant impacts of sea state in this area.

The SS-CCI AD team has the responsibility to improve and develop novel retracking algorithms for estimating the SWH parameters yielding increased signal-to-noise ratio (SNR) and better performance in the coastal zone. The new estimation techniques shall generate consistent results in terms of precision and accuracy during the past 25 years of satellite altimetry data. Two novel retracking algorithms with the best retracking performance shall be selected for production, one for each of the two main operational modes of satellite altimetry, i.e. Low Resolution Mode (LRM) and SAR Mode (SARM; also called Delay-Doppler Mode).

In accordance with other ESA CCI projects, a Round Robin (RR) exercise for algorithm evaluation and selection open to both internal and external teams is being conducted. This section will illustrate the selection procedure and present an overview of the results of the different candidate algorithms. The RR is focused on input data sets of the two missions Jason-3 and Sentinel-3A covering up to two years of data and spanning different sea state conditions. To evaluate the overall performance of the retracker, a series of criteria have been defined, including criteria for both internal statistics and for a comparison against in-situ (buoys) and model data. In the evaluation process, a differentiation is made between open-ocean and coastal regions and also for different sea states, in order to identify the general applicability of the individual retracking algorithms. There has not been any other RR exercise so far, which has conducted a similar objective comparison between different retracking algorithms. A further distinction is the use of a quasi-global selection of the satellite tracks, a long time-series spanning up to two years, and the validation against both wave models and in-situ data.

Based on the ALES-retracker³, within the project, DGFI-TUM developed an subwaveform re-tracker focused on wave height estimation (WHALES) for LRM and SARM, that is also part of the RR experiment. Fig. 2.6 shows a comparison of two 1-Hz, retracked data sets against the ERA5-h wave model in a 2D-histogram plot comparing the baseline retracking algorithm (a) SAMOSA-based (as included in the ESA/EUMETSAT Level-2 products) and (b) WHALES-SAR. As compared to the standard product, the correlation of WHALES-SAR against ERA5-h is improved significantly from 0.881 to 0.963. Likewise, the standard deviation of differences has improved from 0.531 to 0.289 m.

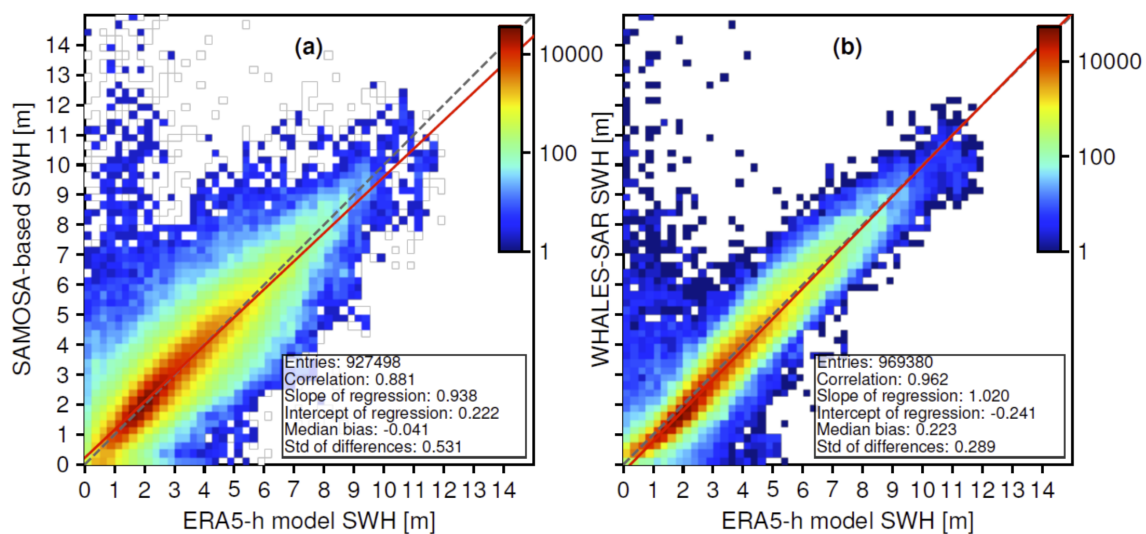


Figure 2.6: 2D-histogram of a comparison of the retracked data set against ERA5-h model comparing the retrackers (a) SAMOSA-based and (b) WHALES-SAR. An SWH-interval bin size of 0.25 m is used.

There is also a significant improvement of the intrinsic noise (computed as the standard deviation of a 20-Hz measurement) of the retracked data sets. Fig. 2.7 shows a plot of the noise versus the SWH (using an interval bin size of 0.25 m). Novel retracker significantly outperform the baseline algorithms MLE-4 and SAMOSA-based for all sea states, while Adaptive and STARv2 (LRM) and LR-RMC_HFA and STARv2-PLRM showing the best performance.

Concluding the results of the RR assessment, it can be stated that evaluating the overall performances of the retracking algorithms strongly depends on the distance to coast and the sea

³Passaro M., Cipollini P., Vignudelli S., Quartly G., Snaith H.: ALES: A multi-mission subwaveform retracker for coastal and open ocean altimetry. Remote Sensing of Environment 145, 173-189, doi:10.1016/j.rse.2014.02.008, 2014

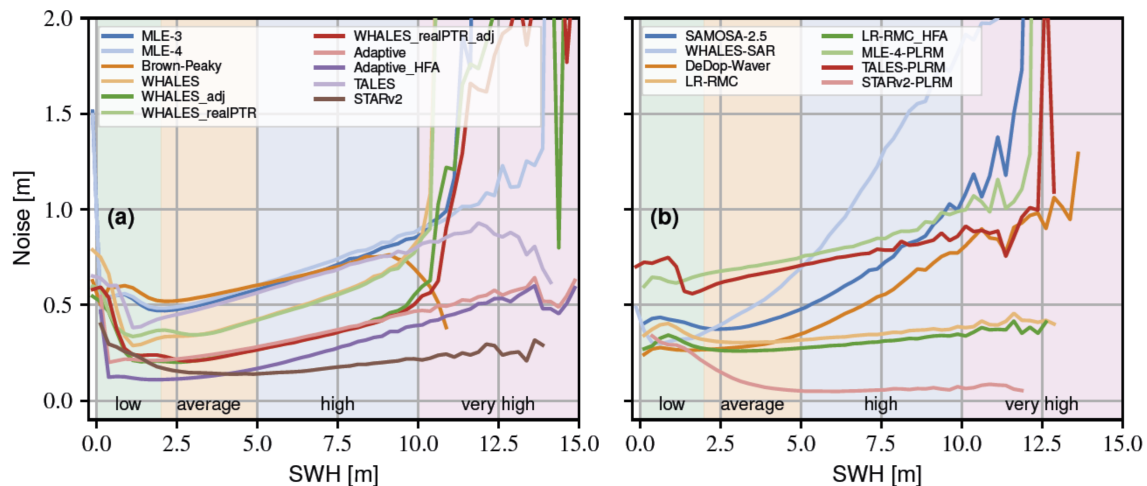


Figure 2.7: Intrinsic noise level of the individual retracers as a function of SWH for (a) LRM- and (b) SARM-retracking algorithms with the sea state noted at the bottom.

state. Defining an overall best performance to select the algorithms for production is a challenging task. For instance, some algorithms show high correlations with model and in-situ data, but significantly deteriorate the large-scale wave spectral variability.

The RR exercise of the ESA SS-CCI project is an excellent opportunity to harmonize the procedures for retracers' evaluation and can be reused in other projects that involve satellite altimetry. Our results show the strong improvements that most novel algorithms achieve with respect to the current baseline algorithms MLE-4 (LRM) and SAMOSA-based (SARM) in the coastal zone and therefore the analysis is relevant also for future choices of wave products tailored for the coast.

Coastal vertical land motion

Coastal vertical land motions (VLM) significantly contribute to relative sea level change (SLC). With rates of several millimeters per year, VLM range in the same order of the contemporary global sea level rise of about 3 mm/year. Consequently, VLM affects coastal impacts of climate-sensitive processes and can regionally account for large fractions of the observed and projected coastal sea level change signal itself. The accurate estimation of VLM is thus vital, not only to disentangle climatic from geodynamic SLC signatures, but also to obtain more robust estimates of past and future relative sea level and its associated uncertainties.

The aim of the DFG-funded **Project VLAD** (Vertical Land motion by satellite Altimetry and tide gauge Difference) is to generate global coastal VLM estimates using a multi-technique approach of tide gauge and satellite altimetry observations, validated by GNSS measurements. Even if the quality of GNSS-derived VLM is very good, the number of coastal permanent stations with a long data record is limited. In contrast, the number of tide gauge stations is much higher. By combining their relative sea level measurements with absolute sea level measurements from satellite altimetry, local VLM can be derived. The main benefit of this "satellite altimetry minus tide-gauge" (SAT-TG) approach is that it strongly complements GNSS VLM measurements and increases the geographical distribution of VLM estimates.

The major innovations of the first project phase are the enhancement of quality and resolution of altimetry data, as well as the method of combining sea level anomalies (SLAs) measured by altimetry and tide gauge records. In order to ensure precise altimetry observations close to

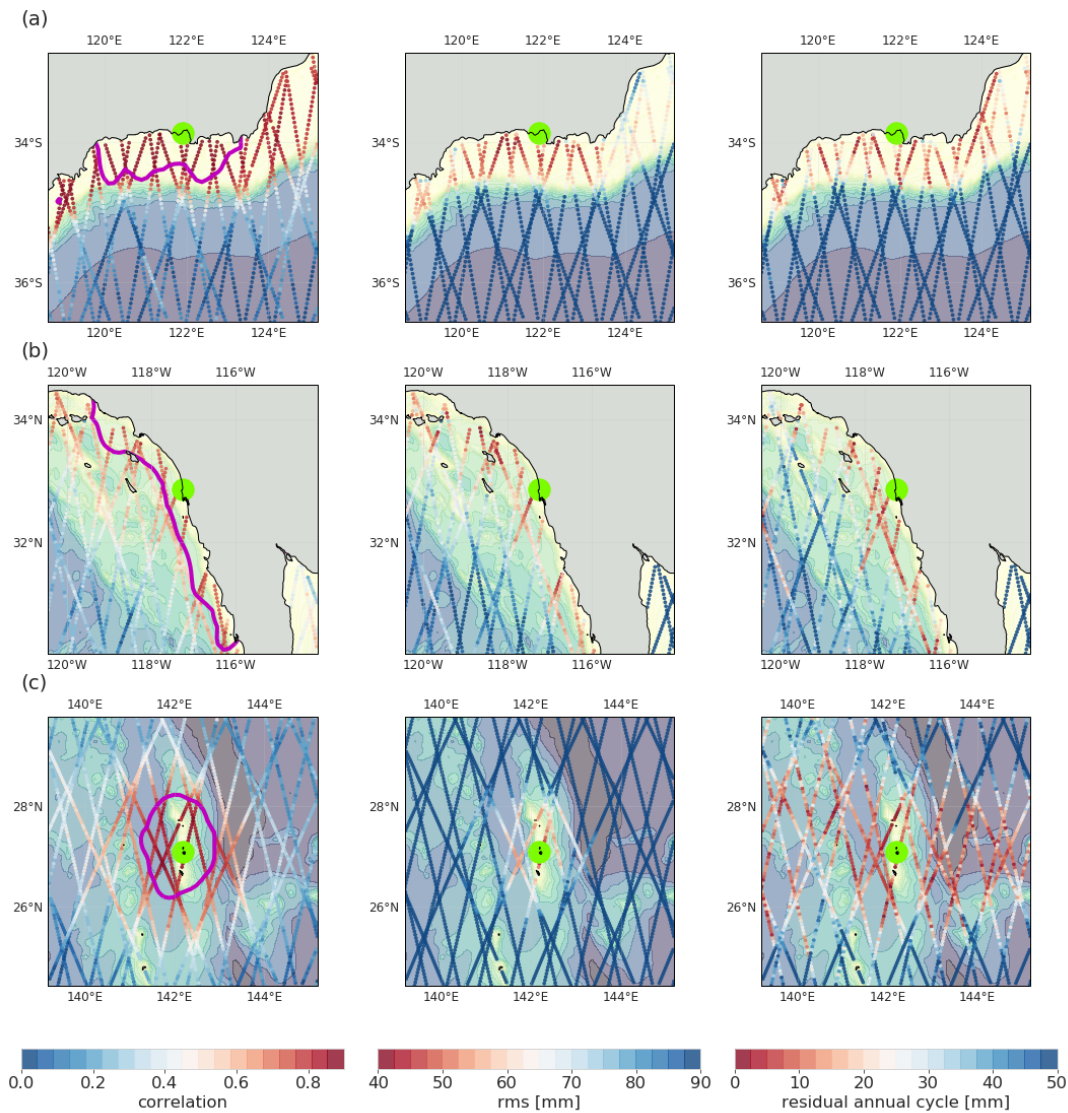


Figure 2.8: Zone of Influence: Different coherent zones of SL-variability are identified by different statistical criteria. Columns show correlations, RMS and the residual annual cycle from left to right with respect to the tide gauge highlighted in green (center). (a) South coast of Western Australia, (b) Western coast of North America near San Diego, (c) Chichijima island (Japan). The bold contour in the first column indicates a Zone-of-Influence built from 20% of the best-correlated SLAs within a 300km radius. The underlying contours denote the bathymetry, where light colors indicate shallow and blue colors deep water.

the coast, a dedicated coastal along-track data set based on the ALES retracker⁴ is used to compute the absolute sea level change in the proximity of tide gauge stations. We couple those 1 Hz altimetry data with high-frequency tide-gauge observations from the Global Extreme Sea Level Analysis (GESLA) project⁵. For this purpose, only altimetry observations in a so-called "Zone of Influence" (ZOI) are used, defined as regions of sea level variability that show maximum coherency with tide-gauge observations. Using the concept of a ZOI, we aim to decrease noise of the differenced, high-frequent SAT-TG time series to hone trends and uncertainties estimates.

⁴Passaro M., Cipollini P., Vignudelli S., Quartly G., Snaith H.: ALES: A multi-mission subwaveform retracker for coastal and open ocean altimetry. Remote Sensing of Environment 145, 173-189, doi:10.1016/j.rse.2014.02.008, 2014

⁵Woodworth P., Hunter J.R., Marcos M., Caldwell P., Menéndez M., Haigh I.: Towards a global higher-frequency sea level data set. Geoscience Data Journal, 3(2), 50-59, doi:10.1002/gdj3.42, 2016

To construct the ZOI, we investigate several criteria of comparability: correlation, RMS and residual annual cycle of the differenced SAT-TG time series. Figure 2.8 shows three different tide-gauge locations and different statistical criteria which indicate the levels of comparability of the 1 Hz along-track data. The contours in the first column confine 20% of the top-performing SLAs (in terms of correlation) for each individual station in a 300 km radius. This ZOI represents the region where altimetry detects the high-frequent sea level variability that is measured at the tide-gauge.

We elaborate which relative threshold, i.e. the fraction of the best-performing altimetry data, yields a globally valid ZOI definition and, correspondingly, highest accuracies and lowest uncertainties of VLM trend estimates. Thereto we compute different trend estimates for different relative thresholds at 72 tide-gauge locations with co-located GPS station (within 1 km distance; for validation). We derive for each threshold the RMS of the differences of SAT-TG and GPS trends as well as the median uncertainties of SAT-TG trend estimates for all considered stations. As a result, not only the RMS but also trend uncertainties strongly improve by 15% (RMS) and 30% (uncertainties), when increasing the relative thresholds (see Fig. 2.9). Based on this, we define an optimum relative level of 20% to construct ZOI. This optimum relative threshold represents a compromise between data comparability (SAT-TG) and data redundancy, as at very high relative thresholds, i.e. higher comparability, less records are taken into account. Comparing our results to conventional gridded altimetry combinations, we reduce the RMS with respect to GNSS by 20% and trend uncertainties by 25%.

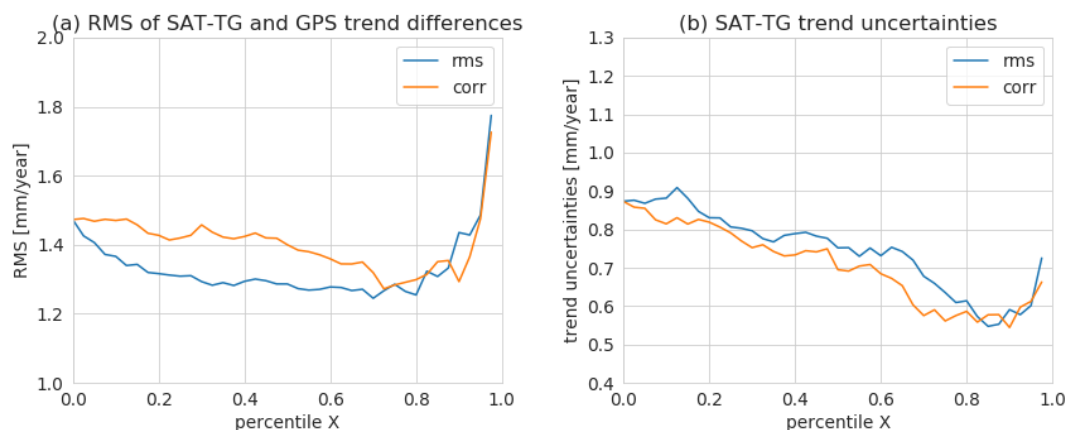


Figure 2.9: Impact of ZOI definition on performance of VLM trend estimates: (a) RMS of the difference of SAT-TG and GPS trends for different relative thresholds (stepsize 0.25%) and different selection criteria. Blue: RMS; red: correlation. (b) same as (a) but for median uncertainties of SAT-TG VLM.

Ocean tides

In 2019, the work on an updated Empirical Ocean Tide model (EOT) continued. Investigations performed in the frame of the DFG-funded Research Unit 2736 NEROGRAV (**Project TIDUS**) focused on improving the accuracy of tidal information in coastal waters. The estimation is based on multi-mission data of more than 25 years and a weighted least-squares approach, whereby data of different missions is automatically weighted by variance component estimation (VCE). A preliminary model, EOT19p, was created using coast-dedicated altimetric data in two critical regions: the North Sea and the Malay Archipelago. The performance of the new model has been assessed by comparison to external state-of-the-art ocean tide models and by validation against in-situ observations from tide gauges, e.g. from the TICON dataset (Piccioni et al., 2019a). Comparisons to tide gauge stations show (Fig. 2.10) that the new model improved

with respect to its former version (EOT11a) by 35% in the North Sea and 21% in the Malay Archipelago. The most significant improvements are visible in complex coastal areas such as the English Channel or the Irish Sea. Moreover, in both regions, EOT19p is in line with the latest models from other institutions (i.e. DTU16, TPXO8, GOT4.8). Comparison with FES2014, used as a reference, showed that the Root Sum Square (RSS) of Median Absolute Difference (MAD) decreases from 4.84 (FES2014) to 4.49 cm (EOT19p) in the North Sea and from 2.86 to 2.79 cm in the Malay Archipelago. However, some of the tidal constituents are less well represented than in FES2014, especially K1, which will further be investigated. More details on the performance of the EOT19p in the two study areas are provided by Piccioni et al. (2019b).

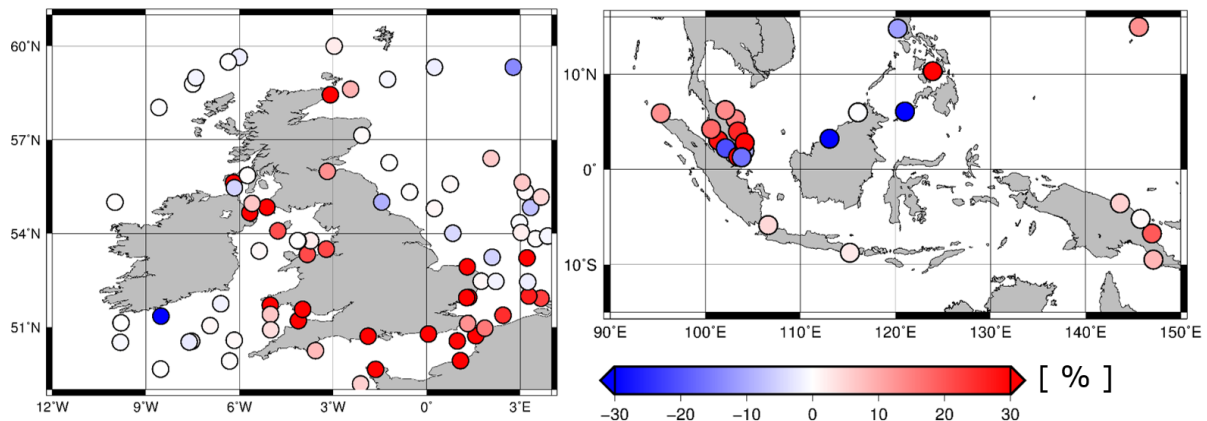


Figure 2.10: RSS relative improvement of EOT19p with respect to EOT11a at in-situ stations in the North Sea (left) and in the Malay Archipelago (right). Red dots indicate areas in which the new model outperforms its predecessor.

2.3 Inland Altimetry

Enhancement of the Database for Hydrological Time Series of Inland Waters (DAHITI)

The DGFI-TUM has been maintaining the *Database for Hydrological Time Series of Inland Waters* (DAHITI) since 2013 (see also Section 4.6). The goal of DAHITI is to provide satellite-based information for lakes, rivers, and reservoirs. Originally limited to time series of water levels from satellite altimetry, DAHITI today also provides time series of surface areas and volume changes of globally distributed inland water bodies. Currently, water stage information for about 2500 targets is available (see Fig. 2.11). More than 800 users are registered in DAHITI, and the international community makes use of the data for a wide variety of applications and studies.

The algorithm for estimating water level time series combines an extended outlier detection and a Kalman filter approach⁶. Since 2018, the data holding of DAHITI has continuously been extended for time series of surface extent which are meanwhile available for about 50 targets. The applied approach for the computation of surface areas, named AWAX (Automated Extraction of Time-Variable Water Surfaces), is described in detail by Schwatke et al. (2019). Recently,

⁶Schwatke C., Dettmering D., Bosch W., Seitz F.: DAHITI – an innovative approach for estimating water level time series over inland waters using multi-mission satellite altimetry. *Hydrology and Earth System Sciences* 19(10), doi:10.5194/hess-19-4345-2015, 2015

this approach has been updated from a monthly-based to a scene-based processing, which increases the temporal resolution of the resulting time series.

In 2019, we extended the data holding of DAHITI by an additional data type, namely by time series of volume changes of lakes and reservoirs. The approach for the volume computation is described below.



Figure 2.11: Global distribution of inland water bodies currently available in DAHITI

Volume time series of lakes and reservoirs

In the debate of climate change impacts, the availability and accessibility of freshwater on Earth is an extremely important topic. Storage changes of larger inland water bodies can be derived from a combination of satellite altimetry (water levels) with optical imagery (surface areas). For example, Busker et al. (2019) used DAHITI water level time series in combination with the JRC Global Surface Water (GSW) data set⁷ for generating time series of volume changes in lakes and reservoirs between 1984 and 2015 for 137 lakes over all continents.

During 2019 we developed an improved approach for the combination of water levels and surface areas which is divided into three steps: First, a hypsometry model describing the relationship between water levels and surface areas needs to be generated. For that purpose, a well established approach developed by A. Strahler in 1952⁸ is used and modified for this application. The level/area relationship is applied to derive a water level for each observed lake area. In a second step, a lake bathymetry between minimum and maximum observed surface area is derived. This is done by stacking land-water masks from DAHITI with the water levels estimated from the hypsometry model. Finally, the third step comprises the intersection of water levels with bathymetry in order to estimate volume time series with respect to the minimum observed water level. At the example of Ray Roberts Lake in USA (DAHITI-ID 10146) the results of the three steps are shown in Figure 2.12.

⁷Pekel J.-F., Cottam A., Gorelick, N., Belward, A.S.: High-resolution mapping of global surface water and its long-term changes. *Nature*, 540, doi:[10.1038/nature20584](https://doi.org/10.1038/nature20584), 2016.

⁸Strahler A.N.: Hypsometric (area-altitude) analysis of erosional topography. *GSA Bulletin*, 63(11), doi:[10.1130/0016-7606\(1952\)63\[1117:HAAOET\]2.0.CO;2](https://doi.org/10.1130/0016-7606(1952)63[1117:HAAOET]2.0.CO;2)

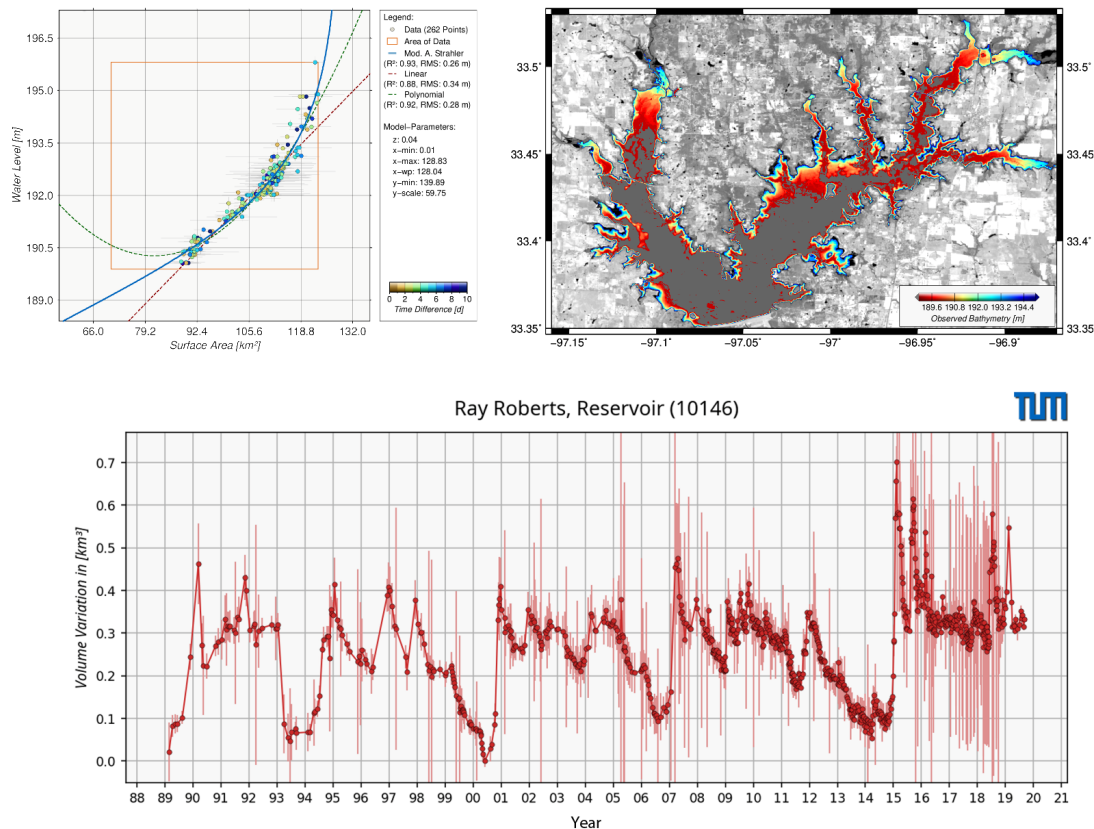


Figure 2.12: Water volume variations of Ray Roberts Lake, USA (bottom), its hypsometry (top left) and bathymetry (top right).

Improved lake level time series base on time-dependent land/water masks

Accurate water level time series of inland water bodies contain important information about regional hydrological regimes, water resources and their dynamics. Satellite altimetry has demonstrated its potential to complement measurements from in-situ gauging stations by providing absolute water level heights with good quality not only for the open ocean but also for larger inland waters. Observations from satellite altimetry do not only allow for the determination of seasonal fluctuations or short-term variations of water storage and discharge, but also for the detection of long-term trends and the tracking and prediction of impacts of extreme events.

Within the DFG-funded Research Unit 2630 GlobalCDA (**Project WALES**), DGFI-TUM is working on the development of new algorithms and approaches enabling the automated and fast generation of water level series at the highest possible accuracy for all major water bodies on global scale. This data will be applied for a subsequent computation of water volume and discharge series to be used in a calibration/data assimilation approach to improve a global hydrological model.

In order to obtain reliable water level series also for smaller lakes, the data quality has to be ensured by a rigorous data preprocessing. This involves in particular the identification of corrupted measurements, e.g. due to land reflections. A common approach to separate radar reflections from water surfaces and land is based on static land/water masks. However, the extent of water surface areas can be subject to significant temporal changes, especially in the cases of meandering rivers and wetlands. Here, the usage of time-dependent land/water masks instead of static ones can considerably change the resulting water level time series. This impact has been investigated by calculating water level series for several water bodies using both approaches (static and time-variable). The results were validated against in-situ

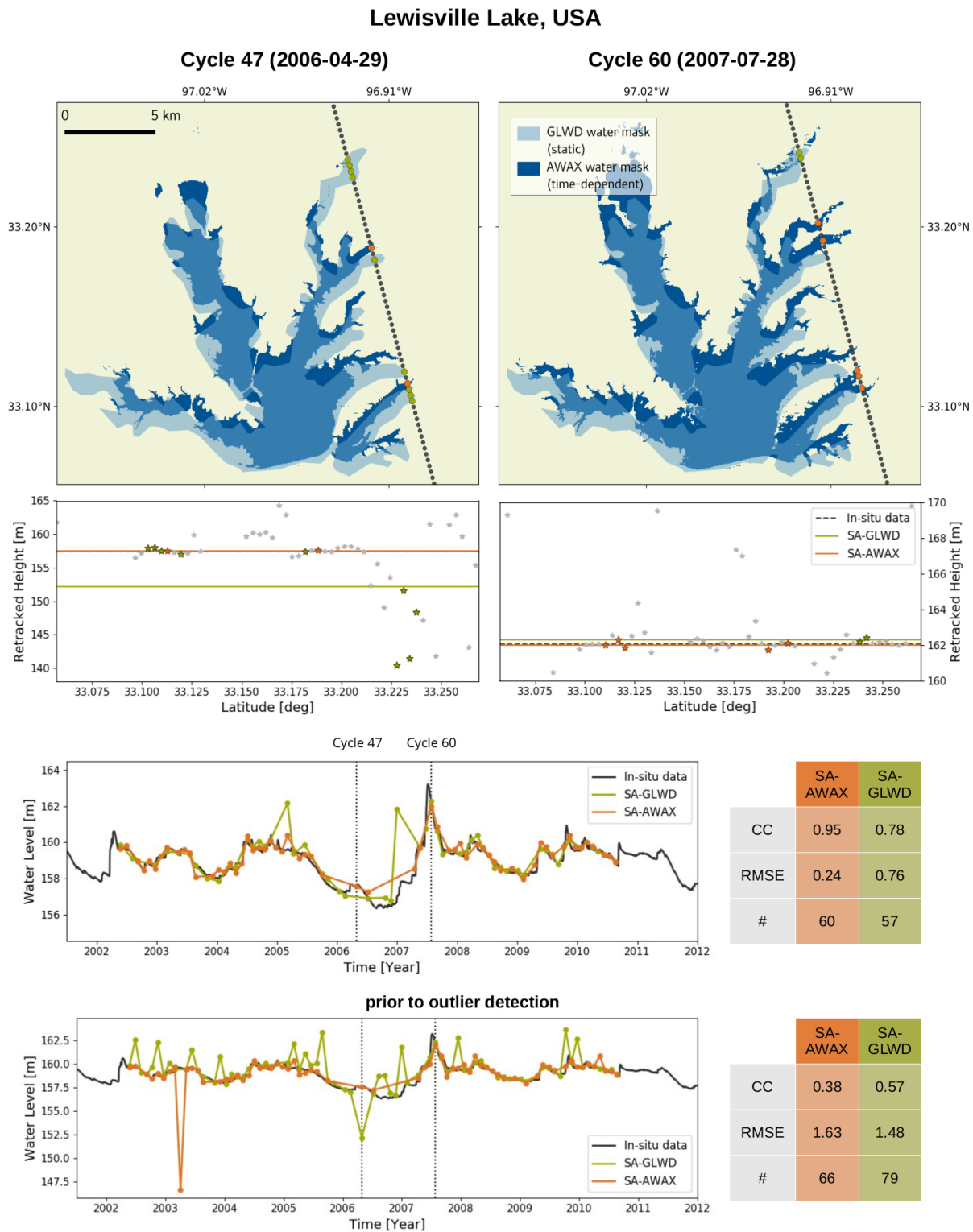


Figure 2.13: Top: surface area extent of Lake Lewisville, USA, for a low-water (Cycle 47) and a high-water period (Cycle 60). Time-dependent masks from DAHITI are shown in dark blue. They are overlain by the static GLWD product. Envisat high-frequency measurement points are marked as gray dots; data points considered to be water returns using the time-dependent mask are shown in orange, whereas points considered as water returns using the static GLWD mask are colored in green. Middle: Along-track measurements for the two cycles. Bottom: Resulting time series in comparison with in-situ data (black).

measurements. The static masks were taken from the Global Lakes and Wetlands Database (GLWD)⁹, the time-dependent masks from DAHITI (see above).

It was found that using time-variable masks improved the accuracy and data coverage in most cases. But the improvement strongly depends on particular characteristics of the respective water body, and it is, as expected, small for water bodies with stable extent. Since the time-variable masks lead to a better localization of the water returns, less errors are contained in the water level series. Figure 2.13 shows results for Lake Lewisville, USA. Here, the number of corrupted altimeter measurements could be reduced significantly by correctly identifying measurements in the northern tributary as land returns during low-water.

River discharge

Contrary to the increasing interest in monitoring data of inland waters, the availability of data from in-situ stations is strongly decreasing. In order to compensate the lack of ground data, approaches based on remote sensing techniques are being developed.

In 2019, DGFI-TUM began to develop a new *at-a-station* hydraulic geometry approach in order to estimate the discharge of large rivers by combining different long-term remote sensing data sets with physical flow equations. The approach makes use of water levels from multi-mission satellite altimetry and surface areas from optical satellite images, both provided by DAHITI (see above). It is independent from in-situ data, however ground data are used for validation (Scherer 2019). The data sets are combined by fitting a hypsometric curve. This curve is then applied to estimate the water level at the epoch of each acquisition of the long-term multi-spectral remote sensing images. This way, the temporal resolution can be improved which increases also the chance to detect water level extremes. Moreover, a bathymetry can be estimated from the time series of water surface extents. Below the minimum hypsometric water level, the river bed elevation is estimated by using an empirical width-to-depth relationship in order to determine the final cross-sectional geometry. An example for the Mississippi River is shown in Fig. 2.14.

⁹ Lehner, B. and Doell, P.: Development and Validation of a Global Database of Lakes, Reservoirs and Wetlands. Journal of Hydrology, 296, 1-22, 2004

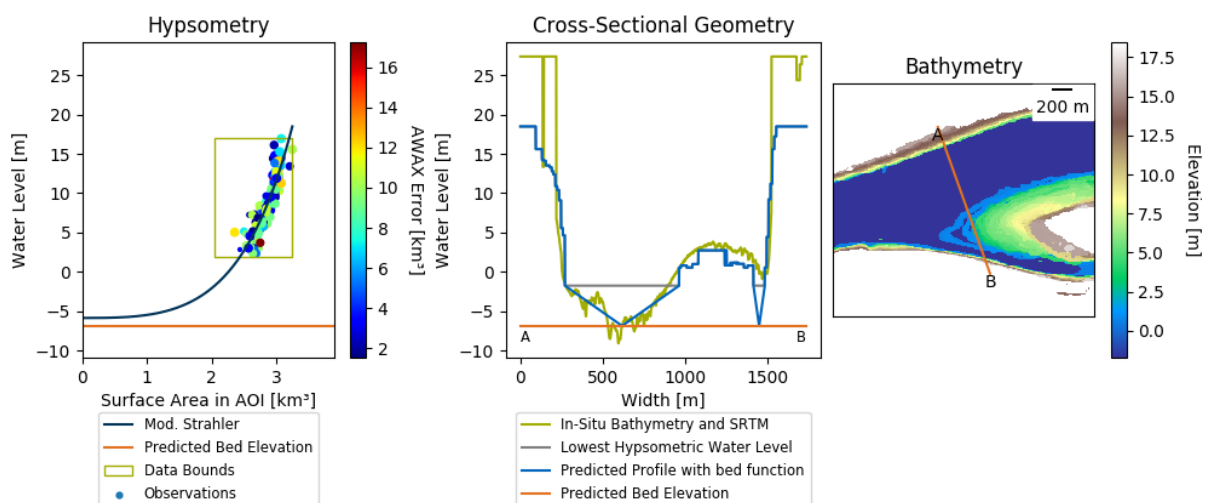


Figure 2.14: Hypsometric relationship of surface area and water level observations (left), derived bathymetry (right) and extracted cross-sectional geometry (center) at river kilometer 439,4 of the Mississippi River.

In order to describe the river flow, a simple Manning-Strickler equation is used¹⁰. We compute the required flow gradient based on a linear adjustment of multi-mission altimetry data. Thereby, the differences between all synchronously observed water levels at various virtual stations along the river are considered. The roughness coefficient is estimated based on geomorphological features. Respective adjustment factors are chosen based on remote sensing data and a literature decision guide.

The validation of the method at the Lower Mississippi River with ground data shows that the developed algorithm yields best results for uniform and straight river sections. Figure 2.15 displays a validation result with an RMSE of $2212 \text{ m}^3/\text{s}$ (12.8%). The results are comparable to other studies, but vary strongly depending on the location. Further studies will make use of an *at-many-stations* approach, where the described methodology will be applied to multiple stations along a river section. Based on the conservation of mass and river equilibrium principles, this advanced approach is expected to deliver better results by averaging the parameters over a section.

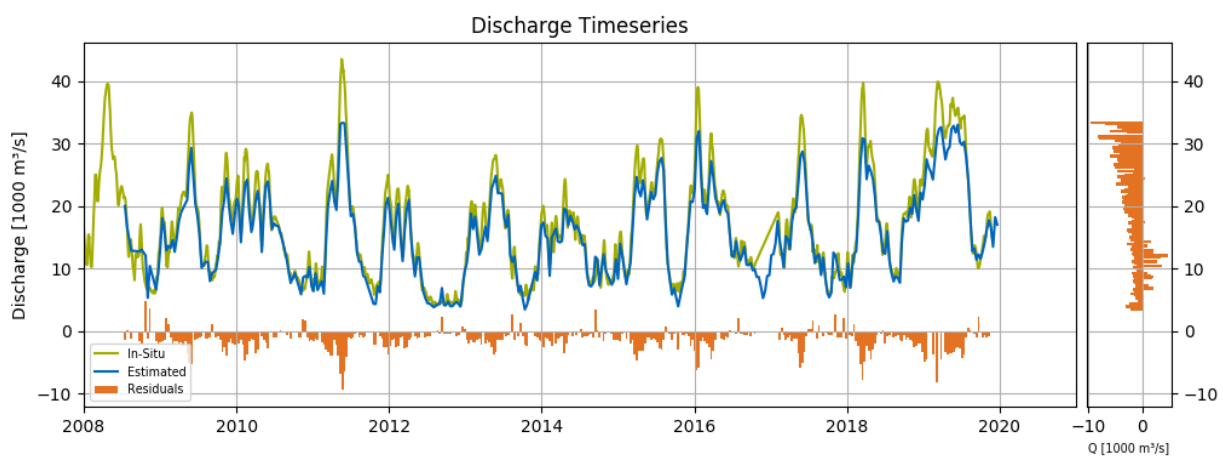


Figure 2.15: Time series of estimated and in-situ discharge for the Mississippi River at river kilometer 439,4 with residuals.

Related publications

Benveniste J., Cazenave A., Vignudelli S., Fenoglio-Marc L., Shah R., Almar R., Andersen O., Birol F., Bonnefond P., Bouffard J., Calafat F., Cardellach E., Cipollini P., Le Cozannet G., Dufau C., Fernandes M.J., Frappart F., Garrison J., Gommenginger C., Han G., Hoyer J.L., Kourafalou V., Leuliette E., Li, Z., Loisel H., Madsen K., Marcos M., Melet A., Meyssignac B., Pascual A., Passaro M., Ribó S., Scharroo R., Song Y.T., Speich S., Wilkin J., Woodworth P., Wöppelmann, G.: *Requirements for a Coastal Hazards Observing System*. *Frontiers in Marine Science*, 6:348, doi:[10.3389/fmars.2019.00348](https://doi.org/10.3389/fmars.2019.00348), 2019

Busker T., de Roo A., Gelati E., Schwatke C., Adamovic M., Bisselink B., Pekel J.-F., Cotnam A.: *A global lake and reservoir volume analysis using a surface water dataset and satellite altimetry*. *Hydrology and Earth System Sciences*, 23(2), 669-690, doi:[10.5194/hess-23-669-2019](https://doi.org/10.5194/hess-23-669-2019), 2019

¹⁰Manning, R.: On the flow of water in open channels and pipes. *Transactions of the Institution of Civil Engineers of Ireland* 1891, 20, 161–207

- Dettmering D., Schwatke C.: *Multi-Mission Cross-Calibration of Satellite Altimeters - Systematic Differences between Sentinel-3A and Jason-3*. International Association of Geodesy Symposia, 150, Springer, doi:[10.1007/1345_2019_58](https://doi.org/10.1007/1345_2019_58), 2019
- Marti F., Cazenave A., Birol F., Passaro M., Leger F., Nino F., Almar R. Benveniste J., Legeais J.F.: *Altimetry-based sea level trends along the coast of Western Africa*. Advances in Space Research, doi:[10.1016/j.asr.2019.05.033](https://doi.org/10.1016/j.asr.2019.05.033), 2019
- Müller F., Wekerle C., Dettmering D., Passaro M., Bosch W., Seitz F.: *Dynamic ocean topography of the northern Nordic seas: a comparison between satellite altimetry and ocean modeling*. The Cryosphere, 13, 611–626, doi:[10.5194/tc-13-611-2019](https://doi.org/10.5194/tc-13-611-2019), 2019a
- Müller F., Dettmering D., Wekerle C., Schwatke C., Passaro M., Bosch W., Seitz F.: *Geostrophic currents in the northern Nordic Seas from a combination of multi-mission satellite altimetry and ocean modeling*. Earth System Science Data, 11(4), 1765-1781, doi:[10.5194/essd-11-1765-2019](https://doi.org/10.5194/essd-11-1765-2019), 2019b
- Müller F., Dettmering D., Wekerle C., Schwatke C., Bosch W., Seitz F.: *Geostrophic Currents in the northern Nordic Seas: A Combined Dataset of Multi-Mission Satellite Altimetry and Ocean Modeling (data)*. Deutsches Geodätisches Forschungsinstitut, Munich, doi:[10.1594/PANGAEA.900691](https://doi.org/10.1594/PANGAEA.900691), 2019c
- Piccioni G., Dettmering D., Bosch W., Seitz F.: *TICON: Tidal CONstants based on GESLA sea-level records from globally located tide gauges*. Geoscience Data Journal, 6(2), 97-104, doi:[10.1002/gdj3.72](https://doi.org/10.1002/gdj3.72), 2019a
- Piccioni G., Dettmering D., Schwatke C., Passaro M., Seitz F.: *Design and regional assessment of an empirical tidal model based on FES2014 and coastal altimetry*. Advances in Space Research, doi:[10.1016/j.asr.2019.08.030](https://doi.org/10.1016/j.asr.2019.08.030), 2019b
- Quartly G., Rinne E., Passaro M., Andersen O. B., Dinardo S., Fleury S., Guillot A., Hendricks S., Kurekin A., Müller F. L., Ricker R., Skourup H., Tsamados M.: *Retrieving Sea Level and Freeboard in the Arctic: A Review of Current Radar Altimetry Methodologies and Future Perspectives*. Remote Sensing, 11(7), doi:[10.3390/rs11070881](https://doi.org/10.3390/rs11070881), 2019a
- Quartly G., Smith W., Passaro M.: *Removing Intra-1-Hz Covariant Error to Improve Altimetric Profiles of σ^0 and Sea Surface Height*. IEEE Transactions on Geoscience and Remote Sensing, 57(6), 3741-3752, doi:[10.1109/tgrs.2018.2886998](https://doi.org/10.1109/tgrs.2018.2886998), 2019b
- Rose S.K., Andersen O.B., Passaro M., Ludwigsen C.A., Schwatke C.: *Arctic Ocean Sea Level Record from the Complete Radar Altimetry Era: 1991–2018*. Remote Sensing, 11(14), 1672, doi:[10.3390/rs11141672](https://doi.org/10.3390/rs11141672), 2019
- Rudenko S., Esselborn S., Schöne T., Dettmering D.: *Impact of terrestrial reference frame realizations on altimetry satellite orbit quality and global and regional sea level trends: a switch from ITRF2008 to ITRF2014*. Solid Earth, 10(1), 293-305, doi:[10.5194/se-10-293-2019](https://doi.org/10.5194/se-10-293-2019), 2019
- Scherer D.: *Estimation of River Discharge using Satellite Altimetry and optical Remote Sensing Images*. Master Thesis, University of Applied Sciences Munich, 2019
- Schwatke C., Scherer D., Dettmering D.: *Automated Extraction of Consistent Time-Variable Water Surfaces of Lakes and Reservoirs Based on Landsat and Sentinel-2*. Remote Sensing, 11(9), 1010, doi:[10.3390/rs11091010](https://doi.org/10.3390/rs11091010), 2019

3 Cross-Cutting Research Topics

DGFI-TUM's Research Areas Reference Systems and Satellite Altimetry are closely interconnected with three overarching research topics: Atmosphere, Regional Gravity Field, and Standards and Conventions.

The atmosphere (Section 3.1) plays a key role in the analysis of all space-geodetic observations. Satellite orbits are disturbed by atmospheric drag, and the measurement signals are affected by refraction and signal delay. Such effects must be properly handled in precise orbit determination and geodetic data analysis, and the optimization of respective correction models means a significant research challenge. On the other hand, the disturbances of the different signals carry valuable information on the state and dynamics of the atmosphere. This information can be used to investigate atmospheric processes and space weather impacts, and it is of great interest for other disciplines. Space weather, in particular, is given more and more attention by politics and sciences as it can cause severe damage to modern infrastructure, such as navigation systems, power supply and communication facilities. Over the past years, DGFI-TUM has built up strong expertise in modeling and predicting global and regional structures of the electron and the neutral density within the Earth's ionosphere and thermosphere, respectively, from the joint analysis of different space geodetic observations. The institute participated in the preparation of a position paper on space weather research in Germany, and it closely cooperates with the German Space Situational Awareness Center (Weltraumlagezentrum) and the DLR since many years. Furthermore, DGFI-TUM chairs the Focus Area on Geodetic Space Weather Research of the Global Geodetic Observing System (GGOS).

The precise knowledge of the Earth's gravity field (Section 3.2) is of high relevance for various applications in geodesy, such as the realization and unification of height systems or the determination of high-precision satellite orbits. The latter are a prerequisite for the computation of accurate reference frames or for reliable estimates of water heights from satellite altimetry. Furthermore, the geoid provides the reference surface for the ocean circulation. Temporal changes of the gravity field contain information about mass transports in the Earth system and are of great interest, for example, for the investigation of dynamic processes in the Earth's interior or within the hydrosphere. DGFI-TUM primarily focuses on theoretical and practical aspects of regional gravity field determination. The goal is the creation of high-resolution and high-precision potential fields for delimited areas through a combination of different data types, such as space- and airborne gravity measurements, satellite altimetry, and terrestrial and ship gravimetry.

Common standards and conventions (Section 3.3) are essential to assure highest consistency of different geodetic parameters and products. On the international level, DGFI-TUM is deeply involved in the activities of the competent bodies for defining standards in geodesy and monitoring their implementation. DGFI-TUM chairs the GGOS Bureau of Products and Standards (BPS) and operates it jointly with partners. In the frame of the United Nations Global Spatial Information Management (UN-GGIM), DGFI-TUM provides the IAG representative for the Key Area "Data Sharing and Development of Standards" to the UN-GGIM Subcommittee Geodesy.

3.1 Atmosphere

According to different physical parameters, such as temperature or charge state, the Earth's atmosphere can be structured into different layers. With respect to the charge state, we distinguish mainly between the neutral atmosphere up to about 50 km altitude and the ionosphere

approximately between 50 km and 1000 km altitude. The plasmasphere is a part of the Earth's magnetosphere and is located above the ionosphere. Both the plasmasphere and the ionosphere can be characterized by the number of free electrons, i.e. the electron density distribution, and thus play a key role in monitoring space weather and its impacts.

Figure 3.1 gives an overview about the 2019 project collection of DGFI-TUM in the frame of atmosphere modeling. On the left-hand side of the figure we added as further research field the plasmasphere; for more details see Fig. 3.2.

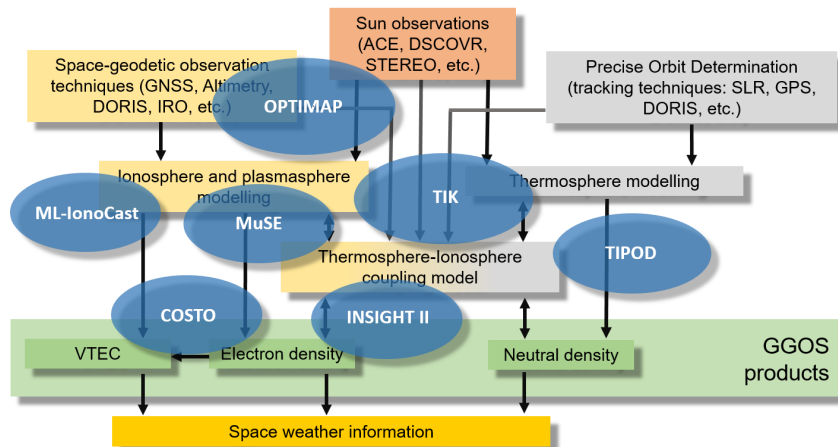


Figure 3.1: Work structure of the Research Topic 'Atmosphere' in 2019: the blue colored oval areas visualize the third-party funded projects running at DGFI-TUM (project acronyms written in white letters). The location of such an oval area reflects the scientific content of the project and demonstrates its role in the structure of the research topic.

The blue colored oval areas in Fig. 3.1 indicate the altogether seven third-party funded projects running at DGFI-TUM during 2019. The **Projects OPTIMAP** (Operational Tool for Ionospheric Mapping And Prediction), funded by Bundeswehr GeoInformation Centre (BGIC), **TIK** (Operational prototype for the determination of the thermospheric density on the basis of a coupled thermosphere-ionosphere model), funded by the German Ministry for Economic Affairs and Energy (BMWi) via German Aerospace Center (DLR), as well as the three projects **MuSE** (Multi-Satellite Ionosphere-Plasmasphere Electron Density Reconstruction), **INSIGHT-II** (Interactions of Low-Orbiting Satellites with the Surrounding Ionosphere and Thermosphere) and **TIPOD** (Development of High-precision Thermosphere Models for Improving Precise Orbit Determination of Low-Earth-Orbiting Satellites) all funded by the German Research Foundation (DFG) within the Special Priority Programme (SPP) 1788 'Dynamic Earth', have already been presented in the Annual Reports of DGFI-TUM of the recent years. The new ESA project **COSTO** (Contribution of Swarm Data to the Prompt Detection of Tsunamis and Other Natural Hazards) with a running time of 15 months starting at June 1, 2019, is focusing on a better characterization, understanding and discovering of coupling processes and interactions between the ionosphere/magnetosphere, the lower atmosphere as well as the Earth's surface and sea level vertical displacements. The acronym **ML-IonoCast** (Machine Learning for Forecasting the Ionospheric Total Electron Content) stands for a scholarship of the DAAD (German Academic Exchange Service) supporting (1) the development of an accurate model for nowcasting and forecasting the ionospheric vertical total electron content (VTEC) taking into account physical aspects and state-of-art machine learning techniques, as well as (2) understanding and describing the complex Sun-Earth relation including space weather effects and their impact on the ionosphere and GNSS technology.

In the following, we will present results of our investigations (1) on modeling the electron density within the plasmasphere, (2) on modeling key parameters of the electron density within

the ionosphere considering inequality constraints and (3) on the analysis of empirical thermospheric density models during high solar activity.

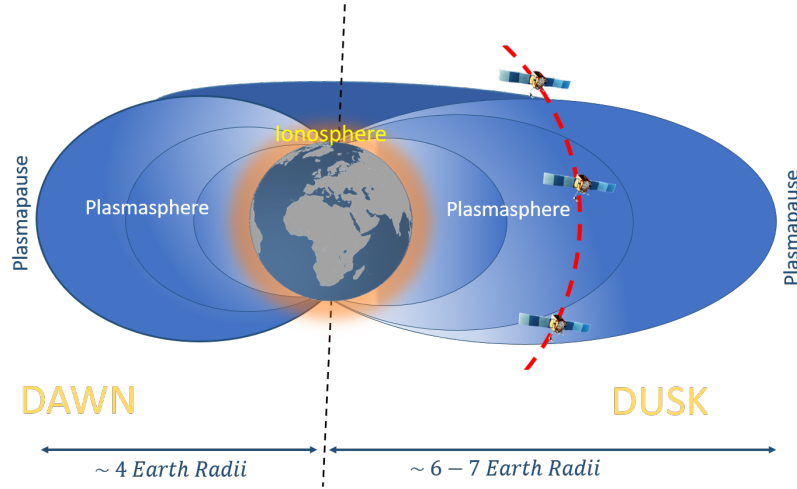


Figure 3.2: The ionosphere is enveloping the Earth as a spherical layer; geometrically the plasmasphere is a torus of cold, dense (tens to thousands of particles per cubic centimeter) plasma that occupies roughly the same region as the inner magnetosphere; the sharp edge of the plasmasphere is called plasmapause at equatorial distances of 4 to 7 Earth radii; figure inspired by ESA (<https://sci.esa.int/web/cluster>).

Modeling the electron density within the plasmasphere

Space weather events affect different components of the System Earth (mainly magnetosphere, plasmasphere, ionosphere and thermosphere) and their mutual couplings in very complex and different ways. Consequently, the accuracy, quality and availability of precise point positioning and satellite navigation as well as remote sensing and telecommunication depend on the influence of space weather. Since space weather is reflected by the electron density distribution, it causes refraction, scattering, reflection and a propagation delay of microwave signals. Around 50% of such a delay for an L-band signal, e.g. used in GNSS, originates from altitudes above the F_2 layer, i.e. from the topside ionosphere and plasmasphere. Consequently, the knowledge of the three-dimensional (3D) electron density distribution of the topside ionosphere and plasmasphere is of great importance. Unfortunately, it is not well described yet. Figure 3.3 shows a sketch of the characteristic altitude behavior of the electron density.

In general, the majority of data, available for modeling the electron density within the ionosphere and plasmasphere, are Slant Total Electron Content (STEC) values derived from GNSS measurements to low-Earth-orbiting (LEO) satellites or ground-based receiver stations, i.e. for each ray-path S between a transmitting GNSS satellite T and a receiver station R the integral equation

$$STEC_R^T(t) = \int_R^T N_e(\varphi, \lambda, h, t) ds \quad (3.1)$$

can be set up, where φ is the latitude, λ the longitude, h the height above the Earth's surface and t the time. The absence of horizontal measurements, such as radio occultations, makes the modeling of the height-dependency of the electron density to a major challenge. Further difficulties in realizing a topside ionosphere and plasmasphere model originate (1) from the rarity of pure electron density measurements and (2) from the low plasma density at high altitudes. Since ground-based STEC values are significantly affected by the electron density of the F_2 layer, in particular, of the part below the peak height $h_m^{F_2}$, it was decided in the project MuSE to avoid the utilization of ground-based STEC data and to concentrate on the upper part of the

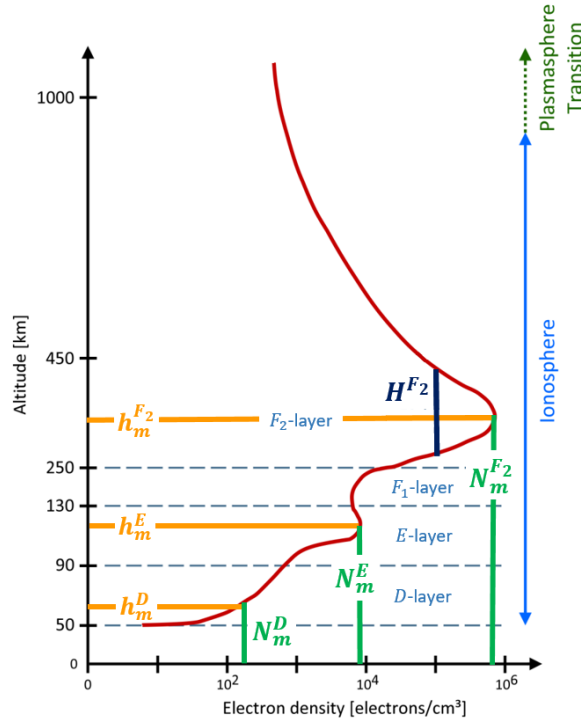


Figure 3.3: Sketch of an electron density (N_e) profile (red line); the 4 ionospheric layers D, E, F_1, F_2 can each be represented by the Chapman function (see Eq. (3.6)), characterized by the maximum value N_m^Q , the corresponding peak height h_m^Q and the scale height H^Q with $Q \in \{D, E, F_1, F_2\}$. The plasmaspheric part of the N_e profile is characterized by an exponential decay with increasing altitude (see Eq. (3.7)).

ionosphere and the plasmasphere. Consequently, a topside ionosphere-plasmasphere model was developed at DGFI-TUM, which is capable to assimilate measurements from various satellite missions. The procedure exploits mainly observations of LEO satellites, in particular the three satellites of the constellation mission Swarm, the six satellites of the Formosat-3/COSMIC mission as well as the two GRACE satellites, TerraSAR-X, MetOp-A and MetOp-B. A considerable part thereby is the implementation of a plasmopause location model (PLM) into the assimilation procedure. A new PLM was developed in MuSE by our project partners from GFZ Potsdam and the Tihany Geophysical Observatory in Hungary, based on field-aligned current signatures, deduced from Swarm magnetic field data¹. The first version of this model was validated by means of electron density data collected on board of NASA's satellite mission Van Allen Probes (https://www.nasa.gov/mission_pages/rbsp/mission/index.html). Because of the rarity of plasmopause measurements, the derived PLM is important as an anchor point for the construction of the plasmasphere.

As mentioned before, the majority of the usable data to estimate the electron density of the topside ionosphere and plasmasphere are STEC observations derived from GPS measurements on board of LEO satellites. To represent the electron density we introduce a series expansion

$$N_e(\varphi, \lambda, h, t) \approx \sum_{k=1}^N c_k(t) \phi_k(\varphi, \lambda, h) \quad (3.2)$$

in terms of given 3D basis functions $\phi_k(\varphi, \lambda, h)$ and unknown time-dependent series coefficients

¹Heilig B., Lühr H.: Quantifying the relationship between the plasmopause and the inner boundary of small-scale field-aligned currents, as deduced from Swarm observations, *Annales Geophysicae*, doi:10.5194/angeo-36-595-2018, 2018

$c_k(t)$. Inserting Eq. (3.2) into Eq. (3.1) yields the observation equation

$$STEC_R^T(t) + e_R^T(t) = \sum_{k=1}^N c_k(t) \int_R^T \phi_k(\varphi, \lambda, h) ds = \sum_{k=1}^N c_k(t) a_{R;k}^T \quad (3.3)$$

where $e_R^T(t)$ means the measurement error. To interpret Eq. (3.3) we consider a straight line propagation along the ray-path S between the transmitter T on board of a GPS satellite and a GPS receiver R on board of the LEO satellite through the plasmasphere and ionosphere discretized by means of 3D voxels. In this scenario, a coefficient $c_k(t)$ describes the electron density within a voxel V_k "illuminated" by the GPS observation $STEC_R^T(t)$ at time t . The quantity $a_{R;k}^T$ means the length of the ray-path through the voxel V_k . Collecting all observations $STEC_R^T(t)$ at time epoch t in the vector $\mathbf{y}(t)$, the corresponding measurement errors $e_R^T(t)$ in the vector $\mathbf{e}(t)$, the N coefficients $c_k(t)$ in the vector $\mathbf{c}(t)$ and the elements $a_{R;k}^T$ in the matrix \mathbf{A} , the linear equation system

$$\mathbf{y}(t) + \mathbf{e}(t) = \mathbf{A} \mathbf{c}(t) \quad (3.4)$$

results. It is generally characterized by a poor observation geometry, a huge number of unknown coefficients compared to the limited number of observations and the existence of significant measurement errors. To solve this ill-posed problem, we developed a 4D assimilation procedure based on Ensemble Kalman filtering. It allows the combination of all available observations with ionospheric background and forecast information, describing the time evolution of the ionosphere. Further, an Ensemble Kalman filter (EnKF) allows for using covariance information in form of an observation covariance matrix, a background model error covariance matrix and a covariance matrix of the forecast model errors. The application of this information means a big advantage of statistical data assimilation methods. Additionally, it generates not just a solution but also provides its accuracy. Figure 3.4 shows the estimated electron density distribution for the lower part of the plasmasphere.

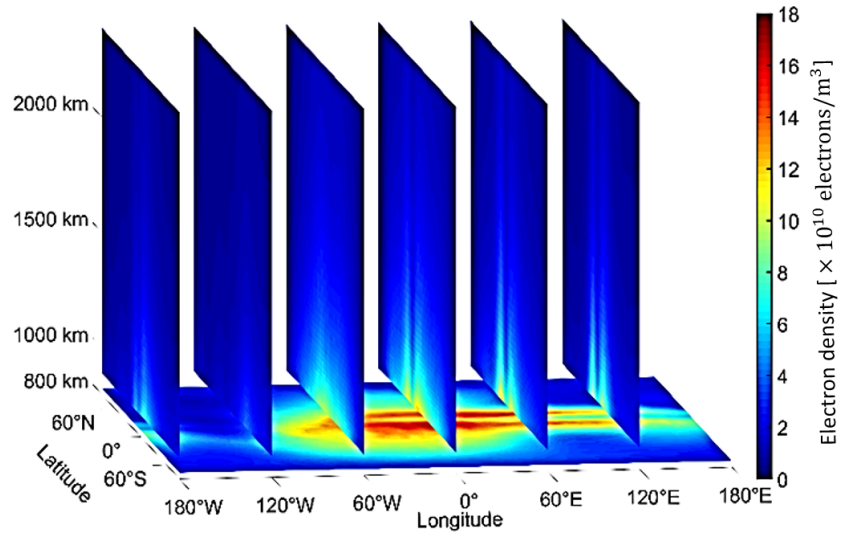


Figure 3.4: Estimated electron density distribution above 800 km altitude at February 10, 2015 at 14:00 UT visualized by one horizontal layer at an altitude of 800 km and six vertical layers at different fixed longitudes.

To validate this result in-situ data are used, namely Langmuir probe electron density data from the three Swarm satellites as well as electron density observations derived from the Van Allen Probes mission. Since these data are rather noisy at altitudes below the orbits of the GPS satellites, an algorithm was developed to eliminate outliers and to compute a running mean for validation purpose.

The capacity of the procedure to estimate the state of the topside ionosphere and plasmasphere is highly depending on the quality of the assimilated data, especially during solar or geo-

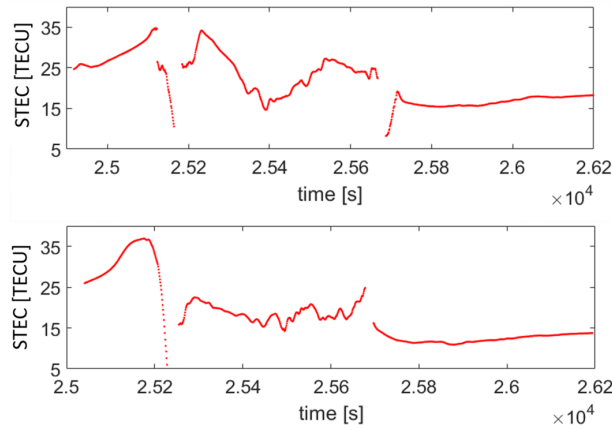


Figure 3.5: STEC data measured on Swarm-A to GPS satellite PRN 2 (top) and on Swarm-C to PRN 2 (bottom), both at February 10, 2015. Since, the distance between the two Swarm satellites is around 100 to 200 km, similar and continuously measured STEC values are expected.

magnetic disturbed conditions. Errors and inconsistencies in the data from different sources (see e.g. Fig. 3.5) can dramatically decrease the quality of the results. This reflects a serious problem for all data driven approaches. We treat this problem by putting special attention on the data filtering methods. Three different STEC data filtering methods are developed at DGFI-TUM. The first method is based on the assumption that the STEC – measured between a fixed LEO satellite and a fixed GNSS satellite – does not change significantly within a short time span. Under this assumption, an adaptive filter for the detection of irregularities in STEC data along the arc was developed. This method is sensitive to the ionospheric, solar and magnetospheric conditions. It takes into account, e.g., the expected seasonal and daily variations of the plasma density. Furthermore, it uses the geomagnetic three-hour Kp index as an input quantity which is seen as a proxy for the energy input from the solar wind. The second method is based on the assumption that the measured STEC along a fixed arc is in average comparable to the one calculated from the corresponding background model. As background model, we used the NeQuick 2.0.2 ionosphere electron density model. Also this second filter is sensitive to the solar and geomagnetic variations. The third method is developed especially for the Swarm-A and Swarm-C satellites, flying side by side at a small distance from each other and thus, could be expected to deliver very similar STEC measurements.

Modeling the electron density within the ionosphere using inequality constraints

The vertical electron density profile as visualized in Fig. 3.3 can be approximated by the so-called multi-layer approach

$$N_e(h) = N_e^D(h) + N_e^E(h) + N_e^{F_1}(h) + N_e^{F_2}(h) + N_e^P(h) = \sum_Q N_e^Q(h) + N_e^P(h) \quad (3.5)$$

as already introduced in DGFI-TUM's Annual Report 2015. In Eq. (3.5) the notations D , E , F_1 , F_2 and P refer to the D –, E –, F_1 – and F_2 –layer as well as to the plasmasphere. We use the Chapman function

$$N_e^Q(h) = N_m^Q \exp \left(\frac{1}{2} \left(1 - \frac{h - h_m^Q}{H^Q} - \exp \left(-\frac{h - h_m^Q}{H^Q} \right) \right) \right) \quad (3.6)$$

to describe approximately the vertical electron density distribution of the Q –layer. Herein, the three quantities N_m^Q (= maximum electron density value), h_m^Q (= peak height) and H^Q (= scale

height) are defined as the key parameters of the Q -layer. In the same manner the function

$$N_e^P(h) = N_0^P \exp\left(-\frac{|h - h_m^{F_2}|}{H^P}\right) \quad (3.7)$$

approximates the decay of the electron density in the plasmasphere with height h above the Earth's surface. The quantities N_0^P (= basis density of the plasmasphere) and H^P (= scale height of the plasmasphere) are the two key parameters of the plasmasphere. Consequently, the multi-layer Chapman model (3.5) to (3.7) includes the set

$$\mathcal{K} = \{N_m^D, h_m^D, H^D, N_m^E, h_m^E, H^E, N_m^{F_1}, h_m^{F_1}, H^{F_1}, N_m^{F_2}, h_m^{F_2}, H^{F_2}, N_0^P, H^P\} \quad (3.8)$$

of altogether 14 key parameters. It can be further extended, e.g. by choosing different scale heights for the top side and the bottom side of each layer.

For a global representation of a key parameter $\kappa \in \mathcal{K}$ we apply the series expansion

$$\kappa(\varphi, \lambda) = \sum_{k_1=0}^{K_{J_1}-1} \sum_{k_2=0}^{K_{J_2}-1} d_{k_1, k_2; \kappa}^{J_1, J_2} N_{J_1, k_1}^2(\varphi) T_{J_2, k_2}^2(\lambda) \quad (3.9)$$

in terms of tensor products of polynomial endpoint-interpolating B-spline functions $N_{J_1, k_1}^2(\varphi)$ and trigonometric B-spline functions $T_{J_2, k_2}^2(\lambda)$, respectively, as introduced in DGFI-TUM's Annual Report 2017 on page 42. Note, that in Eq. (3.9) the levels J_1 and J_2 have to be adapted to the spectral content of the chosen key parameter κ , the corresponding truncation error is omitted; for details on the relations between spectral content, sampling intervals and B-spline levels see Goss et al. (2019, 2020). The $K_{J_1} \cdot K_{J_2}$ unknown series coefficients $d_{k_1, k_2; \kappa}^{J_1, J_2}$ in Eq. (3.9) have to be determined from observed functionals of the electron density, such as STEC measurements (3.1) or ionospheric radio occultation (IRO) measurements.

Since the key parameters of the set \mathcal{K} describe the electron density distribution of the ionosphere and the plasmasphere according to Eq. (3.1) via the Chapman function (3.6) and the exponential decay function (3.7), it is expected that significant correlations exist between the estimated sets of B-spline coefficients $d_{k_1, k_2; \kappa_1}^{J_1, J_2}$ and $d_{k_1, k_2; \kappa_2}^{J_1, J_2}$ of various pairs (κ_1, κ_2) of key parameters κ . Here we have to distinguish between physical and statistical or mathematical correlations. Whereas the latter, for instance, exists between $h_m^{F_1}$ and $h_m^{F_2}$, a physical correlation has to be considered between $N_m^{F_2}$ and $h_m^{F_2}$. Consequently, the joint estimation of all 14 key parameters means a great, in fact unsolvable, challenge. A possible solution of this problem is to select a subset \mathcal{K}_1 of key parameters to be estimated and to assume the other key parameters $\kappa \in \mathcal{K}_2$ are given, e.g. by model values. Note, that $\mathcal{K}_2 = \mathcal{K} \setminus \mathcal{K}_1$ means the complementary set of \mathcal{K}_1 in \mathcal{K} .

The key parameters are subject to constraints, e.g. the inequality relations $h_m^{F_1} < h_m^{F_2}$ and $N_m^{F_2} > 0$ must hold. Consequently, we developed an estimation procedure for the B-spline coefficients $d_{k_1, k_2; \kappa}^{J_1, J_2}$ of the selected key parameters $\kappa \in \mathcal{K}_1$ subject to the inequality constraints

$$\kappa_l(\varphi, \lambda) < \kappa(\varphi, \lambda) < \kappa_u(\varphi, \lambda) \quad (3.10)$$

where the lower bound functions $\kappa_l(\varphi, \lambda)$ and the upper bound functions $\kappa_u(\varphi, \lambda)$ are given and represent physically realistic limits. Besides the inequality constraints (3.10) the equality constraints

$$\kappa(\varphi, \lambda) = \kappa_e(\varphi, \lambda) \quad (3.11)$$

must hold for the remaining key parameters $\kappa \in \mathcal{K}_2$ with given, physically realistic bound functions $\kappa_e(\varphi, \lambda)$. Using the series expansion (3.9) the bound functions $\kappa_l(\varphi, \lambda)$, $\kappa_u(\varphi, \lambda)$ and $\kappa_e(\varphi, \lambda)$ can be transformed into the B-spline coefficients $d_{k_1, k_2; \kappa_l}^{J_1, J_2}$, $d_{k_1, k_2; \kappa_u}^{J_1, J_2}$ and $d_{k_1, k_2; \kappa_e}^{J_1, J_2}$. Although

the B-spline levels J_1 and J_2 can be chosen individually for each key parameter, for simplicity reasons we use fixed level values in our approach, resulting in the same number of coefficients for each key parameter $\kappa \in \mathcal{K}$. It is worth to be mentioned again, that in case no inequality constraints (3.10) are considered, the estimated B-spline coefficients might lead to physically unrealistic results for the key parameters $\kappa \in \mathcal{K}_1$, e.g., $N_m^{F_2} < N_m^{F_1}$ or $N_m^{F_1} < 0$. An example of realistic constraint bounds for the peak density $N_m^{F_2}$ and the corresponding peak height $h_m^{F_2}$ is shown in Fig. 3.6.

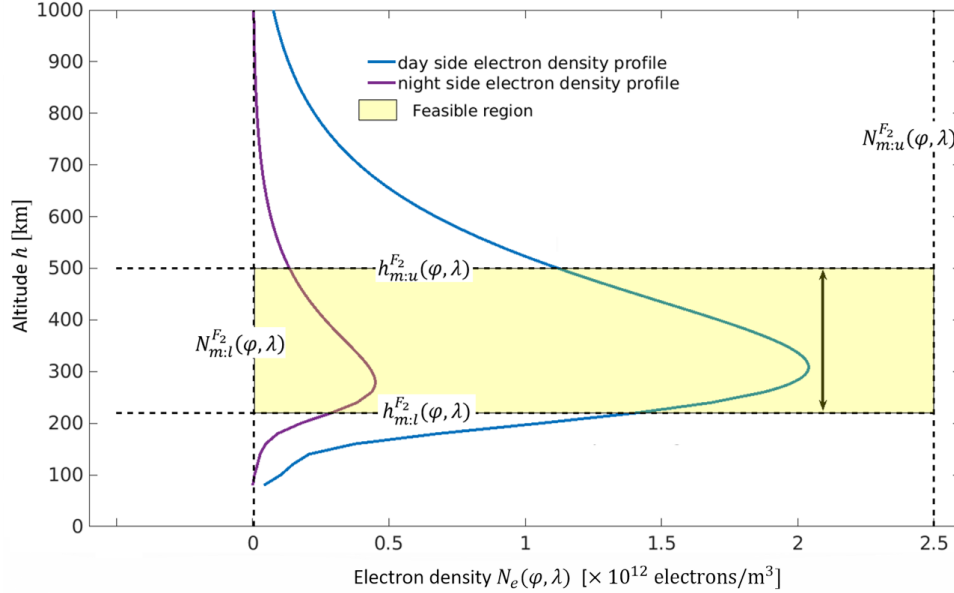


Figure 3.6: Example for the definition of the feasible region in case of the two key parameters $N_m^{F_2}$ and $h_m^{F_2}$ of the F_2 -layer to be estimated at a certain location (φ, λ) . The values $N_{m;l}^{F_2}$, $N_{m;u}^{F_2}$ as well as $h_{m;l}^{F_2}$, $h_{m;u}^{F_2}$ are the lower and upper bounds of the key parameters $N_m^{F_2}$ and $h_m^{F_2}$, respectively, according to the inequality constraints (3.10).

The region enclosed by the constraint bounds $N_{m;l}^{F_2}$, $N_{m;u}^{F_2}$, $h_{m;l}^{F_2}$ and $h_{m;u}^{F_2}$ is called the feasible region $\mathcal{F}_{\mathcal{R}}$ for the key parameters $N_m^{F_2}$ and $h_m^{F_2}$. The final solution of the estimation process must be a pair $(N_m^{F_2}, h_m^{F_2}) \in \mathcal{F}_{\mathcal{R}}$. Figure 3.6 also shows that the lower and upper bounds for the key parameters can be chosen differently for day and night.

For setting up the parameter estimation model we have to linearize Eq. (3.5) for the electron density profile by considering the Eqs. (3.6) and (3.7) with respect to the B-spline coefficients $d_{k_1, k_2; \kappa}^{J_1, J_2}$ of the selected key parameters $\kappa \in \mathcal{K}_1$. Collecting the B-spline coefficients in the vector $\mathbf{d}_{\kappa} = [d_{0,0;\kappa}^{J_1, J_2}, d_{0,1;\kappa}^{J_1, J_2}, \dots, d_{K_{J_1}-1, K_{J_2}-1;\kappa}^{J_1, J_2}]^T$ and decomposing it into the vector $\mathbf{d}_{\kappa;0}$ of the initial values related to the feasible region for the key parameter κ and the vector $\Delta \mathbf{d}_{\kappa}$ of corrections, the inequality constraints (3.10) can be rewritten as matrix equation $\mathbf{B}_{\kappa} \Delta \mathbf{d}_{\kappa} < \mathbf{b}_{\kappa}$, where \mathbf{B}_{κ} is the constraint coefficient matrix and \mathbf{b}_{κ} means the constraint bound vector related to the lower bound function $\kappa_l(\varphi, \lambda)$ and the upper bound function $\kappa_u(\varphi, \lambda)$ of the key parameter $\kappa \in \mathcal{K}_1$.

To demonstrate the developed procedure we introduce the subset

$$\mathcal{K}_1 = \{\kappa_1 = N_m^{F_2}, \kappa_2 = h_m^{F_2}, \kappa_3 = H^{F_2}, \kappa_4 = N_0^P, \kappa_5 = H^P\} \quad (3.12)$$

of the 5 key parameters of the F_2 -layer and the plasmasphere. To set up the estimation model, we introduce the vector $\mathbf{d} = [\mathbf{d}_{\kappa_1}^T, \dots, \mathbf{d}_{\kappa_5}^T]^T$ of the B-spline coefficients for all 5 key parameters κ_1 to κ_5 , the corresponding vector $\mathbf{d}_0 = [\mathbf{d}_{\kappa_1;0}^T, \dots, \mathbf{d}_{\kappa_5;0}^T]^T$ of the initial B-spline coefficient values, the vector $\Delta \mathbf{d} = [\Delta \mathbf{d}_{\kappa_1}^T, \dots, \Delta \mathbf{d}_{\kappa_5}^T]^T$ of the B-spline coefficient corrections and the vector $\mathbf{b} = [\mathbf{b}_{\kappa_1}^T, \dots, \mathbf{b}_{\kappa_5}^T]^T$ of the constraint bounds as well as the matrix $\mathbf{B} = [\mathbf{B}_{\kappa_1}, \dots, \mathbf{B}_{\kappa_5}]$ of the constraint

coefficient matrices and the matrix $\mathbf{A} = [\mathbf{A}_{\kappa_1}, \dots, \mathbf{A}_{\kappa_5}]$ of the partial derivatives of the electron density with respect to the B-spline coefficients of the key parameters κ_1 to κ_5 . Next, we define according to Eq. (3.11) the equality constraints $\mathbf{E}_\kappa \mathbf{d}_\kappa = \mathbf{e}_\kappa$, where \mathbf{E}_κ is the constraint coefficient matrix and \mathbf{e}_κ means the constraint bound vector related to the bound function $\kappa_e(\varphi, \lambda)$ of the key parameter $\kappa \in \mathcal{K}_2$. Finally, we introduce the vector $\Delta \mathbf{n}_e = \mathbf{n}_e - \mathbf{n}_{e;0}$ of the differences between the observed electron density values $\mathbf{n}_e = (N_e(\varphi, \lambda, h))$ and the vector $\mathbf{n}_{e;0}$ of the corresponding values computed from the vector \mathbf{d}_0 of the initial B-spline coefficient values and the vectors \mathbf{d}_κ for the key parameters $\kappa \in \mathcal{K}_2$.

With the aforementioned matrices and vectors, we introduce the Gauss-Markov model

$$\Delta \mathbf{n}_e + \mathbf{e} = \mathbf{A} \Delta \mathbf{d} \quad \text{with} \quad D(\Delta \mathbf{n}_e) = \sigma_0^2 \mathbf{P}^{-1} \quad (3.13)$$

subject to the inequality and equality constraints

$$\mathbf{B}_\kappa \Delta \mathbf{d}_\kappa < \mathbf{b}_\kappa \quad \text{for} \quad \kappa \in \mathcal{K}_1, \quad (3.14)$$

$$\mathbf{E}_\kappa \mathbf{d}_\kappa = \mathbf{e}_\kappa \quad \text{for} \quad \kappa \in \mathcal{K}_2. \quad (3.15)$$

In the model part (3.13) \mathbf{e} means the random vector of the unknown measurement errors, \mathbf{P} is a given positive definite weight matrix of the observations and σ_0^2 means an unknown variance factor.

To solve for the unknown B-spline coefficient correction vector $\Delta \mathbf{d}$ we applied the optimization approach based on the interior point method². We estimate the unknown B-spline coefficients by minimizing the Lagrangian function

$$L(\Delta \mathbf{d}, \boldsymbol{\lambda}, \mathbf{y}) = (\Delta \mathbf{n}_e - \mathbf{A} \Delta \mathbf{d})^T \mathbf{P} (\Delta \mathbf{n}_e - \mathbf{A} \Delta \mathbf{d}) + \boldsymbol{\lambda}^T (\mathbf{B} \Delta \mathbf{d} - \mathbf{b} + \mathbf{y}) \quad (3.16)$$

with respect to the three optimization variables, namely, the B-spline correction vector $\Delta \mathbf{d}$, the vector $\boldsymbol{\lambda}$ of the Lagrange multipliers and the vector \mathbf{y} of the so-called slack variables. From the definition of the objective function (3.16) it has to be stated that the inequality constraints (3.14) for the key parameters $\kappa \in \mathcal{K}_1$, or more correct the corresponding sets of B-spline coefficients, respectively, are transferred to the inequality constraint $\mathbf{y} > \mathbf{0}$ to the vector of the slack variables. However, the interior point method allows for a combined estimation of all optimization variables³.

A software prototype was developed within the reporting period using electron density observations from different sources. As shown in Fig. 3.7 the first input interface is for a VTEC product generated primarily from GNSS observations but also using observations from DORIS and satellite altimetry; for details see Erdogan et al. (2020). The VTEC data is transferred to electron density using the so-called separability approach⁴. The second interface is for IRO measurements from the Formosat-3/COSMIC mission. Accordingly, the third interface is for IRO measurements from the GRACE, GRACE-FO and the CHAMP missions. This interface has been developed also to support additional in-situ observations from Langmuir probe on board of the Swarm satellites.

The electron density observations are collected in the input vector \mathbf{n}_e of the Gauss-Markov model (3.13). The applied optimization approach based on the Lagrangian function (3.16) considers the inequality constraints (3.14) and estimates the B-spline coefficients which are

²Rose-Koerner L.R.: Convex Optimization for Inequality Constrained Adjustment Problems. PhD thesis, Deutsche Geodätische Kommission, Reihe C, 759, München, ISBN 978-3-7696-5171-3, 2015

³Nocedal J., Wright S.J.: Numerical Optimization. Second edition, Springer, ISBN-13: 978-0387-30303-1, 2006

⁴Hernandez-Pajares M., Juan J. M., Sanz J.: Improving the Abel inversion by adding ground GPS data to LEO radio occultations in ionospheric sounding. Geophysical Research Letters, 27(16), 2473–2476, doi: 10.1029/2000GL000032, 2000

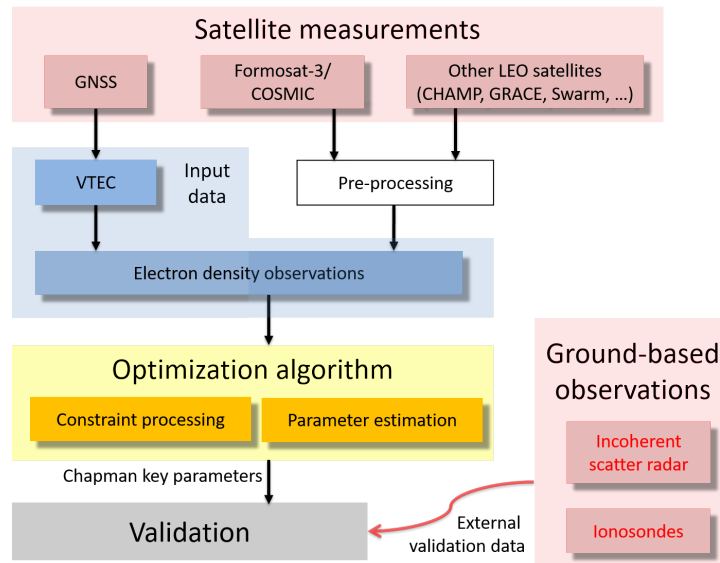


Figure 3.7: Flowchart of the developed procedure to estimate the electron density of the ionosphere and plasmasphere following the optimization approach based on the interior point method by using inequality constraints for selected key parameters.

subsequently transformed to the respective key parameters according to Eq. (3.9). The final validation is independently performed with data from ionosonde and incoherent scatter radar (ISR) data. The complete data flow is visualized in Fig. 3.7. However as a first step, for testing the optimization software routines, we performed a closed-loop validation using IRI model data and adding a 5% noise on the electron density observations. These input data were then used to model the five key parameters listed in the subset (3.12). In Fig. 3.8 the results for the F_2 -layer peak height $h_m^{F_2}(\varphi, \lambda)$ are shown. The estimated peak height values and the reference data from the IRI model are visualized in the top right and the top left panel of Fig. 3.8, respectively. The deviations between these two maps are shown in the bottom left panel and reveal a rather random behavior. Finally, a Monte-Carlo approach was used to obtain the standard deviation map of the estimated peak height in the bottom right panel.

Analysis of empirical thermosphere models during high solar activity

The motion of a satellite depends on gravitational and non-gravitational accelerations. A major problem in the precise orbit determination (POD) of LEO satellites is modeling the non-gravitational perturbations. Among them, the atmospheric drag acceleration — mainly depending on the thermospheric density — is the largest for LEOs with altitudes lower than 1000 km. Consequently, the knowledge of thermospheric density is of crucial importance in many geoscientific applications such as remote sensing, satellite altimetry and satellite gravity missions, where orbits with an accuracy of a few millimeters are required. The comparison of neutral density values of the currently used thermosphere models shows significant differences, especially during times of high solar activity; see Fig. 3.9.

Studies at DGFI-TUM dealt with the spectral analysis of thermospheric density time series from different empirical models to understand which information is contained in these models and how it affects POD. For this purpose, different tools are used, such as Fourier analysis and wavelet analysis. In contrast to the classical Fourier transform, the wavelet transform can detect time-varying amplitudes and/or frequencies of the signal under investigation. Usually, for the visual representation of the wavelet transform the wavelet scalogram is used. It represents the energy distribution in the phase space, which is spanned by the (time) shift b and the scale

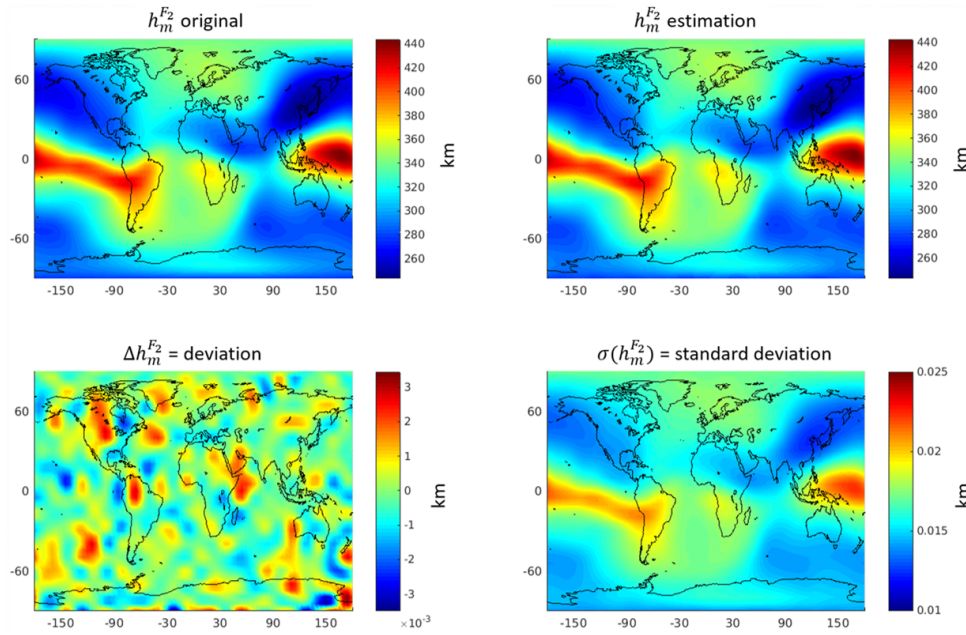


Figure 3.8: Estimation of the peak height h_m^{F2} of the F_2 -layer using electron density observations from the separability approach (incl. 5% noise) and validation in a closed loop by means of the IRI model

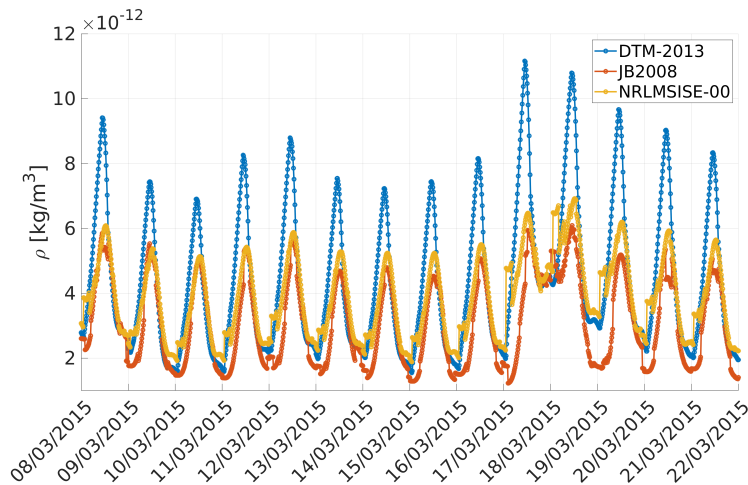


Figure 3.9: Time series for a single location (longitude $\lambda = 5^\circ$, latitude $\phi = 15^\circ$) of the thermospheric density ρ around the St. Patrick Storm day (March 17th, 2015) at an altitude of $h = 400$ km. The choice of the thermosphere model affects considerably the estimation of POD unknowns such as the semi-major axis of the Keplerian ellipse⁵.

parameter a . Applying the Morlet function as wavelet function the scale parameter can be interpreted as the period $T = 2\pi/\omega$ where ω is the angular frequency, the variable of the Fourier transform. In addition, the wavelet variance can also be displayed, which indicates the energy distribution as a function of the scale parameter, i.e. the angular frequency; for more details see Schmidt (2000)⁶. Comparing the wavelet scalograms $W_{x,x}(b,a)$ and $W_{y,y}(b,a)$ of the two time series $x(t)$ and $y(t)$ of the global mean values of the thermospheric density computed from DTM-2013 (Fig. 3.10) and from JB2008 (Fig. 3.11), respectively, the similarities and differences of the time-dependent frequency contents of the two signals can be detected. Clearly visible in the two scalograms

⁶Schmidt M.: Grundzüge der Wavelet-Analyse und Anwendungen in der Geodäsie. Post doctoral thesis, Shaker, 2000

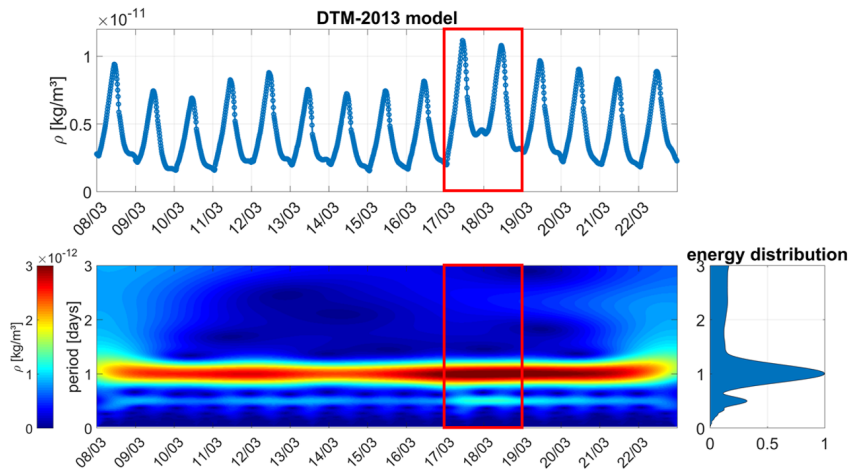


Figure 3.10: Time series $x(t)$ of the global mean values of the thermospheric density from DTM-2013 (top), the related homogenized Morlet-scalogram $\Omega_{x,x}(b,a)$ (bottom left) and the normalized wavelet variance (bottom right) based on the Morlet function defined with shape parameter $\sigma = 1$ and constant $\kappa_0 = 2\pi$; see Schmidt (2000).

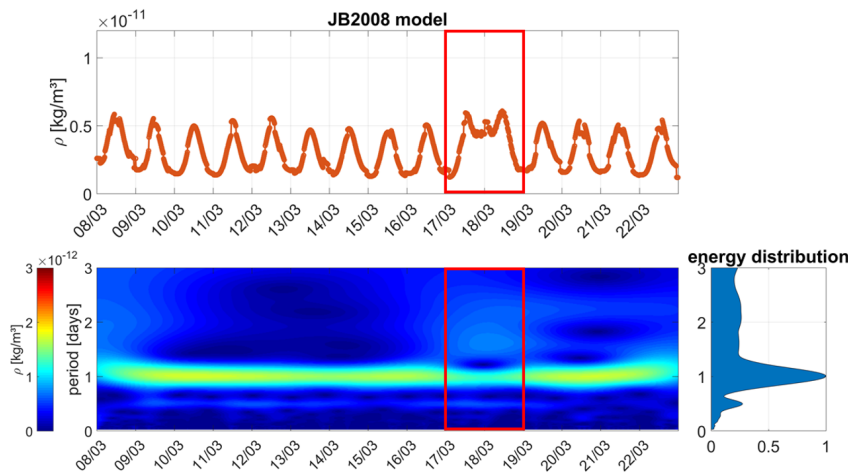


Figure 3.11: Time series $y(t)$ of the global mean values of the thermospheric density from JB2008 (top), the related homogenized Morlet-scalogram $\Omega_{y,y}(b,a)$ (bottom left) and the normalized wavelet variance (bottom right) based on the Morlet function defined with shape parameter $\sigma = 1$ and constant $\kappa_0 = 2\pi$; see Schmidt (2000).

are the period bands at one day and at half a day, which are not constant in time but vary over the 15 days. Thereby, the energy increases and decreases again. Interestingly, both scalograms show a different energy behavior during the St. Patrick Storm event. In DTM-2013 the energy in the 1-day and in the 0.5-day period band increases during this time, in contrast the JB2008 shows lower energy values, this can be explained by the different magnitude values of the time series. Interestingly, the JB2008 shows additional energy in an area larger than 1 day during the St. Patrick Storm event.

Comparing the similarity of the two time series $x(t)$ and $y(t)$, this can be done from the homogenized cross-scalogram $\Omega_{x,y}(b,a) = (\Omega_{x,x}(b,a) \cdot \Omega_{y,y}(b,a))^{1/2}$ which shows values close to 1 where high energy is present in both of the individual scalograms. $\Omega_{x,y}(b,a)$ has values equal to zero if either both scalograms $\Omega_{x,x}(b,a)$ and $\Omega_{y,y}(b,a)$ are equal to zero or only one of them. In the first case the energy distribution of both signals is the same, in the latter case totally different. To detect the similarities the normalized wavelet-coherence $|\Gamma_{x,y}(a)|^2$ has to be analyzed which can be interpreted as a correlation coefficient. In the aforementioned study $|\Gamma_{x,y}(a)|^2$ shows large values around the 1-day period, which indicates a high correlation. In the other

periods it shows particularly lower values because there are differences between the individual wavelet scalograms, especially in the period range between 1.5 days and 2.0 days. From the two panels in Fig. 3.12 it can be concluded that the spectral contents of the two time series are predominantly quite similar. However, during the St. Patrick Storm event the JB2008 model contains obviously more spectral information than DTM-2013. This shows that, in particular, during high solar activity a user must decide very careful which thermospheric model shall be applied. Our investigations further indicate that the currently used thermosphere models need urgently a significant improvement.

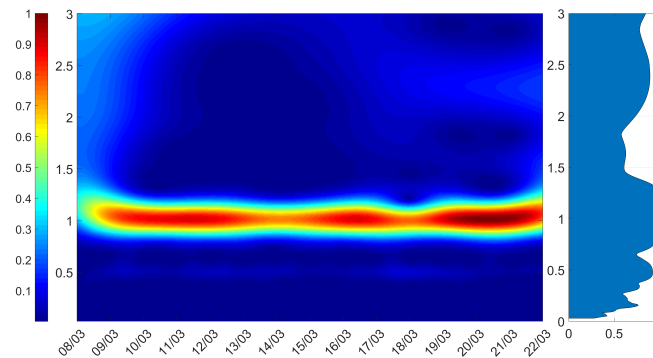


Figure 3.12: Homogenized quadratic cross-scalogram $|\Omega_{x,y}(b,a)|^2$ (left) and normalized wavelet coherence $|\Gamma_{x,y}(a)|^2$ (right).

A further study within the TIPOD project is to extend the empirical thermosphere model, namely CH-Therm 2018 (developed by our GFZ project partners during the DFG-SPP 1788 project INSIGHT; for details see Xiong et al. (2018)⁷), to get a better representation of the height dependency of the thermospheric density. Up to now only a simple exponential function is used, which shall be replaced.

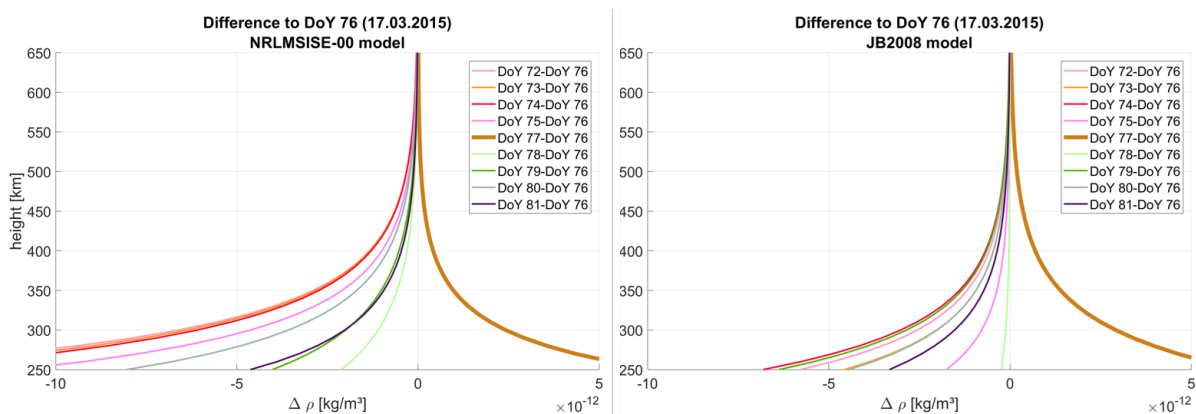


Figure 3.13: Differences of the height profiles of the days DoY 72 (March 13, 2015) to DoY 81 (March 22, 2015) w.r.t the height profile of the St. Patrick Storm day (DoY 76, March 17, 2015) at a single location (longitude $\lambda = 5^\circ$, latitude $\phi = 15^\circ$) at 11:00 UT for the NRLMSISE-00 model (left) and for JB2008 (right).

Figure 3.13 shows the differences of the height profiles of the thermospheric density over a time period of 9 days each after subtracting the height profile for the St. Patrick Storm day. Comparing the thermospheric density values with VTEC values of the ionosphere, it is plainly visible, that the St. Patrick Storm occurred on March 17, 2015, characterized by two peaks at around 12:00 UT and 18:00 UT (see the purple colored curve in Fig. 3.14. This behavior is

⁷Xiong C., Lüher, Schmidt M., Bloßfeld M., Rudenko S.: An empirical model (CH-Therm-2018) of the thermospheric mass density derived from CHAMP satellite. *Annales Geophysicae*, 36(4), 1141-1152, doi:[10.5194/angeo-36-1141-2018](https://doi.org/10.5194/angeo-36-1141-2018), 2018

not reflected by the thermospheric density, because the profile difference of DoY 77 w.r.t. DoY 76 is positive value, indicating that the thermospheric density values on DoY 77 are higher than on DoY 76. This different behavior between the ionospheric and thermospheric density is still under investigation. These studies will contribute to a better understanding and modeling of the thermospheric density and of the coupled thermosphere-ionosphere processes, i.e. the interaction of the neutral particles of the thermosphere with the charged particles of the ionosphere.

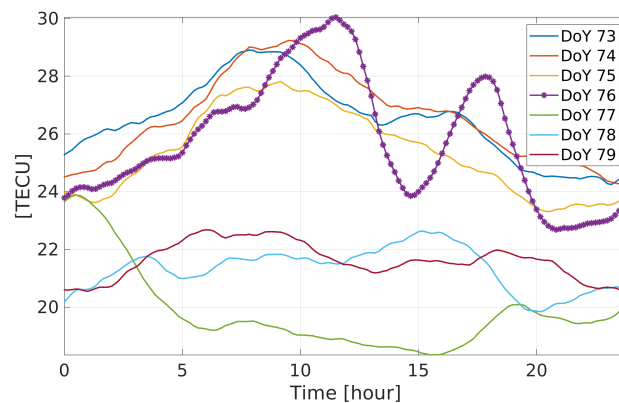


Figure 3.14: Temporal evolution of the global mean VTEC values from DoY 73 (March 14, 2015) to DoY 79 ((March 20, 2015)). Whereas at DoY 76 two VTEC peaks are clearly visible, at the following days DoY 77 to DoY 79 the mean VTEC variations are dramatically decreasing as can be seen from the green, light blue and dark red colored curves.

Related publications

Erdogan E., Schmidt M., Goss A., Görres B., Seitz F.: *Adaptive Modeling of the Global Ionosphere Vertical Total Electron Content*. Remote Sensing, 2020 (in review)

Goss A., Schmidt M., Erdogan E., Görres B., Seitz F.: *High-resolution vertical total electron content maps based on multi-scale B-spline representations*. Annales Geophysicae, 37(4), doi:[10.5194/angeo-37-699-2019](https://doi.org/10.5194/angeo-37-699-2019), 2019

Goss A., Schmidt M., Erdogan E., Seitz F.: *Global and Regional VTEC Modeling with High Resolution Using a Two-Step B-Spline Model*. Remote Sensing, 2020 (in press)

3.2 Regional Gravity Field

The unification of physical height systems is an essential geodetic application of the Earth's gravity field. It is important and urgent to have a global height system consistent within a few centimeters or better, for both scientific and societal demands. A high-resolution and high-precision geoid model is the key to a physical height system. In addition to the global models, regional gravity measurements such as airborne, shipborne or terrestrial gravity observations can be used for regional geoid refinement. High-resolution regional gravity modeling is especially inevitable in mountainous areas, since the very short wavelengths are correlated with local topography to a large extent.

The 1-cm Geoid Experiment

The *1-cm Geoid Experiment*, also known as the *Colorado Experiment*, was proposed by four scientific groups within the International Association of Geodesy (term 2015-2019), namely (1) the Global Geodetic Observing System (GGOS) Joint Working Group (JWG) 0.1.2 "Strategy for the realization of the IHRs", (2) the IAG JWG 2.2.2 "The 1 cm geoid experiment", (3) the IAG Sub-Commission (SC) 2.2 "Methodology for geoid and physical height systems", and (4) the Inter-Commission Committee on Theory (ICCT) Joint Study Group (JSG) 0.15 "Regional geoid/quasi-geoid modeling – Theoretical framework for the sub-centimeter accuracy". 1-cm Geoid Experiment focuses on the computation of geoid heights, height anomalies, and geopotential values (as IHRs coordinates) in Colorado, USA. With altogether fourteen contributions worldwide involved in this experiment with different methodologies, the comparison of the results highlights the disparities between the methods. We contributed to this exercise with the approach of spherical radial basis functions (SRBF) that has been developed and enhanced by DGFI-TUM since many years. The research work is performed within the framework of the DFG-funded **Project ORG4Heights**.

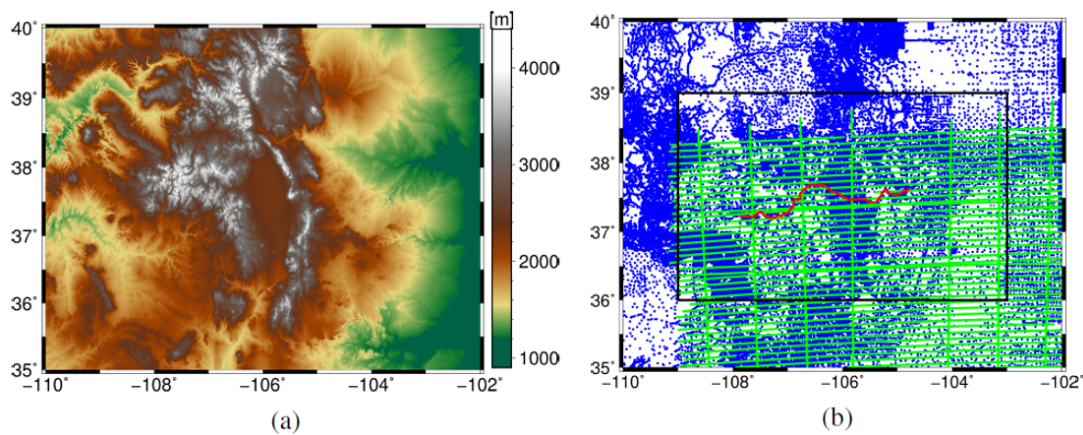


Figure 3.15: (a) Terrain map of the study area; (b) given terrestrial (blue points) and airborne (green flight tracks) gravity data, GSVS17 benchmarks (223 points along the red line) as well as the model grid area (black rectangle)

As shown in Fig. 3.15 (a), Colorado is a mountainous area with a mean elevation of 2017 m and thus a challenging study area for regional gravity field determination. Two data sets are provided within the 1-cm Geoid Experiment: terrestrial gravity data (blue points in Fig. 3.15 (b)) and airborne gravity data (green flight tracks in Fig. 3.15 (b)). Height anomalies and geoid heights as output gravity functionals have to be calculated along the Geoid Slope Validation Survey 2017 (GSVS17) benchmarks (red line in Fig. 3.15 (b)) and at regular grid points between -109° and -103° longitude and between 36° and 39° latitude (black box in Fig. 3.15 (b)) with a spatial resolution of $1' \times 1'$.

The remove-compute-restore (RCR) procedure was applied. Usually, the removed part is the long wavelength component of a global gravity model (GGM), since existing global models approximate this part very accurately. Besides the GGM, topographic models are included additionally to achieve a further improvement of the modeling results. The XGM2016⁸ is chosen as the global gravity model, as topography models we used dV_ELL_Earth2014 as well as ERTM2160. Figure 3.16 visualizes the RCR procedure. It is clear that after the remove step the gravity field becomes much smoother, especially in regions with varying elevation, for instance, the central part of the study area.

⁸Pail R., Fecher T., Barnes D., Factor J., Holmes S., Gruber T., Zingerle P.: Short note: the experimental geopotential model xgm2016. *Journal of Geodesy* 92(4): 443–451, 2018.

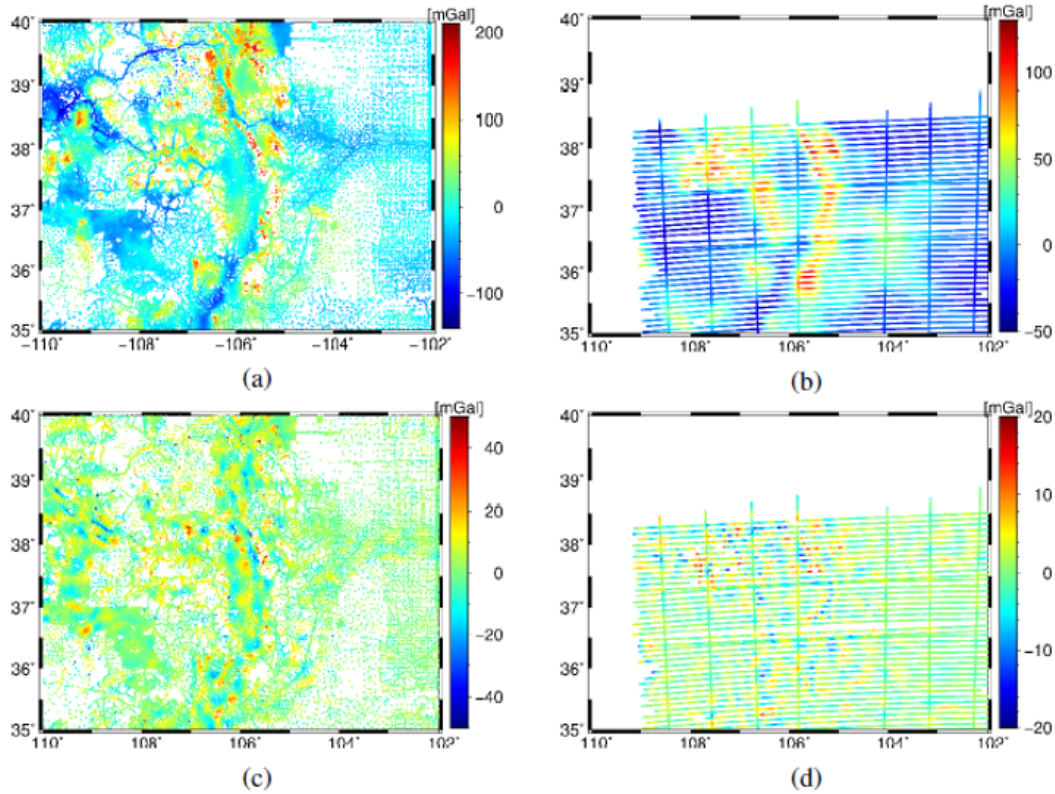


Figure 3.16: The observations (top row) and the remaining parts (bottom row) following the application of the RCR procedure for the terrestrial data (left column, panels (a) and (c)) and the airborne data (right column, panels (b) and (d))

Among the different types of basis functions (see e.g. Schmidt et al., 2007⁹), two types are considered here, namely

1. Shannon function: the low-pass filter properties are given by the Legendre coefficients

$$B_n = \begin{cases} 1 & \text{for } n \in [0, n_{\max}] \\ 0 & \text{else} \end{cases} . \quad (3.17)$$

2. Cubic polynomial (CuP) function: the low-pass filter properties are given by the Legendre coefficients

$$B_n = \begin{cases} (1 - \frac{n}{n_{\max}})^2 (1 + \frac{2n}{n_{\max}}) & \text{for } n \in [0, n_{\max}] \\ 0 & \text{else} \end{cases} . \quad (3.18)$$

As shown in Fig. 3.17, the Shannon function has the properties of an optimal low-pass filter in the spectral domain, but also strong oscillations in the spatial domain. The CuP function has less oscillations in the spatial domain but a smoothing decay in the spectral domain (Liu et al., 2020a).

Mathematically, it can be proven that any convolution of an input signal with a kernel is equivalent to a linear equation system with the same set of series coefficients as long as the used basis functions cover the same spectral domain and are band-limited (Schmidt et al., 2007⁹; Liu et al., 2020b). Thus, as a consequence of this theorem, we can use different SRBFs as kernels for different data sets and can use different SRBFs in the analysis and the synthesis step, respectively, as long as they cover the same frequency range. In this study, we apply the

⁹Schmidt M., Fengler M., Mayer-Gürr T., Eicker A., Kusche J., Sánchez L., Han S.C.: Regional gravity modeling in terms of spherical base functions. *Journal of Geodesy*, 81(1), 17-38, doi:10.1007/s00190-006-0101-5, 2007

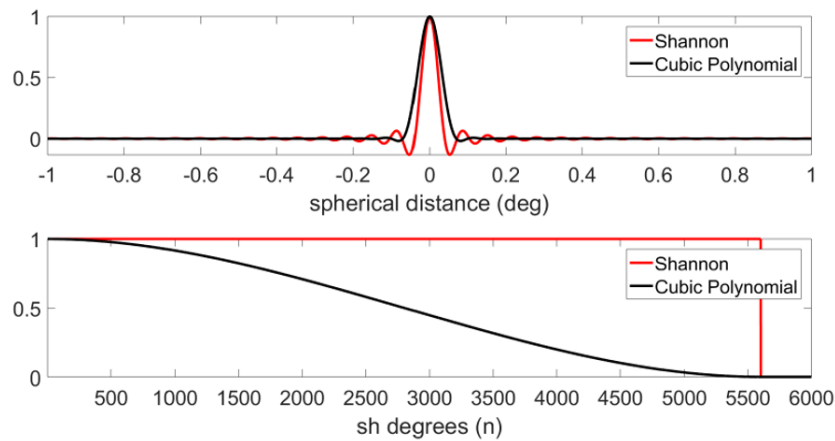


Figure 3.17: Different SRBFs in the spatial domain (top, ordinate values are normed to 1) and the spectral domain (bottom) up to $n_{max} = 5600$

CuP function in the synthesis step to reduce erroneous systematic effects. In the analysis step, the Shannon function is applied to the terrestrial data to avoid the loss of spectral information. The CuP function is applied to the airborne data as a low-pass filter and thus, for filtering the high-frequency noise in the airborne data.

Figure 3.18 shows the deviations of DGFI-TUM's height anomaly (red) and geoid height (blue) results w.r.t. the mean values of the solutions from the fourteen contributing institutions in the 1-cm Geoid Experiment at the GSVS17 benchmarks. A detailed overview about the comparisons is given by Wang et al. (2020). The RMS value of our results compared to the mean of all the participants is 1.0 cm and 1.3 cm for the height anomaly and the geoid height, respectively, which are the smallest among all contributions. The geoid height results are slightly worse than the height anomaly because geoid height is a derived value from the height anomaly. Figure 3.19 visualizes the quasi-geoid as well as the geoid models for the whole investigation area; for more details see Liu et al. (2020b).

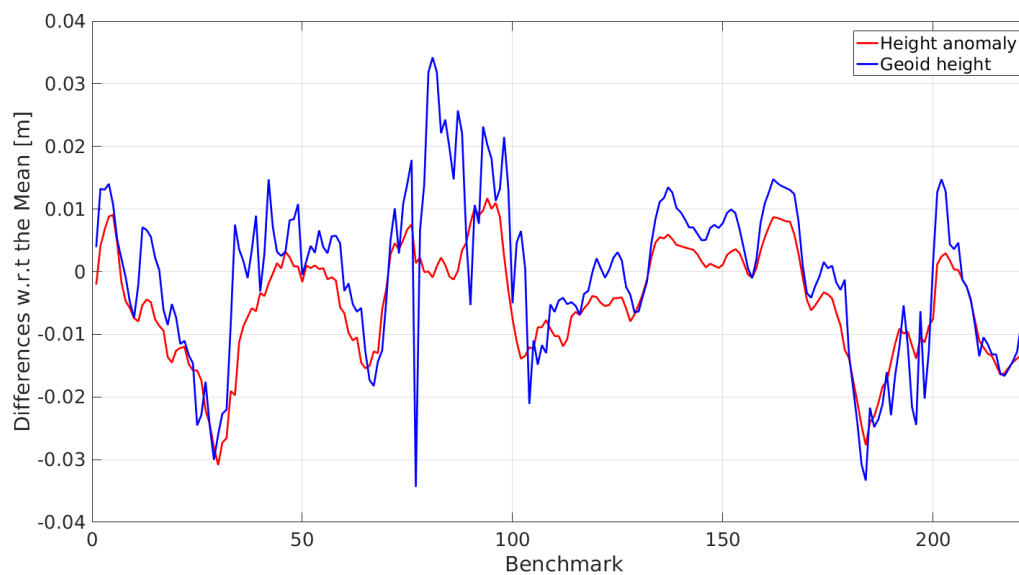


Figure 3.18: Deviations of DGFI-TUM's results for the height anomaly and the geoid height w.r.t. the mean values of the fourteen participants in the "1-cm Geoid Experiment" at the 223 GSVS17 benchmarks.

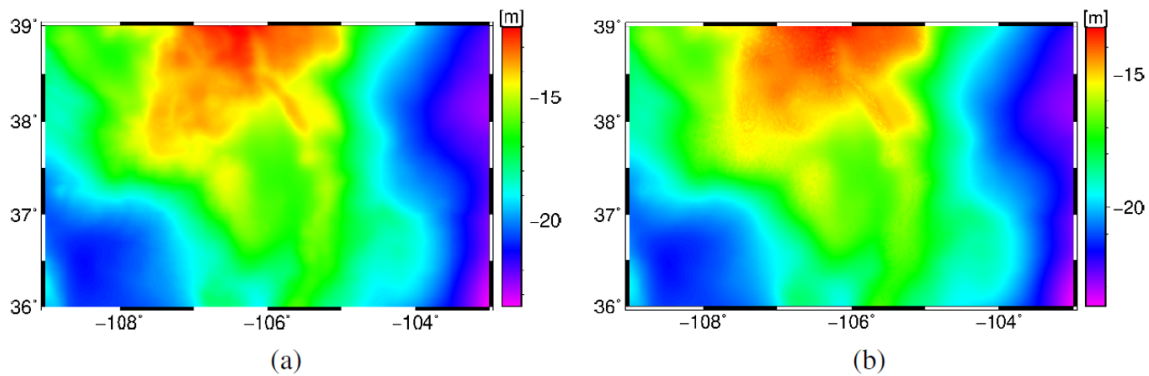


Figure 3.19: (a): Quasi-geoid (a) and geoid (b) model in the area of investigation visualized by the black rectangle in Fig. 3.15 (b).

Related publications

Liu Q., Schmidt M., Pail R., Willberg M.: *Determination of the regularization parameter to combine heterogeneous observations in regional gravity field modeling*. Remote Sensing, 2020a (in review)

Liu Q., Schmidt M., Sánchez L., Willberg M.: *Regional gravity field refinement for (quasi) geoid determination based on spherical radial basis functions in Colorado*. Journal of Geodesy, 2020b (in review)

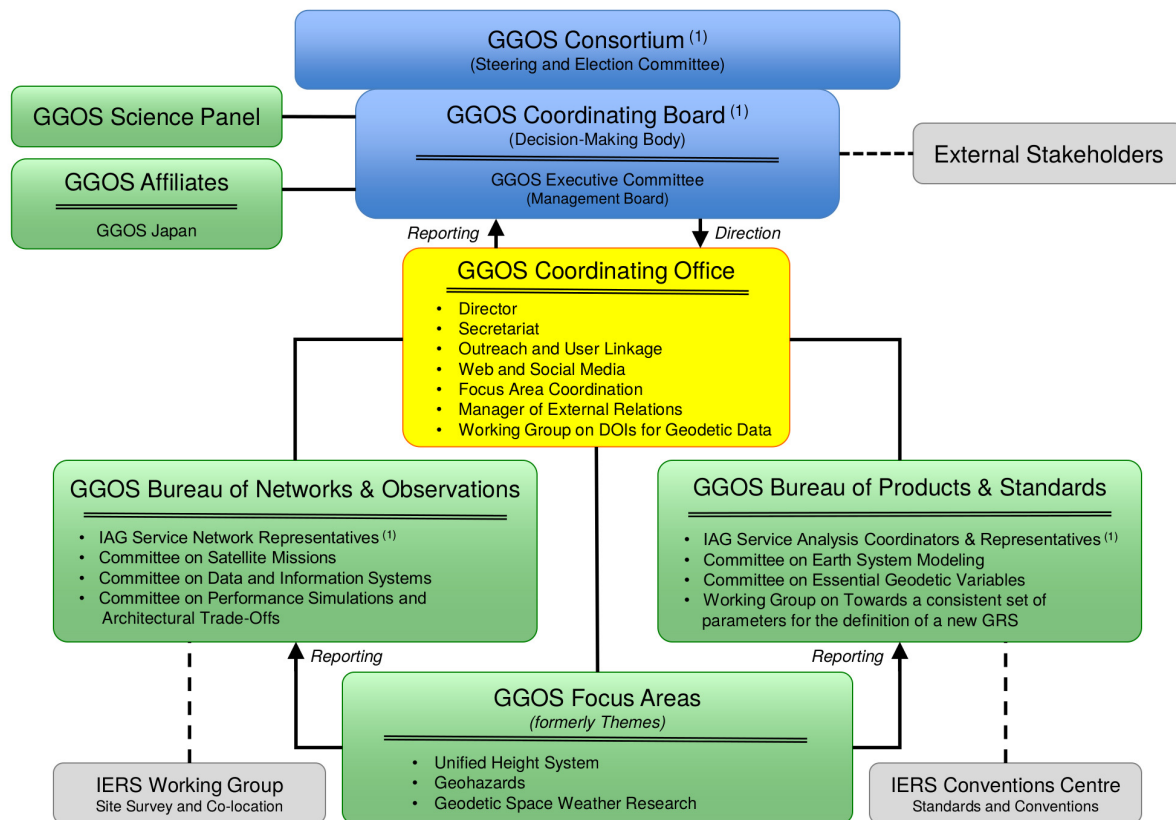
Wang Y.M., Sánchez L., Liu Q., Schmidt M., et al.: *Colorado geoid computation experiment: Overview and summary*. Journal of Geodesy, 2020 (in review)

3.3 Standards and Conventions

The creation and provision of geodetic results and products of highest precision and consistency through the integration of geometric and gravimetric observation data from different sensors is the primary task of the Global Geodetic Observing System (GGOS) of the International Association of Geodesy (IAG). The implementation of this objective relies fundamentally on unified standards and conventions.

Research on the relevance of consistency in parametrization and data analysis for the combination of geodetic space observations has been an important field of study at DGFI-TUM since many years. Also on the international level, DGFI-TUM is strongly involved in the definition and implementation of unified standards and conventions as it chairs the *GGOS Bureau of Products and Standards (BPS)*, one of two GGOS Bureaus (the second one is the Bureau of Networks and Communication, chaired by the Harvard Smithsonian Center for Astrophysics).

In the framework of GGOS, the DGFI-TUM also provides the current GGOS Vice President (Dr. Laura Sánchez) and chairs two of the three GGOS Focus Areas: The FA Unified Height System (see Section 1.4) and the FA Geodetic Space Weather Research (see Section 3.1) (the third FA on Geohazards is chaired by NASA). An overview of the organizational structure of GGOS (current period: 2019-2023) is given in Fig. 3.20.



⁽¹⁾ GGOS is built upon the foundation provided by the IAG Services, Commissions, and Inter-Commission Committees

Figure 3.20: Organizational structure of IAG's Global Geodetic Observing System (GGOS).

GGOS Bureau of Products and Standards

The BPS is chaired by the DGFI-TUM and operated jointly with TUM's Chair of Astronomical and Physical Geodesy within the Research Group Satellite Geodesy (Forschungsgruppe Satellitengeodäsie, FGS). The Bureau supports GGOS in its goal to obtain consistent science data products describing the Earth's surface geometry, its rotation and gravity field as well as the temporal changes of these quantities in mm-accuracy. Such data are of paramount importance for Earth system sciences and provide the fundament for reliably monitoring global change phenomena and geodynamic processes (such as global sea level rise, the melting of glaciers and ice caps, tectonics or earthquakes), see Figure 3.21.

A key objective of the BPS is to keep track of adopted geodetic standards and conventions across all IAG components and to initiate steps to close gaps and deficiencies. The work is primarily built on research activities in data analysis and data combination in the framework of IAG's Scientific Services. The BPS acts as contact and coordinating point regarding homogenization of standards and IAG products. Moreover, the BPS interacts with external stakeholders that are involved in standards and conventions, such as the International Organization for Standardization (ISO), the Bureau International des Poids et Mesures (BIPM), the Committee on Data for Science and Technology (CODATA), the International Astronomical Union (IAU) and the UN GGIM Subcommittee on Geodesy (UM GGIM SCoG).

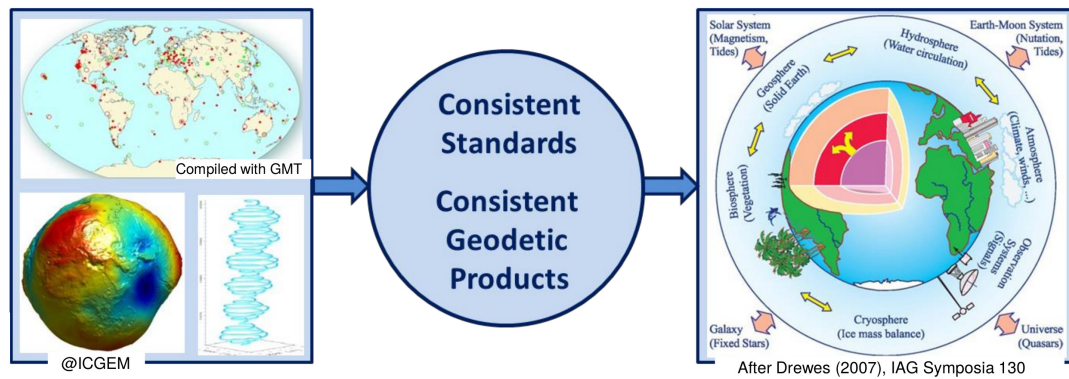


Figure 3.21: The key role of unified standards and conventions: Consistent geodetic science data products for Earth system and climate research.

The tasks of the Bureau of Products and Standards are to:

- act as IAG representative to ISO/TC 211 and to the UN-GGIM GGRF Working Group "Data Sharing and Development of Geodetic Standards";
- contribute to the UN GGIM Subcommittee on Geodesy, mainly to the Working Group "Data Sharing and Development of Geodetic Standards";
- regularly update the inventory on standards and conventions used for the generation of IAG products to incorporate the latest developments in these fields;
- contribute to the re-writing/revision of the IERS Conventions, mainly in the function as Chapter Expert for Chapter 1 "General definitions and numerical standards";
- focus on the integration of geometric and gravimetric observations, and to support the development of integrated products (e.g., GGRF, IHRF, atmosphere products);
- contribute to the Committee on Essential Geodetic Variables (EGV). Such EGVs shall serve as a basis for a gap analysis to identify requirements concerning observational properties and networks, accuracy, spatial and temporal resolution and latency;
- contribute to the newly established GGOS BPS Working Group "Towards a consistent set of parameters for the definition of a new GRS";
- contribute to the GGOS DOI Working Group, focusing on Digital Object Identifier (DOI) for geodetic data and products to improve traceability of data sets and to ensure that data providers receive proper credit for their published data;
- perform activities in organization and coordination as well as in representation and outreach. This includes the organization of internal BPS meetings (every two months), external Bureau meetings (twice per year), the representation of the BPS within IAG and at conferences and workshops, and the presentation and publication of BPS results.

Summary of BPS activities in 2019

A major activity in 2019 was the update of the first version of the BPS Inventory of Standards and Conventions used for the Generation of IAG Products (Angermann et al. 2016¹⁰). The second version of the BPS inventory has been prepared for the publication in the Geodesists Handbook 2020 and takes into account the latest developments. It comprises various updates in the field of standards and conventions, such as the newly released ISO standards by ISO/TC211 covering geographic information and geomatics, the activities of the GGRF Working Group "Data Sharing and Development of Geodetic Standards" within the UN-GGIM Subcommittee on Geodesy, the re-writing/revision of the IERS Conventions initiated by the IERS Conventions Centers, and the recently adopted resolutions by IAG, IUGG and IAU relevant for geodetic standards and products.

In the framework of the re-writing/revision of the IERS Conventions, the director of the BPS (Dr. Detlef Angermann) has been nominated as Chapter Expert for Chapter 1 "General definitions and numerical standards". For the first time, also representatives of the International Gravity Field Service (IGFS) are contributing to the re-writing of this chapter which allows for the consideration of both geometry and gravity field related aspects in the general definitions and numerical standards.

A new GGOS Working Group "Towards a consistent set of parameters for the definition of a new GRS" has been established as a component of the BPS at the end of 2019 in order to solve open problems concerning numerical standards in the context of time and tide systems. The fact that various definitions are in use within the geodetic community is a potential source for inconsistencies and even errors of geodetic products. The BPS recommends to resolve these inconsistencies and to develop a new Geodetic Reference System.

The second version of the BPS inventory also includes an update of the product-based review. New versions of IERS products have been released for the Celestial (ICRF) and Terrestrial (ICRF) Reference Frames as well as for the Earth Orientation Parameters (EOP), namely ICRF3, ITRF2014 and EOP 14C04. Although a significant progress has been achieved compared to the previous realizations, there are still some deficiencies and open problems that are addressed in the inventory. Recommendations are provided to further improve the accuracy and consistency of these products. Concerning GNSS satellite orbits, the modeling has been improved and some missing information has been provided by the satellite operators, but there are still remaining deficiencies. A remarkable progress has been achieved in the field of gravity and geoid related data and results, including the establishment of the IGFS Central Bureau and the development of a dedicated data and products portal based on online applications for the creation of metadata for gravity and geoid data. Also the latest developments and achievements in the field of height systems and their realizations are reported (see Section 1.4 for more information on DGFI-TUM's research concerning Height Systems).

BPS staff and representation of IAG components and other entities

The present BPS staff members are Detlef Angermann (director), Thomas Gruber (deputy director), Michael Gerstl, Urs Hugentobler and Laura Sánchez (all from Technical University of Munich), as well as Robert Heinkelmann (GFZ Potsdam, Germany) and Peter Steigenberger (DLR Oberpfaffenhofen, Germany).

¹⁰Angermann D., Gruber T., Gerstl M., Heinkelmann R., Hugentobler U., Sánchez L., Steigenberger P.: GGOS Bureau of Products and Standards: Inventory of standards and conventions used for the generation of IAG products. In: Drewes H., Kuglitsch F., Adám J. (Eds.) The Geodesist's Handbook 2016, Journal of Geodesy, 90(10), 1095-1156, doi:[10.1007/s00190-016-0948-z](https://doi.org/10.1007/s00190-016-0948-z), 2016

In its current structure, the following GGOS entities are associated with the BPS:

- Committee “Contributions to Earth System Modelling”, Chair: M. Thomas (GFZ Potsdam, Germany);
- Committee “Definition of Essential Geodetic Variables (EGVs)”, Chair: R. Gross (NASA, USA);
- Working Group “Towards a consistent set of parameters for the definition of a new GRS”, Chair: U. Marti (Swisstopo, Switzerland).

According to its charter, the work of the BPS requires a close interaction with the IAG Analysis and Combination Centers regarding the homogenization of standards and products. The IAG Services and the other entities involved in standards and geodetic products have chosen their representatives as associated members of the BPS. The Bureau comprises the staff members, the chairs of the associated GGOS components, the two committees and the working group as listed above, as well as representatives of the IAG Services and other entities. The status of December 2019 is summarized in Table 3.1. Regarding the development of standards, there is a direct link with the IERS Conventions Center as well as with ISO (with its Technical Committee ISO/TC211), BIPM, CODATA, IAU and the UM GGIM SCoG.

Table 3.1: Associated members of the BPS, representing the IAG Services, IAU and other entities (status: December 2019).

T. Herring, N. Stamatakis, USA	International Earth Rotation and Reference Systems Service (IERS)
U. Hugentobler, Germany	International GNSS Service (IGS)
E. Pavlis, USA	International Laser Ranging Service (ILRS)
J. Gipson, USA	International VLBI Service for Geodesy and Astrometry (IVS)
F. Lemoine, J. Ries, USA	International DORIS Service (IDS)
J.-M. Lemoine, H. Capdeville, France	International DORIS Service (IDS)
R. Barzaghi, Italy	International Gravity Field Service (IGFS)
S. Bonvalot, France	Bureau Gravimetric International (BGI)
M. Reguzzoni, Italy	International Service for the Geoid (ISG)
E. Ince, Germany	International Center for Global Earth Models (ICGEM)
K. M. Kelly, USA	International Digital Elevation Model Service (IDEMS)
H. Wziontek, Germany	International Geodynamics and Earth Tide Service (IGETS)
J. L. Hilton, USA	IAU Commission A3 Representative
M. Craymer, Canada	Chair of Control Body for ISO Geodetic Registry Network
L. Hothem, USA	Vice-Chair of Control Body for ISO Geodetic Registry Network
J. Ádám, Hungary	IAG Communication and Outreach Branch
D. Angermann, Germany	IAG representative to ISO/TC211
J. Kusche, Germany	Representative of gravity community

4 Scientific Transfer

The transfer of knowledge, results and data within the scientific community and with the public is an essential element of scientific working. The following section sets out DGFI-TUM's efforts with respect to the most relevant instruments for the exchange of information: the cooperation in scientific organizations and collaborative research programs on national and international level, scientific publications and presentations, the participation in scientific meetings, guest researchers and the operation of internet portals.

Section 4.1 provides a compilation of the positions and involvement of DGFI-TUM staff in national and international scientific organizations. The institute is strongly networked with other institutions worldwide, in particular through research activities in the framework of the International Union of Geodesy and Geophysics (IUGG), the International Astronomical Union (IAU), and the International Association of Geodesy (IAG). The DGFI-TUM is a key player in IAG's Global Geodetic Observing System (GGOS) (cf. Section 3.3), and it operates, mostly by virtue of long-term commitments, research centers, analysis centers, and data centers (cf. Section 1). Scientists of the institute collaborate in various cooperative projects, working and study groups, and, in accordance with DGFI-TUM's international strategy, DGFI-TUM staff takes numerous key positions and functions in management and support to actively contribute to shaping the future direction of international geodetic research.

Sections 4.2 lists the articles printed or published online in 2019. Section 4.3 contains the directory of posters and talks presented by DGFI-TUM staff at the numerous national and international conferences, symposia and workshops listed in Section 4.4. Guests who visited DGFI-TUM in the frame of research cooperations during 2019 are listed in Section 4.5. In order to share scientific information and to exchange results and data with partners and the interested public, the DGFI-TUM maintains several web sites, public databases and a facebook page. An overview of the portals operated is provided in Section 4.6.

4.1 Functions in Scientific Bodies

United Nations Global Spatial Information Management (UN-GGIM)

- Subcommittee “Geodesy” (Working Group for a Global Geodetic Reference Frame, GGRF)
IAG Representative for the Working Group “Data Sharing and Development of Standards”:
Angermann D.

International Astronomical Union (IAU)

- Commission A.2, Rotation of the Earth,
President: Seitz F., Member: Seitz M.
- Division A, Fundamental Astronomy,
Member of the Steering Committee: Seitz F.
- Joint IAU CA.2/IAG/IERS Working Group Consistent Realization of TRF, CRF and EOP,
Vice-Chair: Seitz M., Member: Seitz F.
- Joint IAU CA.2/IAG Working Group Theory of Earth Rotation and Validation,
Member: Seitz F.

International Union of Geodesy and Geophysics (IUGG)

- *Representative to the Panamerican Institute for Geodesy and History (PAIGH):*
Sánchez L.

International Association of Geodesy (IAG)

- Global Geodetic Observing System (GGOS),
Vice-president: Sánchez L.
- Global Geodetic Observing System (GGOS) Coordinating Board,
Member: Angermann D., Sánchez L., Schmidt M.
- Global Geodetic Observing System (GGOS) Executive Committee,
Member: Angermann D.
- Global Geodetic Observing System (GGOS) Bureau of Products and Standards,
Director: Angermann D., Member: Sánchez L.
- Global Geodetic Observing System (GGOS) Focus Area Unified Height System,
Lead: Sánchez L.
- Global Geodetic Observing System (GGOS) Focus Area Geodetic Space Weather Research,
Lead: Schmidt M.
- Global Geodetic Observing System (GGOS) GGOS Bureau of Products and Standards, Working Group Towards a consistent set of parameters for the definition of a new GRS, *IHRF representative: Sánchez L.*
- Global Geodetic Observing System (GGOS) Focus Area Unified Height System, Joint Working Group Implementation of the International Height Reference Frame (IHRF),
Chair: Sánchez L.
- Global Geodetic Observing System (GGOS) Focus Area Geodetic Space Weather Research, Joint Working Group 1 Electron density modeling,
Member: Gerzen T., Goss A., Schmidt M.
- Global Geodetic Observing System (GGOS) Joint Working Group Validation of VTEC models for high-precision and high resolution applications,
Member: Goss A.
- Global Geodetic Observing System (GGOS) Joint Working Group on Improvement of thermosphere models,
Member: Schmidt M., Zeitler L.
- Global Geodetic Observing System (GGOS) Joint Working Group on the Realization of the IHRF,
Chair: Sánchez L.
- Global Geodetic Observing System (GGOS) Joint Working Group for the establishment of the Global Geodetic Reference Frame (GGRF),
Member: Angermann D., Sánchez L.
- Global Geodetic Observing System (GGOS) Working Group on DOIs for Geodetic Data,
Member: Schwatke C.
- Global Geodetic Observing System (GGOS) Working Group on Performance Simulations and Architectural Trade-Offs (PLATO),
Member: Bloßfeld M., Kehm A., Seitz M.

- IAG Symposia Series,
Assistant Editor-in-Chief: Sánchez L.
- Commission 1 Sub-Commission 1.4 Interaction of celestial and terrestrial reference frames,
Member: Seitz M.
- Commission 1 Working Group 1.3.1 Time dependent transformations between reference frames,
Member: Sánchez L.
- Commission 1 Joint Working Group 0.22 Definition of next generation terrestrial reference frames,
Member: Bloßfeld M., Seitz M.
- Commission 2 Joint Working Group 2.1.1 Establishment of the International Gravity Reference Frame,
Corresponding member, IHRF representative: Sánchez L.
- Commission 2 Joint Working Group 2.2.2 Error assessment of the 1 cm geoid experiment,
Member: Sánchez L., Liu Q.
- Commission 3 Joint Working Group C.1 Climate Signatures in Earth Orientation Parameters,
Member: Göttl F.
- Commission 4 Sub-Commission 4.3 Atmosphere Remote Sensing,
Chair: Schmidt M.
- Commission 4 Joint Working Group 4.3.3 Combination of Observation Techniques for Multi-dimensional Ionosphere Modeling,
Member: Erdogan E.
- Commission 4 Working Group 4.3.1 Real Time Ionosphere Monitoring,
Member: Dettmering D., Erdogan E., Goss A.
- Commission 4 Working Group 4.3.2 Ionosphere Predictions,
Vice-Chair: Erdogan E.
- Commission 4 Working Group 4.3.3 Ionosphere Scintillations,
Member: Schmidt M.
- ICCT Joint Study Group 0.14 Fusion of multi-technique satellite geodetic data,
Member: Bloßfeld M.
- ICCT Joint Study Group 0.19 Time series analysis in geodesy,
Member: Schmidt M.
- ICCT Joint Study Group 0.20 Space weather and ionosphere,
Member: Lalgudi Gopalakrishnan G.
- ICCT Joint Study Group Geoid/quasi-geoid modeling for realization of the geopotential height datum,
Member: Sánchez L.

International Association of Geodesy (IAG) and International Earth Rotation and Reference Systems Service (IERS)

- Joint Working Group on Site Survey and Co-location,
Member: Angermann D., Seitz M.

International Earth Rotation and Reference Systems Service (IERS)

- Directing Board,
Associate member: Angermann D., Bloßfeld M., Seitz M.
- ITRS Combination Center,
Chair: Seitz M., Member: Bloßfeld M.
- Working Group on SINEX Format,
Member: Seitz M.
- Working Group on Site Coordinate Time Series Format,
Member: Seitz M.

International Laser Ranging Service (ILRS)

- Analysis Standing Committee,
Member: Bloßfeld M., Kehm A., Schwatke C.
- EUROLAS Data Center (EDC),
Chair: Schwatke C.
- Data Formats and Procedures Standing Committee,
Chair: Schwatke C.
- Governing Board,
Member: Schwatke C.
- Networks and Engineering Standing Committee,
Member: Schwatke C.
- ILRS Operations Center,
Chair: Schwatke C.
- Study Group on Data Format Update,
Member: Schwatke C.
- Study Group on ILRS Software Library,
Member: Schwatke C.

International VLBI Service for Geodesy and Astrometry (IVS)

- Operational Analysis Center,
Member: Glomsda M., Seitz M.
- Combination Center (jointly with BKG),
Member: Bloßfeld M., Seitz M.

International DORIS Service (IDS)

- Associate Analysis Center,
Member: Bloßfeld M., Rudenko S.
- DORIS Analysis Working Group,
Member: Bloßfeld M., Rudenko S.
- Governing Board,
Member: Dettmering D.
- Working Group on NRT DORIS data,
Chair: Dettmering D., Member: Erdogan E., Schmidt M.

International GNSS Service (IGS)

- Governing Board,
Network Representative: Sánchez L.
- GPS Tide Gauge Benchmark Monitoring - Working Group,
Member: Sánchez L.
- Ionosphere Working Group,
Member: Schmidt M.
- Regional Network Associate Analysis Center for SIRGAS,
Chair: Sanchez L.

International Service for the Geoid (ISG)

- *Scientific Advisor: Sánchez L.*

European Geosciences Union (EGU)

- Early career scientist representative, Division Geodesy,
Bloßfeld M.
- Vening Meinesz Medal Committee,
Chair: Schmidt M.

European Commission (EC)

- Coastal Waters Research Synergy Framework (CoReSyF) User Board,
Member: Passaro M.

European Commission (EC) / European Space Agency (ESA)

- Copernicus POD Quality Working Group,
Member: Dettmering D.

European Space Agency (ESA)

- CryoSat Expert Group,
Member: Passaro M.
- Coastal Altimetry Workshop Organizing Committee,
Member: Passaro M.

European Space Agency (ESA) / Centre National d'Etudes Spatiales (CNES)

- Scientific Committee of "25 Years of Progress in Radar Altimetry Symposium",
Member: Passaro M.

European Space Agency (ESA) / European Organisation for the Exploitation of Meteorological Satellites (EUMETSAT)

- Sentinel-3 Validation Team, Altimetry sub-group,
Member: Dettmering D.

Centre National d'Etudes Spatiales (CNES) / National Aeronautics and Space Administration (NASA)

- Ocean Surface Topography Science Team,
Member: Dettmering D., Passaro M., Schwatke C.

Sistema de Referencia Geocéntrico para las Américas (SIRGAS)

- Scientific Committee,
Member: *Sánchez L.*
- SIRGAS Analysis Center,
Chair: *Sánchez L.*

Forschungsgruppe Satellitengeodäsie (FGS)

- Deputy Speaker: *Seitz F.*
- Managing Board,
Member: *Schmidt M., Seitz F.*

Ausschuss Geodäsie der Bayerischen Akademie der Wissenschaften (Deutsche Geodätische Kommission, DGK)

- Member: *Seitz F.*

Deutsche Gesellschaft für Geodäsie, Geoinformation und Landmanagement (DVW)

- Working Group 7: Experimentelle, Angewandte und Theoretische Geodäsie,
Member: *Schmidt M., Seitz F.*

4.2 Publications

Angermann D., Gruber T., Gerstl M., Heinkelmann R., Hugentobler U., Sanchez L., Steigenberger P.: *GGOS Bureau of Products and Standards*. In: Drewes H., Kuglitsch F. (Eds.), Reports 2015-2019 of the International Association of Geodesy, Travaux de l'AIG 41, 2019

Ardhuin F., Stopa J., Chapron B., Collard F., Husson R., Jensen R.E., Johannessen J., Mouche A., Passaro M., Quartly G., Swail V., Young I.: *Observing Sea States*. Frontiers in Marine Science, 6:124, doi:[10.3389/fmars.2019.00124](https://doi.org/10.3389/fmars.2019.00124), 2019

Benveniste J., Cazenave A., Vignudelli S., Fenoglio-Marc L., Shah R., Almar R., Andersen O., Birol F., Bonnefond P., Bouffard J., Calafat F., Cardellach E., Cipollini P., Le Cozannet G., Dufau C., Fernandes M.J., Frappart F., Garrison J., Gommenginger C., Han G., Hoyer J.L., Kourafalou V., Leuliette E., Li, Z., Loisel H., Madsen K., Marcos M., Melet A., Meyssignac B., Pascual A., Passaro M., Ribó S., Scharroo R., Song Y.T., Speich S., Wilkin J., Woodworth P., Wöppelmann, G.: *Requirements for a Coastal Hazards Observing System*. Frontiers in Marine Science, 6:348, doi:[10.3389/fmars.2019.00348](https://doi.org/10.3389/fmars.2019.00348), 2019

Boergens E., Dettmering D., Seitz F.: *Observing water level extremes in the Mekong River Basin: The benefit of long-repeat orbit missions in a multi-mission satellite altimetry approach*. Journal of Hydrology, 570, 463-472, doi:[10.1016/j.jhydrol.2018.12.041](https://doi.org/10.1016/j.jhydrol.2018.12.041), 2019

Busker T., de Roo A., Gelati E., Schwatke C., Adamovic M., Bisselink B., Pekel J.-F., Cotnam A.: *A global lake and reservoir volume analysis using a surface water dataset and satellite altimetry*. Hydrology and Earth System Sciences, 23(2), 669-690, doi:[10.5194/hess-23-669-2019](https://doi.org/10.5194/hess-23-669-2019), 2019

Chereskin T., Gille S., Rocha C., Menemenlis D., Passaro M.: *Characterizing the transition from balanced to unbalanced motions in the southern California Current*. Journal of Geophysical Research: Oceans, doi:[10.1029/2018jc014583](https://doi.org/10.1029/2018jc014583), 2019

- Dettmering D., Passaro M., Braun A.: *Editorial for Special Issue: Advances in Satellite Altimetry and its Application*. Remote Sensing, 11(24), 2913, doi:[10.3390/rs11242913](https://doi.org/10.3390/rs11242913), 2019
- Dettmering D., Schwatke C.: *Multi-Mission Cross-Calibration of Satellite Altimeters - Systematic Differences between Sentinel-3A and Jason-3*. International Association of Geodesy Symposia, 150, Springer, doi:[10.1007/1345_2019_58](https://doi.org/10.1007/1345_2019_58), 2019
- Gómez-Enri J., Vignudelli S., Izquierdo A., Passaro M., González C., Cipollini P., Bruno M., Álvarez Ó., Mañanes R.: *Sea Level Variability in the Strait of Gibraltar from Along-Track High Spatial Resolution Altimeter Products*. International Association of Geodesy Symposia, 150, Springer, doi:[10.1007/1345_2019_54](https://doi.org/10.1007/1345_2019_54), 2019
- Goss A., Schmidt M., Erdogan E., Görres B., Seitz F.: *High-resolution vertical total electron content maps based on multi-scale B-spline representations*. Annales Geophysicae, 37(4), doi:[10.5194/angeo-37-699-2019](https://doi.org/10.5194/angeo-37-699-2019), 2019
- Göttl F., Murböck M., Schmidt M., Seitz F.: *Reducing filter effects in GRACE-derived polar motion excitations*. Earth, Planets and Space, 71(117), doi:[10.1186/s40623-019-1101-z](https://doi.org/10.1186/s40623-019-1101-z), 2019
- Hellmers H., Thaller D., Bloßfeld M., Kehm A., Girdiuk A.: *Combination of VLBI Intensive Sessions with GNSS for generating Low latency Earth Rotation Parameters*. Advances in Geosciences, 50, 49–56, doi:[10.5194/adgeo-50-49-2019](https://doi.org/10.5194/adgeo-50-49-2019), 2019
- Kehm A., Bloßfeld M., König P., Seitz F.: *Future TRFs and GGOS – where to put the next SLR station?* Advances in Geosciences, 50, 17–25, doi:[10.5194/adgeo-50-17-2019](https://doi.org/10.5194/adgeo-50-17-2019), 2019
- Luceri V., Pirri M., Rodríguez J., Appleby G., Pavlis E. C., Müller H.: *Systematic errors in SLR data and their impact on the ILRS products*. Journal of Geodesy, 93, 2357–2366, doi:[10.1007/s00190-019-01319-w](https://doi.org/10.1007/s00190-019-01319-w), 2019
- Marti F., Cazenave A., Birol F., Passaro M., Leger F., Nino F., Almar R., Benveniste J., Legeais J.F.: *Altimetry-based sea level trends along the coast of Western Africa*. Advances in Space Research, doi:[10.1016/j.asr.2019.05.033](https://doi.org/10.1016/j.asr.2019.05.033), 2019
- Müller F., Dettmering D., Wekerle C., Schwatke C., Passaro M., Bosch W., Seitz F.: *Geostrophic currents in the northern Nordic Seas from a combination of multi-mission satellite altimetry and ocean modeling*. Earth System Science Data, 11(4), 1765–1781, doi:[10.5194/essd-11-1765-2019](https://doi.org/10.5194/essd-11-1765-2019), 2019
- Müller F., Dettmering D., Wekerle C., Schwatke C., Bosch W., Seitz F.: *Geostrophic Currents in the northern Nordic Seas: A Combined Dataset of Multi-Mission Satellite Altimetry and Ocean Modeling (data)*. Deutsches Geodätisches Forschungsinstitut, Munich, doi:[10.1594/PANGAEA.900691](https://doi.org/10.1594/PANGAEA.900691), 2019
- Müller F., Wekerle C., Dettmering D., Passaro M., Bosch W., Seitz F.: *Dynamic ocean topography of the northern Nordic seas: a comparison between satellite altimetry and ocean modeling*. The Cryosphere, 13, 611–626, doi:[10.5194/tc-13-611-2019](https://doi.org/10.5194/tc-13-611-2019), 2019
- Pearlman M., Arnold D., Davis M., Barlier F., Biancale R., Vasiliev V., Ciufolini I., Paolozzi A., Pavlis E., Sośnica K., Bloßfeld M.: *Laser geodetic satellites: a high-accuracy scientific tool*. Journal of Geodesy, 93(11), 2181–2194, doi:[10.1007/s00190-019-01228-y](https://doi.org/10.1007/s00190-019-01228-y), 2019
- Piccioni G., Dettmering D., Bosch W., Seitz F.: *TICON: Tidal CONstants based on GESLA sea-level records from globally located tide gauges*. Geoscience Data Journal, 6(2), 97–104, doi:[10.1002/gdj3.72](https://doi.org/10.1002/gdj3.72), 2019

- Piccioni G., Dettmering D., Schwatke C., Passaro M., Seitz F.: *Design and regional assessment of an empirical tidal model based on FES2014 and coastal altimetry*. Advances in Space Research, doi:[10.1016/j.asr.2019.08.030](https://doi.org/10.1016/j.asr.2019.08.030), 2019
- Quartly G., Rinne E., Passaro M., Andersen O. B., Dinardo S., Fleury S., Guillot A., Hendricks S., Kurekin A., Müller F. L., Ricker R., Skourup H., Tsamados M.: *Retrieving Sea Level and Freeboard in the Arctic: A Review of Current Radar Altimetry Methodologies and Future Perspectives*. Remote Sensing, 11(7), doi:[10.3390/rs11070881](https://doi.org/10.3390/rs11070881), 2019
- Quartly G., Smith W., Passaro M.: *Removing Intra-1-Hz Covariant Error to Improve Altimetric Profiles of σ^0 and Sea Surface Height*. IEEE Transactions on Geoscience and Remote Sensing, 57(6), 3741–3752, doi:[10.1109/tgrs.2018.2886998](https://doi.org/10.1109/tgrs.2018.2886998), 2019
- Ren X., Zhang X., Schmidt M., Zhao Z., Chen J., Zhang J., Li X.: *Performance of GNSS Global Ionospheric Modeling augmented by LEO Constellation*. Earth and Space Science, doi:[10.1029/2019ea000898](https://doi.org/10.1029/2019ea000898), 2019
- Reyes R., Noveloso D., Rediang A., Passaro M., Bringas D., Nagai M.: *Tide gauge and satellite altimetry data for possible land motion detection in south east Bohol trench and fault*. ISPRS International Archives of the Photogrammetry, Remote Sensing and Spatial Information Sciences XLII-4/W19, 369–376, doi:[10.5194/isprs-archives-xxii-4-w19-369-2019](https://doi.org/10.5194/isprs-archives-xxii-4-w19-369-2019), 2019
- Riepl S., Müller H., Mähler S., Eckl J., Klügel T., Schreiber U., Schüler T.: *Operating two SLR systems at the Geodetic Observatory Wettzell: from local survey to space ties*. Journal of Geodesy, 93, 2379–2387, doi:[10.1007/s00190-019-01243-z](https://doi.org/10.1007/s00190-019-01243-z), 2019
- Rose S.K., Andersen O.B., Passaro M., Ludwigsen C.A., Schwatke C.: *Arctic Ocean Sea Level Record from the Complete Radar Altimetry Era: 1991–2018*. Remote Sensing, 11(14), 1672, doi:[10.3390/rs11141672](https://doi.org/10.3390/rs11141672), 2019
- Rudenko S., Esselborn S., Schöne T., Dettmering D.: *Impact of terrestrial reference frame realizations on altimetry satellite orbit quality and global and regional sea level trends: a switch from ITRF2008 to ITRF2014*. Solid Earth, 10(1), 293–305, doi:[10.5194/se-10-293-2019](https://doi.org/10.5194/se-10-293-2019), 2019
- Sánchez L.: *Report of the GGOS Focus Area Unified Height System and the Joint Working Group 0.1.2: Strategy for the Realization of the International Height Reference System (IHR)*. Reports 2015–2019 of the International Association of Geodesy, Travaux de l'AIG 41, Global Geodetic Observing System (GGOS), 42–51, 2019
- Sánchez L.: *SIRGAS Regional Network Associate Analysis Centre Technical Report 2018*. In: Villiger A., Dach R. (Eds.), International GNSS Service Technical Report 2018 (IGS Annual Report), 109–125, doi:[10.7892/boris.130408](https://doi.org/10.7892/boris.130408), 2019
- Scherer D.: *Estimation of River Discharge using Satellite Altimetry and optical Remote Sensing Images*. Master Thesis, University of Applied Sciences Munich, 2019
- Schwatke C., Scherer D., Dettmering D.: *Automated Extraction of Consistent Time-Variable Water Surfaces of Lakes and Reservoirs Based on Landsat and Sentinel-2*. Remote Sensing, 11(9), 1010, doi:[10.3390/rs11091010](https://doi.org/10.3390/rs11091010), 2019
- Zeitler L.: *Einfluss des Weltraumwetters auf geodätisch bestimmbare Ionosphärenparameter*. DVW Bayern e. V. Gesellschaft für Geodäsie, Geoinformation und Landmanagement, Mitteilungen, 2019
- Zeithöfler, J.: *Nominal and Observation-Based Attitude Realization for Precise Orbit Determination of the Jason Satellites*. Master Thesis, Technical University of Munich, 2019

4.3 Presentations

- Angermann D., Gruber T., Gerstl M., Heinkelmann R., Hugentobler U., Sanchez L., Steigenberger P.: *The GGOS Bureau of Products and Standards*. EGU General Assembly, Vienna, Austria, 2019 (Poster)
- Angermann D., Gruber T., Gerstl M., Heinkelmann R., Hugentobler U., Sanchez L., Steigenberger P.: *Activities and Plans of the GGOS Bureau of Products and Standards*. 27th IUGG General Assembly, Montréal, Canada, 2019
- Angermann D., Gruber T., Gerstl M., Hugentobler U., Sanchez L., Heinkelmann R., Steigenberger P.: *Bureau of Products and Standards Report*. GGOS Coordinating Board Meeting, Vienna, Austria, 2019
- Angermann D., Gruber T., Gerstl M., Hugentobler U., Sánchez L., Heinkelmann R., Steigenberger P.: *GGOS Bureau of Products and Standards*. UN Workshop for the Implementation of the GGRF in Latin America, Buenos Aires, Argentina, 2019
- Angermann D., Gruber T., Gross R.: *IAG Standards and Policies for Geodetic Data Sharing, Production and Publication*. 27th IUGG General Assembly, Montréal, Canada, 2019
- Angermann D., Stamatakis N.: *Review of Chapter 1 of IERS Conventions*. GGOS/IERS Unified Analysis Workshop, Paris, France, 2019
- Badawi Y., Lee W., Lyu H., Omar H., Goss A.: *Single-Cusp and Dual-Cusp EIA during high and low solar activities*. IRI Workshop, Nicosia, Cyprus, 2019
- Beckley B., Yang X., Zelensky N., Lemoine F., Ray R., Loomis B., Passaro M., Schwatke C., Mitchum G.: *Assessment of Global and Regional Sea-Level Estimates based on Reprocessed TOPEX/Jason Altimetry*. NASA Sea Level Change Science Team, Annapolis, Maryland, USA, 2019 (Poster)
- Bloßfeld M.: *Was bewegt sich wie? Geodätische Referenzsysteme als Grundlage für die Erdsystemforschung*. Geodätisches Kolloquium, Oldenburg, Germany, 2019
- Bloßfeld M.: *DGFI-TUM ILRS AC: status report*. ILRS Analysis Standing Committee Meeting, Paris, France, 2019
- Bloßfeld M.: *Analyzing of SLR observations – what do we do with the data?*. First One-Day Introductory and Refresher Course on Satellite and Lunar Laser Ranging, Stuttgart, Germany, 2019
- Bloßfeld M., Angermann D., Seitz M., Seitz F.: *Geodätische Referenzsysteme als Grundlage für die Erdsystemebeobachtung*. 2nd Symposium on New Perspectives for Earth Observation, Cologne, Germany, 2019
- Bloßfeld M., Jäggi A., Kehm A., Meyer U., Sosnica K.: *Evaluating the potential of combined SLR gravity field solutions*. COST-G Team Meeting, Berne, Switzerland, 2019
- Bloßfeld M., Kehm A.: *Status report of the DGFI-TUM ILRS AC*. ILRS Analysis Standing Committee Meeting, Vienna, Austria, 2019
- Bloßfeld M., Kehm A.: *The potential of increased station performances for scientific SLR products*. ILRS Technical Workshop 2019, Stuttgart, Germany, 2019
- Bloßfeld M., Meyer U., Sosnica K., Jäggi A.: *Combined SLR gravity field time series for continuous Earth System Monitoring*. EGU General Assembly, Vienna, Austria, 2019

- Bloßfeld M., Rudenko S., Zeitlhöfler J.: *Status of the DORIS satellite data processing at DGFI-TUM*. IDS Analysis Working Group Meeting, Munich, Germany, 2019
- Bloßfeld M., Schmidt M., Forootan E., Aibar A. C., dos Santos Prol F., Soja B., Garcia-Rigo A., Siemes C., Vielberg K.: *GGOS Focus Area on Geodetic Space Weather Research: Observation Techniques and Modeling Approaches*. AGU Fall Meeting, San Francisco, USA, 2019
- Bloßfeld M., Seitz M., Glomsda M., Angermann D.: *Improving global reference frame realizations by correcting for non-tidal loading displacements (+DTRF2020 outlook)*. AGU Fall Meeting, San Francisco, USA, 2019
- Boergens E., Passaro M., Arduin F., Cipollini P., Donlon C.: *Estimating Significant Wave Heights from SAR waveforms with a Leading Edge Retracker*. ESA Living Planet Symposium, Milan, Italy, 2019 (Poster)
- Busker T., De Roo A., Gelati E., Schwatke C., Adamovic M., Bisselink B., Pekel, J. F., Cottam A.: *Resilient lakes and reservoirs: making a change with satellite-based global monitoring*. 8th IWA-Aspire 2019, Hong Kong, 2019
- Cazenave A., Birol F., Passaro M., Leger F., Gouzenes Y., Rogel P., Legeais J.F., Benveniste J.: *Present-day Sea Level Changes in the World Coastal Zones*. AGU Fall Meeting, San Francisco, USA, 2019 (Poster)
- Cazenave A., Gouzenes Y., Leger F., Birol F., Passaro M., Legeais J.F., Benveniste J.: *Coastal Sea Level Rise from Reprocessed Altimetry Differs from Offshore*. AGU Fall Meeting, San Francisco, USA, 2019
- Cazenave A., Marti F., Passaro M., Birol F., Leger F., Nino F., Benveniste J.: *Coastal sea level changes from retracked Jason-1 and Jason-2 altimetry along the Western African coasts*. ESA Living Planet Symposium, Milan, Italy, 2019
- Chen. P., Liu H., Zheng N., Schmidt M. : *Response of the ionosphere to the total solar eclipse on August 21, 2017 in the United States*. EGU General Assembly, Vienna, Austria, 2019
- Chereskin T., Gille S., Mazloff M., Cornuelle B., Wang J., Menemenlis D., Passaro M., Schwatke C., Rocha C. : *High-wavenumber variability in the California Current: Evaluating sub-100-km scales with high-resolution altimetry, ADCP, and model output*. Ocean Surface Topography Science Team (OSTST) Meeting 2019, Chicago, USA, 2019
- Dettmering D., Schwatke C.: *Direct comparison of Sentinel-3 SRAL LRM and SAR mode data for inland water level estimation*. ESA Living Planet Symposium, Milan, Italy, 2019 (Poster)
- Dettmering D., Schwatke C.: *Assessment of Sentinel-3A/B ocean data sets: Recent results of DGFI-TUM's multi-mission cross-calibration*. Ocean Surface Topography Science Team (OSTST) Meeting 2019, Chicago, USA, 2019 (Poster)
- Dettmering D., Schwatke C., Scherer D., Ellenbeck L., Seitz F.: *Satellitenaltimetrie: Wasserhöhen, Speichervolumen und Abflüsse aus dem Weltraum*. 2nd Symposium on New Perspectives for Earth Observation, Cologne, Germany, 2019
- Ellenbeck L., Dettmering D., Schwatke C., Seitz F.: *Improving Altimetry-Derived Water Level Time Series of Small Inland Water Bodies: Impact of Introducing Time-Dependent Land-Water Masks*. ESA Living Planet Symposium, Milan, Italy, 2019
- Erdogan E., Goss A.: *Bayesian Approaches for Non-Linear Ionosphere Modelling - Concept and Strategies*. EGU General Assembly, Vienna, Austria, 2019

- Fernandez-Gomez I., Goss A., Schmidt M., Borries C., Schlicht A. : *The performance of empirical and physics based Ionosphere models*. EGU General Assembly, Vienna, Austria, 2019
- Fernández-Gómez I., Goss A., Schmidt M., Codrescu S., Codrescu M., Borries C., Schlicht A.: *The performance of physics - based and empirical models during St. Patrick's day storm 2015*. DFG SPP Dynamic Earth Colloquium 2019, Bad Aibling, Germany, 2019 (Poster)
- Forootan E., Schmidt M., Börger K., Farazaneh S., Lück C., Vielberg K., Kosary M.: *Global Ionospheric and Thermospheric Responses to Solar and Magnetic Activity Derived from Models and Geodetic Observations*. EGU General Assembly, Vienna, Austria, 2019
- Forootan E., Schmidt M., Vielberg K., Börger K., Farazaneh S., Kosary M.: *Essential Geodetic (Space Weather) Variables – Mind the Gap in Thermosphere and Ionosphere*. 27th IUGG General Assembly, Montréal, Canada, 2019
- Gerzen T., B. Heilig, H. Lühr, M. Schmidt: *Multi-Satellite ionosphere-plasmasphere Electron density reconstruction (MuSE): Project overview and first results*. EGU General Assembly, Vienna, Austria, 2019
- Gerzen T., Heilig B., Luer H., Schmidt M., Minkwitz D. : *Overview about the project MuSE: Multi-Satellite ionosphere-plasmasphere Electron density reconstruction*. 27th IUGG General Assembly, Montréal, Canada, 2019
- Gerzen T., Heilig B., Lühr H., Schmidt M., Rashkovetsky D.: *Multi-Satellite ionosphere-plasmasphere Electron density reconstruction (MuSE)*. DFG SPP Dynamic Earth Colloquium 2019, Bad Aibling, Germany, 2019
- Gerzen T., Schmidt M., Minkwitz D., Rashkovetsky D.: *Assimilation of space-based STEC into the NeQuick topside in the frame of the MuSE project*. International Workshop on GNSS Ionosphere, Neustrelitz, 2019
- Glomsda M., Bloßfeld M., Gerstl M., Kwak Y., Seitz M., Angermann D., Seitz F.: *Impact of non-tidal loading in VLBI analysis*. 24th Meeting of the European VLBI Group for Geodesy and Astrometry, Gran Canaria, Spain, 2019
- Glomsda M., Bloßfeld M., Seitz M., Gerstl M., Angermann D., Seitz F.: *Impact of non-tidal loading applied at different levels in VLBI analysis*. INTERGEO/Frontiers of Geodetic Science, Stuttgart, Germany, 2019
- Goss A., Erdogan E., Schmidt M., Dettmering D., Seitz F., Börger K., Müller J., Görres B., Kersten W., Brandert S.: *High-precision and high-resolution VTEC maps based on Multi-Scale B-spline Representations and Near Real-Time Observations*. EGU General Assembly, Vienna, Austria, 2019
- Goss A., Erdogan E., Schmidt M., Dettmering D., Seitz F., Müller J., Görres B., Kersten W.: *Real-Time Modelling of the Vertical Total Electron Content (VTEC) Using B-Splines*. IRI Workshop, Nicosia, Cyprus, 2019
- Goss A., Wang N., Schmidt M., Erdogan E.: *Representing and High-Resolution VTEC maps for Regions With Dense Data Coverage*. 27th IUGG General Assembly, Montréal, Canada, 2019
- Göttl F., Schmidt M., Seitz F.: *Mass-related excitation of polar motion: An assessment of the new RL06 GRACE gravity field models*. EGU General Assembly, Vienna, Austria, 2019

- Hellmers H., Thaller D., Bloßfeld M., Kehm A., Girdiuk A.: *VLBI/GNSS Rapid combination for generating Earth Orientation Parameters*. EGU General Assembly, Vienna, Austria, 2019 (Poster)
- Hellmers H., Thaller D., Bloßfeld M., Kehm A., Girdiuk A.: *Kombination von VLBI Intensive Sessions mit GNSS zur Bestimmung von Erdrotationsparametern mit kurzer Latenzzeit*. INTERGEO/Frontiers of Geodetic Science, Stuttgart, Germany, 2019
- Kehm A.: *Data analysis demonstration – data download and normal point computation*. First One-Day Introductory and Refresher Course on Satellite and Lunar Laser Ranging, Stuttgart, Germany, 2019
- Kehm A., Bloßfeld M., Hellmers H., Dill R., Dobsław H., Seitz F.: *ESA-EOP software for final and rapid combination and prediction*. Implementation Review meeting to ESA project Independent Generation of Earth Orientation Parameters (ESA-EOP), Frankfurt am Main, Germany, 2019
- Kehm A., König P., Bloßfeld M., Seitz F.: *Simulation studies on the location of a future SLR site*. GGOS PLATO Standing Committee Meeting, Vienna, Austria, 2019
- Kehm A., Sánchez L., Bloßfeld M., Angermann D., Drewes H., Seitz F.: *Combination strategies for the realization of an Epoch Reference Frame for South America*. EGU General Assembly, Vienna, Austria, 2019
- Krypiak-Gregorczyk A., Wielgosz P., Jarmolowski W., Erdogan E., Goss A., Schmidt M.: *Comparison of spatio-temporal ionosphere profiles obtained from GNSS and ionosonde data during the severe ionospheric storm at 8th of September 2017*. EGU General Assembly, Vienna, Austria, 2019
- Lalgudi Gopalakrishnan G., Schmidt M.: *Ionosphere electron density modeling using the regularized constraint optimization approach*. EGU General Assembly, Vienna, Austria, 2019
- Lalgudi Gopalakrishnan G., Schmidt M., Gerzen, T.: *Electron density modelling based on Inequality constraints to study the impact of space weather events*. 27th IUGG General Assembly, Montréal, Canada, 2019
- Lalgudi Gopalakrishnan G., Schmidt M., Vielberg K., Kusche J.: *Electron Density and Neutral Density Modelling for Studying Thermosphere-Ionosphere Coupling*. 27th IUGG General Assembly, Montréal, Canada, 2019 (Poster)
- Léger F., Birol F., Niño F., Passaro M., Cazenave A., Legeais J., Schwatke C., Benveniste J.: *The new generation of high-resolution X-TRACK/ALES regional altimetry product*. Ocean Surface Topography Science Team (OSTST) Meeting 2019, Chicago, USA, 2019 (Poster)
- Léger F., Birol F., Niño F., Passaro M., Marti F., Cazenave A.: *X-TRACK/ALES Regional Altimeter Product for Coastal Application: Toward a new multi-mission altimetry product at high resolution*. 39th IGARSS Symposium, Yokohama, Japan, 2019 (Poster)
- Léger F., Birol F., Niño F., Passaro M., Marti F., Fenoglio-Marc L., Cazenave A.: *X-TRACK/ALES: Toward a new coastal multi-mission altimetry product at high rate, combining the ALES re-processing, and the X-TRACK editing algorithms*. ESA Living Planet Symposium, Milan, Italy, 2019 (Poster)
- Le Henaff M., Kersale M., Meinen C., Perez R., Chidichimo M., Passaro M., Schwatke C., Birol F., Faugere Y.: *Combining coastal altimetry and in situ observations to improve Meridional Overturning Circulation estimates: focus on the Southwestern Atlantic*. Ocean Surface Topography Science Team (OSTST) Meeting 2019, Chicago, USA, 2019

- Liu Q., Schmidt M., Willberg M., Pail R., Sánchez L.: *Regional gravity field refinement for the determination of IHRF coordinates based on spherical basis functions*. EGU General Assembly, Vienna, Austria, 2019
- Liu Q., Schmidt M., Willberg M., Pail R., Sánchez L.: *The 1 cm Geoid Experiment based on Spherical Basis Functions using Different Types of Observations*. 27th IUGG General Assembly, Montréal, Canada, 2019
- Martínez W., Mackern M., Drewes H., Rovera H., Brunini C., Sánchez L., Fortes L., Lauría E., Cioce V., Pérez R., de Freitas S., Costa S., Hoyer M., Luz R., Barriga R., Subiza W.: *Status of the SIRGAS reference frame: recent developments and new challenges*. 27th IUGG General Assembly, Montréal, Canada, 2019
- Müller F., Dettmering D., Wekerle C., Bosch W., Seitz F.: *The Dynamic Ocean Topography in the Greenland Sea: Combining Multi-Mission Satellite Altimetry with Ocean Modeling*. ESA Living Planet Symposium, Milan, Italy, 2019
- Müller F., Passaro M., Abulaitijiang A., Andersen O., Dettmering D., Høyer J., Johansson M., Skovgaard Madsen K., Rautiainen L., Ringgaard I., Rinne E., Särkkä J., Scarrott R., Schwatke C., Seitz F., Tuohy E., Tuomi L., Ambrozio A., Restano M., Benveniste J.: *Baltic SEAL: Building a Sea Level Product for Climate Research in a Region Featuring Jagged Coastline and Sea-ice Coverage*. Ocean Surface Topography Science Team (OSTST) Meeting 2019, Chicago, USA, 2019
- Müller F., Passaro M., Dettmering D., Seitz F.: *Geostrophic currents in polar oceans - combining satellite altimetry measurements with model simulations*. World Ocean Circulation User Consultation Meeting, ESA-ESRIN, Frascati, Italy, 2019
- Oelsmann J., Passaro M., Dettmering D., Sanchez L., Schwatke C., Seitz F.: *Comparability of coastal altimetry with tide gauges and application for vertical land motion detection*. INTER-GEO/Frontiers of Geodetic Science, Stuttgart, Germany, 2019
- Passaro M., Quartly G. D., Barbieri E., Ardhuin F., Cipollini P., Donlon C.: *Two decades of Significant Wave Height and σ_0 from altimetry retracked with WHALES: Towards low noise and coastal efficiency*. ESA Living Planet Symposium, Milan, Italy, 2019
- Piccioni G., Dettmering D., Schwatke C., Passaro M., Seitz F.: *Exploiting coastal altimetry to improve tidal estimation*. ESA Living Planet Symposium, Milan, Italy, 2019
- Piccioni G., Dettmering D., Seitz F.: *Analysis of global ocean tide models in critical areas with focus on EOT19 preliminary model*. EGU General Assembly, Vienna, Austria, 2019 (Poster)
- Prol F., Garcia-Rigo A., Hoque M., Schmidt M., Börger K.: *Towards a global 3D ionospheric model for space weather monitoring and GNSS positioning*. 27th IUGG General Assembly, Montréal, Canada, 2019
- Quartly G., Passaro M.: *Can the concept of intra-1 Hz correlations be applied to improve wave height estimates?*. ESA Living Planet Symposium, Milan, Italy, 2019
- Quartly G., Passaro M., Smith W.: *Improving the Agreement between Altimeters by Suppressing Covariant Errors*. ESA Living Planet Symposium, Milan, Italy, 2019 (Poster)
- Ren X., Chen J., Zhang X., Li X., Schmidt M.: *Total Electron content (TEC) estimation and ionosphere monitoring using triple-frequency GPS/Galileo/BDS observations*. 27th IUGG General Assembly, Montréal, Canada, 2019

- Ren X., Zhao Z., Chen J., Zhang X., Li X., Schmidt M.: *Assessment of ionosphere models from the combination of GNSS and LEO constellations*. EGU General Assembly, Vienna, Austria, 2019
- Reyes R., Noveloso D., Rediang A., Passaro M., Bringas D., Nagai M.: *Tide gauge and satellite altimetry data for possible land motion detection in south east Bohol trench and fault*. PhilGEOS x GeoAdvances 2019, Manila, Philippines, 2019
- Rose S., Andersen O., Passaro M., Benveniste J.: *25 years of sea level records from the Arctic Ocean using radar altimetry*. ESA Living Planet Symposium, Milan, Italy, 2019 (Poster)
- Rudenko S., Bloßfeld M., Zeitlhöfner J.: *Status of precise orbit determination of altimetry satellites at DGFI-TUM*. Ocean Surface Topography Science Team (OSTST) Meeting 2019, Chicago, USA, 2019 (Poster)
- Rudenko S., Lalgudi Gopalakrishnan G., Schmidt M., Bloßfeld M.: *Estimation of scale factors from SLR observations to LEO satellites for the thermospheric density computed from empirical and physical models*. ESA Living Planet Symposium, Milan, Italy, 2019 (Poster)
- Rudenko S., Schmidt M., Bloßfeld M., Xiong C., Lühr H.: *Estimation of scaling factors of thermospheric density provided by empirical models using SLR observations to Low Earth Orbiting satellites*. 27th IUGG General Assembly, Montréal, Canada, 2019 (Poster)
- Rudenko S., Zeitlhöfner J., Bloßfeld M., Dettmering D.: *Impact of nominal and measured satellite attitude on SLR- and DORIS-derived orbits of Jason satellites and altimetry results*. Ocean Surface Topography Science Team (OSTST) Meeting 2019, Chicago, USA, 2019
- Sánchez L.: *Permanent tide: a station displacement? Or a permanent component of the station positions?*. GGOS/IERS Unified Analysis Workshop, Paris, France, 2019
- Sánchez L.: *GGOS Focus Area Unified Height System: Status report, ongoing activities, outlook*. GGOS Coordinating Board Meeting, Vienna, Austria, 2019
- Sánchez L.: *The International Height Reference System (IHRF) and its realisation, the International Height Reference Frame (IHRF)*. UN Workshop for the Implementation of the GGRF in Latin America, Buenos Aires, Argentina, 2019
- Sánchez L.: *Status of the International Height Reference Frame - IHRF*. GGOS/IERS Unified Analysis Workshop, Paris, France, 2019
- Sánchez L.: *Activities and plans of the GGOS Focus Area Unified Height System*. GGOS Days 2019, Rio de Janeiro, Brazil, 2019
- Sánchez L., Ågren J., Huang J., Wang Y.M., Mäkinen J., Denker H., Ihde J., Abd-Elmotaal H., Ahlgren K., Amos M., Barzaghi R., Bašić T., Blitzkow D., Carrion D., Claessens S., Erol B., Erol S., Filmer M., Forsberg R., Grigoriadis V.N., Serkan Işık M., Jiang T., Li X., Liu Q., Matos A.C.O.C., Matsuo K., Novák P., Pail R., Pitoňák M., Roman D., Schmidt M., Sideris M., Varga M., Vergos G.S., Véronneau M., Willberg M., Zhang C., Zingerle P.: *IHRF2019: the first realisation of the International Height Reference System*. 27th IUGG General Assembly, Montréal, Canada, 2019
- Sánchez L., Ågren J., Huang J., Wang Y.M., Mäkinen J., Denker H., Ihde J., Abd-Elmotaal H., Ahlgren K., Amos M., Barzaghi R., Bašić T., Blitzkow D., Carrion D., Claessens S., Erol B., Erol S., Filmer M., Forsberg R., Grigoriadis V.N., Serkan Işık M., Jiang T., Li X., Liu Q., Matos A.C.O.C., Matsuo K., Novák P., Pail R., Pitoňák M., Roman R., Schmidt M., Sideris M., Varga M., Vergos G.S., Véronneau M., Willberg M., Zhang V., Zingerle P.: *Advances*

in the realisation of the International Height Reference System. GGOS Days 2019, Rio de Janeiro, Brazil, 2019

Sánchez L., Barzaghi R., Vergos G.: *Operational infrastructure to ensure the long-term sustainability of the IHRs/IHRF.* 27th IUGG General Assembly, Montréal, Canada, 2019

Sánchez L., Brunini C.: *Summary of the workshop on the Implementation of the Global Geodetic Reference Frame (GGRF) in Latin America.* Symposium SIRGAS2019, Rio de Janeiro, Brazil, 2019

Sánchez L., Drewes H.: *Geodetic monitoring of the variable surface deformation in Latin America.* 27th IUGG General Assembly, Montréal, Canada, 2019

Sánchez L., Sideris M., Ihde J.: *Activities and plans of the GGOS Focus Area Unified Height System.* 27th IUGG General Assembly, Montréal, Canada, 2019

Sánchez L., Völksen Ch., Sokolov A., Arenz H., Seitz F.: *Present-day surface deformation of the Alpine Region inferred from geodetic techniques.* 27th IUGG General Assembly, Montréal, Canada, 2019

Scarrott R., Flood S., Passaro M., Müller F. L., Abulaitijiang A., Andersen O. B., Dettmering D., Høyer J., Johansson M., Skovgaard Madsen K., Rautiainen L., Ringgaard I., Rinne E., Särkkä J., Schwatke C., Oelsmann J., Seitz F., Tuomi L., Ambrozio A., Restano M., Benveniste J.: *ESA Baltic SEAL: Setting course to advance satellite-derived sea-level products for jagged coastlines.* 13th Irish Earth Observation Symposium (IEOS), Galway, Ireland, 2019 (Poster)

Schlembach F., Passaro M., Quartly G., Nencioli F., Kurekin A., Dodet G., Piollé J.F., Cipollini P., Schwatke C., Dettmering D., Seitz F., and Donlon C.: *Round Robin Assessment of Radar Altimeter LRM and SAR Retracking Algorithms for Significant Wave Height.* Ocean Surface Topography Science Team (OSTST) Meeting 2019, Chicago, USA, 2019 (Poster)

Schlicht A., Schmidt M., Flury J., Borries C., Kodet J., Eckl J., Goss A., Shabanloui A., Fernandez Gomez I., Hannemann M., Strelnikov B.: *Interactions of Low-orbiting Satellites with the Surrounding Ionosphere and Thermosphere (INSIGHT).* 27th IUGG General Assembly, Montréal, Canada, 2019 (Poster)

Schmidt M.: *Results from the Study and Working Groups of the IAG Sub-Commission 4.3 Atmosphere Remote Sensing.* 27th IUGG General Assembly, Montréal, Canada, 2019

Schmidt M.: *DGFI-TUM's activities on ionosphere modeling and monitoring.* 10th China Satellite Navigation Conference, Beijing, China, 2019

Schmidt M.: *Beobachtung und Modellierung von Solarstürmen in der Geodäsie.* Fachkonferenz Munich Re, München, 2019

Schmidt M., Börger K.: *GGOS Focus Area on Geodetic Space Weather Research.* 27th IUGG General Assembly, Montréal, Canada, 2019 (Poster)

Schmidt M., Börger K., Forootan E.: *GGOS Focus Area on Geodetic Space Weather Research: Essential Geodetic Variables.* EGU General Assembly, Vienna, Austria, 2019 (Poster)

Schmidt M., Erdogan E., Goss A., Dettmering D., Seitz F., Börger K., Müller J., Görres B., Kersten W.F.: *Real-Time Modelling of the Vertical Total Electron Content (VTEC) Using B-Splines.* 27th IUGG General Assembly, Montréal, Canada, 2019

- Schmidt M., Erdogan E., Goss A., Dettmering D., Seitz F., Börger K., Müller J., Görres B., Kersten W.F.: *High-precision and high-resolution VTEC maps based on multi-scale B-spline expansions and near-real time GNSS data*. SGI Workshop 2019, Berlin, Germany, 2019
- Schmidt M., Erdogan E., Goss A., Dettmering D., Seitz F., Müller J., Görres B., Kersten W.F.: *(Near) real-time modelling of the global Vertical Total Electron Content (VTEC) using multi-GNSS ionosphere observations*. International Workshop on GNSS Ionosphere, Neustrelitz, 2019
- Schmidt M., Gerzen T.: *Forschungsthema Atmosphäre - Weltraumwetter*. Weltraumwetter Workshop, Bonn, Germany, 2019
- Schmidt M., Gerzen T.: *Research Topic Atmosphere – Space Weather*. Fachkonferenz GFZ, Potsdam, 2019
- Schmidt M., Göttl F., Seitz F.: *Mass-related excitation of polar motion based on new GRACE RL06 gravity field models*. 27th IUGG General Assembly, Montréal, Canada, 2019
- Schmidt M., Rudenko S., Börger K.: *GGOS Focus Area on Geodetic Space Weather Research – Current Status*. 2019 Living Planet Symposium, Milan, Italy, 2019 (Poster)
- Schmidt M., Zeitler L., Kusche J., Corbin A., Löcher A., Vielberg K., Stolle C., Xiong C., Hugentobler U., Bamann C., Börger K., Forootan E., Schumacher M.: *Development of High-Precision Thermosphere Models for Improving Precise Orbit Determination of Low-Earth-Orbiting Satellites (TIPOD)*. DFG SPP Dynamic Earth Colloquium 2019, Bad Aibling, Germany, 2019
- Schmidt M., Zeitler L., Kusche J., Löcher A., Vielberg K., Stolle C., Xiong C., Hugentobler U., Bamann C., Börger K., Forootan E., Schumacher M.: *Development of High-Precision Thermosphere Models for Improving Precise Orbit Determination of Low-Earth-Orbiting Satellites (TIPOD)*. EGU General Assembly, Vienna, Austria, 2019
- Schwatke C., Scherer D.: *Estimation of gap-less time series of inland waters' surface areas using Landsat and Sentinel-2*. ESA Living Planet Symposium, Milan, Italy, 2019
- Schwatke C., Scherer D., Dettmering D.: *DAHITI: Improving altimetry-derived water level time series of inland waters by a combination with optical remote sensing images from Landsat and Sentinel-2*. ESA Living Planet Symposium, Milan, Italy, 2019
- Schwatke C., Scherer D., Dettmering D.: *AWAX: A new Approach for Automated Extraction of Consistent Time-Variable Water Surfaces of Lakes and Reservoirs using Landsat and Sentinel-2*. 27th IUGG General Assembly, Montréal, Canada, 2019
- Schwatke C., Scherer D., Dettmering D., Ellenbeck L.: *Estimating Long-Term Water Level Time Series of Inland Waters since 1984 by Combining Satellite Altimetry and Optical Remote Sensing Images*. 27th IUGG General Assembly, Montréal, Canada, 2019
- Seitz F.: *One century of Earth rotation research in the framework of IAU: Centennial celebration of IAU Commission A2/19*. Astrometry, Earth Rotation and Reference Systems in the Gaia Era, Paris, France, 2019
- Seitz F.: *Geodätische Erdbeobachtung aus dem Weltraum: Aktuelle Arbeiten am Deutschen Geodätischen Forschungsinstitut*. Einrichtung eines operationellen Dienstes zur Bereitstellung von Ionosphäreninformationen beim Weltraumlagezentrum (OPTIMAP): Zwischenpräsentation des Fachprojekts, Euskirchen, 2019

- Seitz F., Kehm A., König P., Bloßfeld M.: *Future TRFs and GGOS: Where to put the next SLR station?* EGU General Assembly, Vienna, Austria, 2019 (Poster)
- Seitz F., Passaro M.: *Die Veränderung des Meeresspiegels: Wissenschaftliche Beobachtungsergebnisse statt Fake News.* TUM StreetScience, Munich, 2019
- Seitz M., Bloßfeld M., Angermann D., Glomsda M.: *Important issues preparing the ITRS Realizations 2020.* IERS Directing Board Meeting, San Francisco, USA, 2019
- Tarpanelli A., Passaro M., Marti F., Cazenave A., Birol F., Léger F., Niño F., Schwatke C., Camici S., Brocca L., Massari C., Moramarco T., Benveniste J.: *Exploiting Remote Sensing Synergy to Analyse Localised Coastal Sea Level and River Level Trends: the Sassandra River Case Study.* ESA Living Planet Symposium, Milan, Italy, 2019 (Poster)
- Thaller D., Männel B., Glaser S., Kehm A., Bloßfeld M.: *Recent Activities of the GGOS Standing Committee on Performance Simulations and Architectural Trade-Offs (PLATO).* UN Workshop for the Implementation of the GGRF in Latin America, Buenos Aires, Argentina, 2019
- Thaller D., Männel B., Glaser S., Rothacher M., Herrera Pinzón I., Bloßfeld M., Kehm A., Andrich F., Dach R., Böhm J., Pavlis E. C., Pollet A.: *The GGOS Standing Committee on Performance Simulations and Architectural Trade-Offs (PLATO).* 27th IUGG General Assembly, Montréal, Canada, 2019
- Willberg M., Zingerle P., Liu Q., Pail R.: *Filtering of Airborne Observations in the Least Squares Collocation.* 27th IUGG General Assembly, Montréal, Canada, 2019
- Willberg M., Zingerle P., Liu Q., Schmidt M., Pail R.: *The 1 cm geoid experiment with Least Squares Collocation.* EGU General Assembly, Vienna, Austria, 2019
- Zeitler L.: *Einfluss des Weltraumwetters auf geodätisch bestimmbare Ionosphärenparameter.* Wintervortragsreihe 2018/2019 des DVW Bayern e.V., Munich, Germany, 2019
- Zeitler L., Rudenko S., Bloßfeld M., Schmidt M.: *Analyse von thermosphärischen Dichten aus SLR-Beobachtungen zu niedrig fliegenden Satelliten.* INTERGEO/Frontiers of Geodetic Science, Stuttgart, Germany, 2019
- Zeitler L., Rudenko S., Bloßfeld M., Schmidt M., Corbin A., Vielberg K., Löcher A., Kusche J., Xiong C., Stolle C., Bamann C., Hugentobler U., Börger K., Forootan E., Schumacher M.: *Development of High-Precision Thermosphere Models for Improving Precise Orbit Determination of Low-Earth-Orbiting Satellites (TIPOD): First Results.* 27th IUGG General Assembly, Montréal, Canada, 2019 (Poster)
- Zeitler L., Schmidt M., Bloßfeld M., Rudenko S.: *Comparison of neutral density using different empirical thermosphere models.* DFG SPP Dynamic Earth Colloquium 2019, Bad Aibling, Germany, 2019

4.4 Participation in Meetings, Symposia, Conferences

- 2019-01-14/18: **COST-G Team Meeting, Berne, Switzerland**
Bloßfeld M.
- 2019-01-17: **Geodätisches Kolloquium, Jade Hochschule, Oldenburg, Germany**
Bloßfeld M.

- 2019-02-01/02 : **Retreat of the Faculty of Civil, Geo and Environmental Engineering of the TUM, Berg, Germany**
Seitz F.
- 2019-02-06/07 : **Intermediate presentation of project OPTIMAP, Euskirchen, Deutschland**
Schmidt M., Goss A., Seitz F.
- 2019-02-08 : **DFG Round table discussion on the SWOT mission, Universität Bonn, Deutschland**
Dettmering D., Passaro M., Seitz F.
- 2018-02-12 : **FGS Board Meeting, Munich, Germany**
Schmidt M., Seitz F.
- 2019-02-21/22 : **World Ocean Circulation User Consultation Meeting, ESA-ESRIN, Frascati, Italy**
Mueller F. L., Passaro M.
- 2019-03-07 : **Annual meeting of DGK Section Geodesy, Dresden, Germany**
Seitz F.
- 2019-03-14/16 : **3rd IVS VLBI Training School, Las Palmas, Gran Canaria, Spain**
Glomsda M.
- 2019-03-17/19 : **24th Meeting of the European VLBI Service for Geodesy and Astrometry, Las Palmas, Gran Canaria, Spain**
Glomsda M.
- 2019-04-04 : **IDS Analysis Working Group Meeting, Munich, Germany**
Bloßfeld M., Dettmering D., Rudenko S.
- 2019-04-05 : **IDS Governing Board Meeting, Munich, Germany**
Dettmering D.
- 2019-04-06 : **ILRS Analysis Standing Committee Meeting, Vienna, Austria**
Kehm A., Bloßfeld M.
- 2019-04-06 : **GGOS Coordinating Board Meeting, Vienna, Austria**
Sánchez L., Angermann D., Schmidt M.
- 2019-04-07 : **IERS Directing Board Meeting, Vienna, Austria**
Seitz M., Angermann D.
- 2019-04-08 : **GGOS PLATO Standing Committee Meeting, Vienna, Austria**
Kehm A.
- 2019-04-08/12 : **European Geosciences Union (EGU) General Assembly 2019, Vienna, Austria**
Seitz F., Bloßfeld M., Kehm A., Göttl F., Angermann D., Piccioni G., Schmidt M., Erdogan E., Gerzen T.
- 2019-04-10 : **GGOS Bureau of Products and Standards Meeting, Vienna, Austria**
Angermann D.
- 2019-04-11 : **UN-GGIM GGRF Subcommittee of Geodesy, Vienna, Austria**
Angermann D.

- 2019-05-09 : **DFG RU GlobalCDA, First Workshop, Munich, Germany**
Dettmering D., Ellenbeck L.
- 2019-05-10 : **DFG RU GlobalCDA, Second Status Meeting, Munich, Germany**
Dettmering D., Ellenbeck L., Schwatke C., Seitz F.
- 2019-05-13/15 : **Status Meeting of Project OPTIMAP, Uedem, Germany**
Goss A., Schmidt M.
- 2019-05-13/17 : **ESA Living Planet Symposium, Milan, Italy**
Dettmering D., Ellenbeck L., Müller F., Passaro M., Piccioni G., Rudenko S., Schwatke C.
- 2018-05-17 : **FGS Board Meeting, Munich, Germany**
Schmidt M., Seitz F.
- 2019-05-22/25 : **10th China Satellite Navigation Conference, Beijing, China**
Schmidt M.
- 2019-06-03 : **Status Meeting of DFG Project INSIGHT-II, Munich, Germany**
Schmidt M.
- 2019-06-04/06 : **DFG SPP 1788 Dynamic Earth, Colloquium, Bad Aibling, Germany**
Zeitler L., Schmidt M., Gerzen T.
- 2019-06-26 : **8th Copernicus POD Quality WG meeting, Oberpfaffenhofen, Germany**
Dettmering D.
- 2019-07-05 : **Weltraumwetterworkshop, DLR Raumfahrtmanagement, Bonn, Germany**
Schmidt M., Gerzen T.
- 2019-07-08/18 : **27th General Assembly of the International Union of Geodesy and Geophysics (IUGG), Montreal, Canada**
Schmidt M., Angermann D., Sánchez L., Schwatke C., Liu Q.
- 2019-09-06 : **IRI Workshop 2019, Nicosia, Cyprus**
Goss A.
- 2019-09-09 : **Project Meeting 1 of ESA-Project COSTO, Athens, Greece**
Goss A.
- 2019-09-16/20 : **UN Workshop for the Implementation of the GGRF in Latin America, Buenos Aires, Argentina**
Sánchez L.
- 2019-09-17/19 : **INTERGEO/Frontiers of Geodetic Science, Stuttgart, Germany**
Schmidt M., Dettmering D., Zeitler L., Oelsmann J., Glomsda M.
- 2019-09-23/25 : **IWGI 2019, Neustrelitz, Germany**
Schmidt M., Gerzen T.
- 2019-09-25/26 : **Status Meeting of DFG RU NEROGRAV, Berlin, Germany**
Dettmering D., Seitz F., Hart-Davis M.
- 2019-09-26 : **Fachkonferenz Magnetosphäre-Ionosphäre-Thermosphäre, Potsdam, Germany**
Schmidt M.

- 2019-09-27 : **SGI Workshop, Berlin, Germany**
Schmidt M.
- 2019-09-30/10-02 : **Status meeting of DFG project TIPOD, Potsdam, Germany**
Schmidt M., Zeitler L.
- 2019-10-02/04 : **IERS/GGOS Unified Analysis Workshop, Paris, France**
Sánchez L., Angermann D., Bloßfeld M.
- 2019-10-07/09 : **Journees 2019: Astrometry, Earth Rotation and Reference Systems in the Gaia Era, Paris, France**
Seitz F.
- 2019-10-18 : **Implementation Review, ESA project "Independent Generation of Earth Orientation Parameters", Frankfurt, Germany**
Seitz F., Bloßfeld M., Kehm A.
- 2019-10-20 : **SLR Summer School 2019, Stuttgart, Germany**
Bloßfeld M., Kehm A.
- 2019-10-21/25 : **ILRS Technical Workshop 2019, Stuttgart, Germany**
Bloßfeld M., Schwatke C.
- 2019-10-21/25 : **Ocean Surface Topography Science Team (OSTST) Meeting, Chicago, USA**
Dettmering D., Müller F.L., Rudenko S., Schlembach F.
- 2019-11-05/07 : **Status meeting of project OPTIMAP, Munich, Germany**
Schmidt M., Erdogan E., Goss A., Dettmering D., Seitz F.
- 2019-11-11/14 : **Symposium SIRGAS2019, Rio de Janeiro, Brazil**
Sánchez L., Angermann D.
- 2019-11-12/13 : **2nd Symposium on New Perspectives for Earth Observation, Cologne, Germany,**
Bloßfeld M., Dettmering D.
- 2019-11-12/14 : **GGOS Days 2019, Rio de Janeiro, Brazil**
Sánchez L., Angermann D.
- 2019-11-27/29 : **DGK Annual meeting, Munich, Germany**
Seitz F.
- 2019-12-05/06 : **Project Meeting 2 of ESA-Project COSTO, Munich, Germany**
Schmidt M., Goss A., Erdogan E.
- 2019-12-06 : **DFG RU GlobalCDA, Status Meeting, Luxembourg**
Dettmering D., Ellenbeck L.
- 2019-12-08 : **IERS Directing Board Meeting, San Francisco, USA**
Bloßfeld M.
- 2019-12-09/13 : **AGU Fall Meeting 2019, San Francisco, USA**
Bloßfeld M.

4.5 Guests

- 2019-01-01/10-31 : Dr. Ren X., Wuhan University, China
- 2019-01-01/11-30 : Dr. Peng C., College of Geomatics, Xian University of Science and Technology, China
- 2019-01-21 : Prof. Dr. Eicker A., HCU Hamburg, Germany
- 2019-01-22 : Prof. Dr. Güntner A., Deutsches Geoforschungszentrum (GFZ), Germany
- 2019-03-21 : Dr. Arduin, F., Institut Français de Recherche pour l'Exploitation de la Mer, Brest, France
- 2019-05-15 : Roggenbuck O. with a group of students, Jade University, Oldenburg, Germany
- 2019-07-29/08-09 : Roggenbuck O., Jade University, Oldenburg, Germany
- 2019-11-13 : Prof. Dr. Shprits Y., Deutsches Geoforschungszentrum (GFZ), Potsdam, Germany
- 2019-11-20 : Dr. Braun R, Dr. Minkwitz D., Dr. van der Weg W., Beck T., Kirchner M., Airbus Defence and Space, Germany

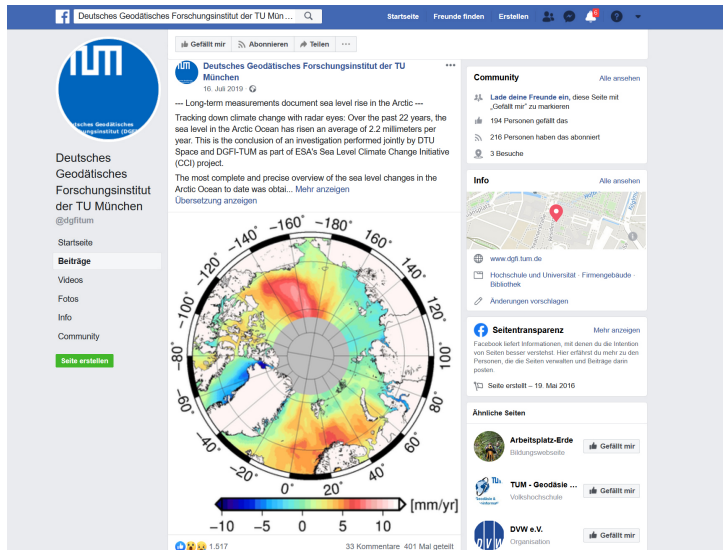
4.6 Internet Portals

In order to exchange scientific knowledge, results and data with national and international partners, interested parties and the public, the DGFI-TUM maintains the following internet portals and public databases:

Deutsches Geodätisches Forschungsinstitut der Technischen Universität München (DGFI-TUM)

The screenshot shows the DGFI-TUM website. On the left is a navigation menu with links like Home, About DGFI-TUM, DGFI-TUM in the media, Research, Projects, Science Data Products, International Services, Staff, Publications, Posters/Presentations, Teaching, Opportunities for Master's Theses / Masterarbeiten, and Location. The main content area features a 'Recent news' section with a headline about surface currents in polar oceans. Below the headline is a map of the North Atlantic showing geostrophic velocities. To the right of the map is a list of 'See also' links, including DGFI Open Altimeter Database (Chorv08), Database for Hydrological Time Series of Inland Waters (DHTS), DGFI Science Data Products, ITRIS Combination Center at DGFI, GGGIS Bureau for Products and Standards, and EURONAS Data Center (EDC) operated by DGFI. At the bottom right, there is a 'Flyer' section with a small image of a satellite and a globe.

The web site of DGFI-TUM at www.dgfi.tum.de highlights the most recent research results and informs about the institute's structure and research. It presents the national and international projects of DGFI-TUM as well as its involvement in various international scientific organizations. The web site contains complete lists of publications, reports and presentations since 1994, and it provides DGFI-TUM's science data products. It has a media section and informs about activities in teaching.



In order to reach out to the public and to students, DGFI-TUM maintains its own facebook site where it publishes latest results, job offers and opportunities for scientific theses. The posts receive considerable feedback and attract several hundred visitors.

Open Altimeter Database (OpenADB)

DGFI-TUM operates an open database for high-level altimetry products. OpenADB provides multi-mission altimetry data and products for scientific and non-expert users free of charge after registration. Currently, the following products are available:

- Sea Surface Heights (SSH)
- Sea Level Anomalies (SLA)
- Adaptive Leading Edge Subwaveform (ALES) Retracker heights
- Instantaneous Dynamic Ocean Topography Profiles (iDOT)
- Empirical Ocean Tide Model (EOT)
- Vertical Total Electron Content (VTEC)

All data is provided along the satellites' tracks in standard data formats. The web site is available at openadb.dgfi.tum.de.

Open Altimeter Database (OpenADB)
Deutsches Geodätisches Forschungsinstitut
Technische Universität München



OpenADB

- Products
- Mean Sea Level
- Missions
- Pass Locator
- Documentation
- Data Access

OpenADB

Open Altimeter Database (OpenADB)

Monitoring Sea Surface Heights

WELCOME TO OPENADB ...

OpenADB is a database for satellite altimetry data and derived high-level products. It shall serve users with little experience in satellite altimetry and scientific users evaluating data, generating new products, models and algorithms.

The following products are available via OpenADB:

- Sea Surface Heights (SSH)
- Sea Level Anomalies (SLA)
- Instantaneous Dynamic Ocean Topography Profiles (iDOT)
- Empirical Ocean Tide Model (EOT)
- Vertical Total Electron Content (VTEC)
- Adaptive Leading Edge Subwaveform (ALES) Retracker

Contact

Christian Schwatke
christian.schwatke@tum.de

80333 München
Arcisstr. 21
Tel. +49 89 23031-1109
Fax +49 89 23031-1240


Database for Hydrological Time Series of Inland Waters (DAHITI)

Database for Hydrological Time Series of Inland Waters (DAHITI)
Deutsches Geodätisches Forschungsinstitut
Technische Universität München

DAHITI
Products
Virtual Stations
Map
Lake/River not found?
Publications
DAHITI-API (Beta)
Tools
Projects

Search ...

Database for Hydrological Time Series of Inland Waters (DAHITI)



Water Level Time Series From Satellite Altimetry

WELCOME TO DAHITI ...

The Database for Hydrological Time Series of Inland Waters (DAHITI) was developed by the Deutsches Geodätisches Forschungsinstitut der Technischen Universität München (DGFI-TUM) in 2013 to provide water level time series of inland waters. Today, DAHITI provides a variety of hydrological information on lakes, reservoirs, rivers, and wetlands derived from satellite data, i.e. from multi-mission satellite altimetry and optical remote sensing imagery. All products are available free of charge for the user community after a short registration process.


DAHITI - Products

Contact
Christian Schwelke
christian.schwelke@tum.de
80333 München
Arcisstr. 21
Tel. +49 89 23031-1109
Fax +49 89 23031-1240

DAHITI-Targets

Africa	804
Asia	377
Australia	21
Europe	58
North America	244
South America	1235
Global	2741

DAHITI-Player



The Database for Hydrological Time Series of Inland Waters (DAHITI) is a public database providing satellite-derived information for more than 2500 globally distributed lakes, reservoirs, rivers and wetlands for hydrological applications. For all targets, water level time series derived from multi-mission satellite altimetry is available. Moreover, for a variety of lakes and reservoirs, DAHITI provides time series of surface water extents based on optical images from Landsat and Sentinel-2, as well as time series of volume change, bathymetry, and water occurrence masks. The integration of discharge information is planned. DAHITI is available at dahiti.dgfi.tum.de.

EUROLAS Data Centre (EDC)


EUROLAS Data Center (EDC)
Deutsches Geodätisches Forschungsinstitut
Technische Universität München

Welcome

About EDC
EUROLAS Terms of Reference

Data
Products
Stations
Satellites
Prediction Provider
Operation Center (OC)
Mailing Lists
Tools
EDC-API (Beta)

Welcome to the EUROLAS Data Center (EDC)



Wettzell, Germany

News

- 2020-01-07 The satellite *Glomos-141 (2008002)* was added to the EDC satellite database.
- 2019-12-09 The satellites *Astrocast-0.1 (2009042)* and *Astrocast-0.2 (2003006)* were added to the EDC satellite database.
- 2019-12-05 The status of station *Wuhan, China (7396)* was changed to validated.
- 2019-11-28 The status of station *San Fernando, Spain (7024)* was changed to validated.
- 2019-11-19 The status of station *Tanegashima, Japan (7558)* was changed to validated.

More News

Live Tracking Status

Station	Date	Satellite	Status	HRS	CPF
Grp	2020-02-10 07:22:36	GLIMS134	OUT		
Hermionou	2020-02-10 07:23:57	GLIMS134	CLR	4036	NEPS401 0.000
MURO-Matras	2020-02-10 07:16:26	Callisto	NKT	(Stat. ing. 07)	9.000
Potliden	2020-02-10 07:24:01		OUT		
Sand	2020-02-10 07:23:47		OUT		
Tanegashima	2020-02-10 07:23:58	GLIMS138	CLR	110	NEPS401 0.000
Zimmerwald	2020-02-10 07:15:03		OUT		

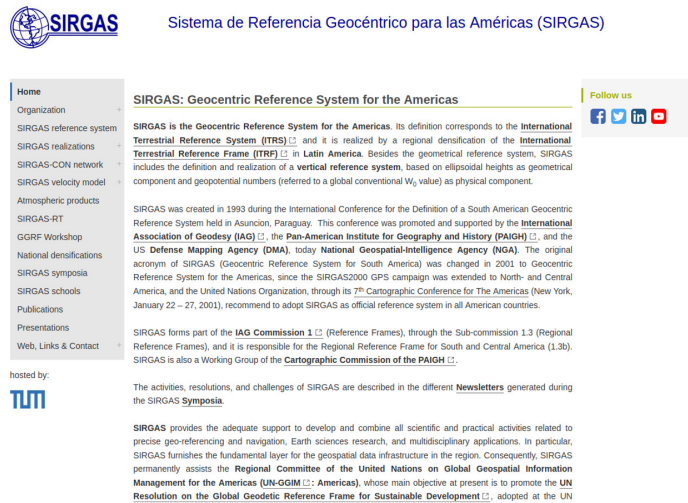
Contact
Christian Schwelke
christian.schwelke@tum.de
80333 München
Arcisstr. 21
Tel. +49 89 23031-1109
Fax +49 89 23031-1240

The EUROLAS Data Center (EDC) operated by DGFI-TUM is one of two global Data Centers of the International Laser Ranging Service (ILRS). The web site at edc.dgfi.tum.de and corresponding FTP at <ftp://edc.dgfi.tum.de> provide access to all SLR original observations and derived products for the ILRS community. Additionally, the EDC web site informs about the real-time data management within the ILRS Operations Center (OC) and about the data holding of the Data Center.

GGOS Focus Area Unified Height System

The DGFI-TUM has been chairing the GGOS Focus Area *Unified Height System* since 2015. Its main objective is the implementation of a global vertical reference system in accordance with the resolution No. 1, 2015 of the International Association of Geodesy for the definition and realization of an International Height Reference System (IHRs). The Focus Area web site operated by DGFI-TUM (ihrs.dgfi.tum.de) summarizes the actions, plans and recent achievements, and it provides an inventory of work documents, relevant publications and presentations.

Geocentric Reference System for the Americas (SIRGAS)



SIRGAS is the Geocentric Reference System for the Americas. The web site (www.sirgas.org) is operated by the IGS Regional Network Associate Analysis Centre for SIRGAS (IGS RNAAC SIRGAS), which has been under the responsibility of DGFI-TUM since 1996. The SIRGAS web site is the primary source of information about SIRGAS. It realizes a unique access point for all SIRGAS science data products (reference frame solutions, deformation models, atmospheric products, etc.), provides detailed meta-data sets for the reference frame components, describes the operational and organizational infrastructures, and contains a detailed inventory of publications and presentations related to SIRGAS.

Office of the International Association of Geodesy (IAG)

DGFI-TUM hosted the Office of the International Association of Geodesy (IAG Office) from the 24th IUGG General Assembly (2007) in Perugia, Italy, until the 27th IUGG General Assembly (2019) in Montreal, Canada. For the same period, the former director of the DGFI, H. Drewes, held the position of the IAG Secretary General, and the DGFI-TUM took the responsibility for all the IAG administration including the IAG budget. The new IAG Office and Secretary General reside at the Finnish Geodetic Institute. During a transition period, the web site of the former IAG Office will continue at iag.dgfi.tum.de.

5 Projects

A large part of DGFI-TUM's research activities is financed through third-party funds from various sources. Funding of the following projects is gratefully acknowledged (in alphabetic order):

Baltic+ SEAL BALTIC+ Sea Level (ESA)

Baltic+ SAR-HSU BALTIC+ Geodetic SAR for Baltic height system unification (ESA)

CIEROT Combination of space geodetic observations for the determination of mass transports in the cryosphere and their impact on Earth rotation (DFG)

COSTO Contribution of SWARM data to the prompt detection of Tsunamis and other natural hazards (ESA)

DAAD Thematic Network Modern Geodetic Space Techniques for Global Change Monitoring (DAAD)

DIGERATI Direct geocentric realisation of the American reference frame by combination of geodetic observation techniques (DFG)

ESA-EOP Independent generation of Earth Orientation Parameters (ESA)

FOR 2630, WALESA Refined estimates of absolute water levels for inland waters from multi-mission satellite altimetry (DFG)

FOR 2736, TIDUS Improved tidal dynamics and uncertainty estimation for satellite gravimetry (DFG)

IONO-WB Assessment and validation of ionospheric models for GNSS application in Western Balkan (DAAD)

ML-IonoCast Machine learning for forecasting the ionospheric total electron content (DAAD)

OPTIMAP Operational Tool for Ionospheric Mapping And Prediction (ZGeoBw)

ORG4Heights Optimally combined regional geoid models for the realization of height systems in developing countries (DFG)

SPP 1788, INSIGHT-2 Interactions of low-orbiting satellites with the surrounding ionosphere and thermosphere (DFG)

SPP 1788, MuSE Multi-satellite reconstruction of the electron density in ionosphere and plasmasphere (DFG)

SPP 1788, TIPOD Development of high-precision thermosphere models for improving precise orbit determination of Low-Earth-Orbiting satellites (DFG)

SL-CCI Plus Sea Level Climate Change Initiative Plus (ESA)

SS-CCI Plus Sea State Climate Change Initiative Plus (ESA)

TIK Entwicklung eines operationellen Prototyps zur Bestimmung der thermosphärischen Dichte auf Basis eines Thermosphären-Ionosphären Kopplungsmodells (BMW/DLR)

VLAD Vertical land motion by satellite altimetry and tide gauge difference (DFG)

6 Personnel

6.1 Lectures and Courses at Universities

Angermann D. : Lecture “Satellite Geodesy: Global Geodata for Society and Politics”,
TUM, SS 2019

Bloßfeld M. : Lecture “Realization and Application of Global Geodetic Reference Systems”,
TUM, SS 2019

Bloßfeld M. : Lecture “Earth System Dynamics”,
TUM, WS 2018/19 and WS 2019/20

Passaro M. : Lecture “Oceanography and Satellite Altimetry”,
TUM, WS 2018/19 and WS 2019/20

Dettmering D. : Lecture “Hydrogeodesy: Monitoring Surface Waters from Space”,
TUM, WS 2018/19 and WS 2019/20

Sánchez L. : Lecture “Advanced Aspects of Height Systems”,
TUM, WS 2018/19 and WS 2019/20

Schmidt M. : Lecture “Numerical Modeling”,
TUM, WS 2018/19 and WS 2019/20

Schmidt M. : Lecture “Numerical Methods in Satellite Geodesy”,
TUM, SS 2019

Schmidt M. : Lecture “Ionosphere Monitoring and Modeling”,
TUM, WS 2018/19 and WS 2019/20

Seitz F. : Lecture “Seminar ESPACE”,
TUM, SS 2019

Seitz F. : Seminar for Doctoral Candidates at the DGFI-TUM,
TUM, WS 2018/19, SS 2019 and WS 2019/20

Seitz F. : Lecture “Earth Rotation”,
TUM, WS 2018/19 and WS 2019/20

6.2 Lectures at Seminars, Schools, and Public Relations

Bloßfeld M. : “Was bewegt sich wie? Geodätische Referenzsysteme als Grundlage für die Erdsystemforschung”. Geodätisches Kolloquium, Jade Hochschule Oldenburg, 2019-01-17

Sánchez L. : “Earth’s surface deformation monitoring based on precise geodetic methods”. Scientists Meet Scientists, Wednesday Coffee Talk of the TUM Institute of Advanced Studies (TUM-IAS), Garching, 2019-02-06

Seitz F., Passaro M. : “Die Veränderung des Meeresspiegels: Wissenschaftliche Beobachtungsergebnisse statt Fake News”. TUM StreetScience, Munich, 2019-09-08

6.3 Thesis Supervision

Master theses

Seitz F., Dettmering D. : Master Thesis Bonas F., TUM: Improving water level estimations of lakes and rivers by advanced analysis of altimeter observations. 2019-04-09

Schmidt M. : Master Thesis Schramm S., TUM: Transformation von VTEC B-Spline Modellen in Kugelflächenfunktionsdarstellungen. 2019-04-29

Schwatke Ch. : Master Thesis Scherer D., Munich University of Applied Sciences: Estimation of river discharge using satellite altimetry and optical remote sensing images. 2019-05-27

Seitz F., Bloßfeld M. : Master Thesis Zeitlhöfler J., TUM: Nominal and observation-based attitude realization for precise orbit determination of the Jason satellites. 2019-06-21

Doctoral theses

Schmidt M. (co-supervisor): Doctoral Thesis Magnet N., TU Wien: Giomo: a robust modelling approach of ionospheric delays for GNSS real-time positioning applications. 2019-04-25

Dettmering D. (examiner): Doctoral Thesis Abulaitijiang A., Technical University of Denmark: Marine gravity and bathymetry modelling from recent satellite altimetry. 2019-06-21

6.4 Awards

Passaro M. : Teaching prize GeodätUM, Technical University of Munich, for the lecture “Oceanography and Satellite Altimetry”, WS 2018/19.

Seitz M. : Appointed as Fellow of the International Association of Geodesy by the IAG Executive Committee in recognition of the services rendered.